AD NUMBER

AD825264

NEW LIMITATION CHANGE

TO

Approved for public release, distribution unlimited

FROM

Distribution authorized to U.S. Gov't. agencies and their contractors; Administrative and Operational Use; Nov 1967. Other requests shall be referred to the Air Force Materials Laboratory, Attn: MAAM - Materials Application Division, Wright-Patterson AFB, OH 45433.

AUTHORITY

USAF, per ltr dtd 2 Mar 1972

AFML-TR-67-257

FRACTURE DATA FOR MATERIALS AT CRYOGENIC TEMPERATURES

W. E. Witzell

Convair division of General Dynamics

TECHNICAL REPORT AFML-TR-67-257

November 1967

Air Force Materials Laboratory
Research and Technology Division
Air Force Systems Command
Wright-Patterson Air Force Base, Ohio

NOTICES

When Government drawings, specifications, or other data are used for any purpose other than in connection with a definitely related Government procurement operation, the United States Government thereby incurs no responsibility nor any obligation whatsoever; and the fact that the Government may have formulated, furnished, or in any way supplied the said drawings, specifications, or other data, is not to be regarded by implication or otherwise as in any manner licensing the holder or any other person or corporation, or conveying any rights or permission to manufacture, use, or sell any patented invention that may in any way be related thereto.

Qualified requesters may obtain copies of this report from the Defense Documentation Center (DDC), Cameron Station, Bldg. 5, 5010 Duke Street, Alexandria, Virginia 22314.

Copies of this report should not be returned unless return is required by security considerations, contractual obligations, or notice on a specific document.

FRACTURE DATA FOR MATERIALS AT CRYOGENIC TEMPERATURES

W. E. Witzell

FOREWORD

This report was prepared by Convair division of General Dynamics, San Diego, California, under USAF Contract No. AF 33(615)-3779 titled "Toughness Data on Materials at Cryogenic Temperatures." The work was administered under the direction of the Air Force Materials Laboratory, Research and Technology Division, Air Force Systems Command, Wright-Patterson Air Force Base, Ohio, Mr. Marvin Knight, MAAM, Project Engineer.

This report covers work conducted from May 1966 to June 1967 under Project Number 7381 "Materials Applications," Task Number 738106 "Design Information Development." The report was submitted by the author in July 1967.

The Convair division Report number is GDC-ZZL67-017.

Mr. Max Spencer of Convair division of General Dynamics performed virtually all the tests reported under this program. In addition, he laid out specimens, supervised manufacture, fatigue cracked notched specimens, collected data, and suggested modifications for test fixtures and instrumentation. In short, Max Spencer was the key man in this program.

Mr. C. J. Kropp of Convair division not only provided the information on thermal treatment of the alloys, but annealed and aged the alloys as required. He also provided other technical assistance both in testing and in data reduction and reporting.

Although obtaining materials for this program was unusually difficult, two material producers were very helpful and kind in supplying alloys.

Alcoa supplied the X2021-T8 E31 aluminum alloy and Kaiser provided the 7039-T64 aluminum.

Mr. Art Mehner of Convair division performed the electron microscopy and analyz l the fractographs.

Many others were helpful in the completion of this project including the AFML projec. monitor, Mr. Marvin Knight.

This technical report has been reviewed and is approved.

D. A. SHINN
Chief, Materials Information Branch
Materials Applications Division
Air Force Materials Laboratory

ABSTRACT

Six potential aerospace alloys were evaluated for toughness at liquid hydrogen temperature (-423° F). They were:

- Titanium 5Al-2.5Sn (ELI)
- Titanium 6Al-4V (ELI)
- INCO 718 (aged) nickel alloy
- Aluminum X2021-T8 E31
- Aluminum 2219-T81
- Aluminum 7039-T64

The first four materials were 0.063-inch thick; the last two were 0.125-inch thick. Sufficient specimens were manufactured to evaluate all of the alloys at four test temperatures, namely: room temperature, -110°F, -320°F, and -423°F.

Convair division has performed tensile, notched tensile, center notched, and single edge notch tests at -423° F for all alloys. In addition, the INCO 718 and X2021 aluminum alloys were investigated at the three other temperatures. The Air Force Materials Laboratory will perform the remainder of tests at room temperature, -110° F, and -320°F.

An attempt was made to obtain both plane stress and plane strain fracture toughness data from the same center notched specimen. Except for the titanium alloys, the net fracture stress exceeded 80 percent of the yield strength for all alloys and test temperatures. In all cases, the net stress at pop-in was well below the yield strength of the material.

The pop-in net fracture stresses for the single edge notch specimens (obtained by a strain gaged compliance gage) were also well below the yield strength.

K_c and K_{Ic} values were calculated for all fracture specimens.

Both the INCO 718 and X2021 aluminum alloys showed good toughness properties as the temperature was decreased to -423° F.

TABLE OF CONTENTS

TABLE OF CONTENTS, Contd

ILLUSTRATIONS

ILLUSTRATIONS, Contd

TABLES

LIST OF SYMBOLS AND ABBREVIATIONS

a	Half crack length for center notched specimen (inches), crack length for SEN specimens (inches), or one half the distance between notches for notched tensile specimens (inches).
a_1	Crack length, adjusted for plastic zone correction (inches) plane strain
a_{c1}	Adjusted crack length (inches) plane stress
a_o	Initial crack length (inches) SEN
B	Specimen thickness (inches)
CN	Center notched
e	Elongation (percent)
E	Modulus of elasticity (ksi)
ELI	Extra low interstitial (impurity)
F_{tu}	Ultimate tensile strength (ksi)
F_{ty}	Tensile yield strength (ksi) (0.2% offset method)
k	Kips (or 1000 pounds)
K_c	Plane stress fracture roughness, or critical crack intensity factor (ksi $\sqrt{\text{in}}$)
K_I	Crack intensity factor (general) (ksi $\sqrt{\text{in}}$)
K_{Ic}	Plane strain fracture toughness, or crack intensity factor at pop-in (ksi $\sqrt{\text{in}}$)
ksi	Kips per square inch
k_t	Notch acuity of notched tensile specimen
P	Maximum load (kips)
P_p	Pop-in load (kips)
r	Radius at the tip of a notch (inches)
SEN	Single-edge-notch
W	Specimen width (inches)

LIST OF SYMBOLS AND ABBREVIATIONS, Contd

σ	Stress (ksi)
σ_G	Maximum gross stress (ksi)
σ_N	Net stress at maximum load (ksi)
σ_P	Gross stress at pop-in (ksi)
σ_{pN}	Net stress at pop-in (ksi)
σ_{yS}	Tensile yield stress (ksi)
μ	Poisson's ratio
2a	Initial crack length (inches), CN
$2a_c$	Critical crack length (inches), CN, or crack length at onset of rapid propagation

SECTION I

INTRODUCTION

This study is part of a program to attempt to determine if a single fracture mechanics specimen could be used to obtain both plane stress and plane strain fracture toughness. The evaluation was performed through utilization of six potential aerospace alloys in thin gauges (0.063 and 0.125 inch) as follows:

Titanium 5Al-2.5Sn (ELI)
Titanium 6Al-4V (ELI)
INCO 718 (aged) nickel alloy
Aluminum X2021-T8 E31
Aluminum 2219-T81
Aluminum 7039-T64

Tests were performed at room temperature and three cryogenic temperatures, -110° F, -320° F, and -423° F. This program is a joint effort by Convair and the Air Force Materials Laboratory; Convair manufactured all specimens and performed all tests at -423° F. In addition, Convair tested INCO 718 and the X2021 aluminum alloy at the other three test temperatures. The X2021 alloy will also be tested by AFML for comparison purposes.

In addition to center notch and single edge notch fracture specimens, smooth and notched tensile specimens were tested to establish basic mechanical properties at the various test temperatures.

This report covers the work done by Convair only. It is anticipated that an additional report will be published at the conclusion of the testing by the Air Force Materials Laboratory.

SECTION II

TEST SPECIMENS

Initially, four types of test specimens were specified: 1) tensile test specimens, 2) notched tensile test specimens, 3) center notched fracture mechanics, and 4) another specimen specified only as a K_{Ic} test specimen. After the program was underway and some results were obtained it was decided to use a single edge notch (SEN) specimen for determination of K_{Ic}. These four specimens are shown in Figures 1, 2, 3, and 4.

1. MECHANICAL PROPERTIES SPECIMENS. Tensile specimens were standard ASTM specimens for flat sheet material. Notched tensile specimens were slightly narrower with medium sharp notches designed to provide a K_t value of slightly less than 7.

2. CENTER NOTCHED SPECIMENS. Design of center notched specimens was somewhat more difficult due to the thickness of the materials under test (0.063 and 0.125 inch). One object of this program was to attempt to obtain both K_c and K_{Ic} from a single specimen. According to Srawley and Brown (Reference 1), width-to-thickness ratios of the two types of specimens are non-overlapping as follows:

$$K_c \quad 16 < W/B < 45$$

$$K_{IC} \quad 5 < W/B < 10$$

For a given thickness, no specimen width could be selected that would satisfy both requirements. Since thin sheet material was designated for this program, it is more probable that conditions of plane stress would exist. Therefore, to emphasize valid K_c values, the greater specimen width was chosen. In addition, for simplification, all specimen widths were to be the same regardless of thickness. Center notches were cut with an electrical discharge machine prior to notch sharpening by tension-tension fatigue at about 20 percent of yield strength (Figure 5). Again, according to Srawley and Brown, the exact machine cut configuration is relatively unimportant as long as the notch is extended by low stress fatigue. The ASTM concurs (Reference 2) as shown in Figure 6. Some differences in opinions are prevalent concerning the total length of the notch. Prior to July 1966, ASTM recommendations suggested a notch length between 30 and 40 percent of the specimen width (Reference 3).

At the ASTM National Convention in July 1966, Brown and Srawley presented a draft of a report that suggests that the crack length should be 50 percent of the specimen width. (Subsequently, a great deal of this report was published as an ASTM Technical Publication, Reference 4.)

NOTE: ALL DIMENSIONS IN INCHES.

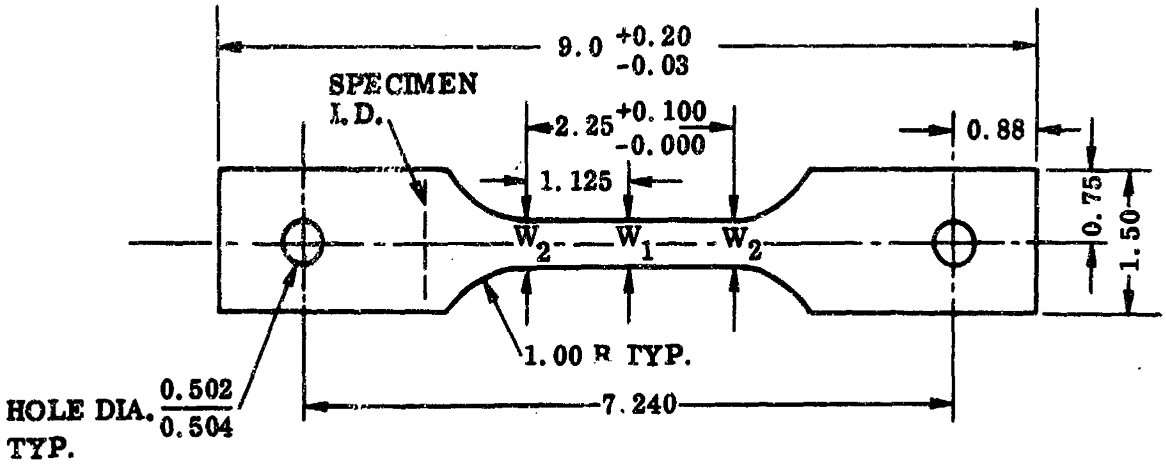

Figure 1. Tensile Specimen

NOTE: ALL DIMENSIONS IN INCHES.

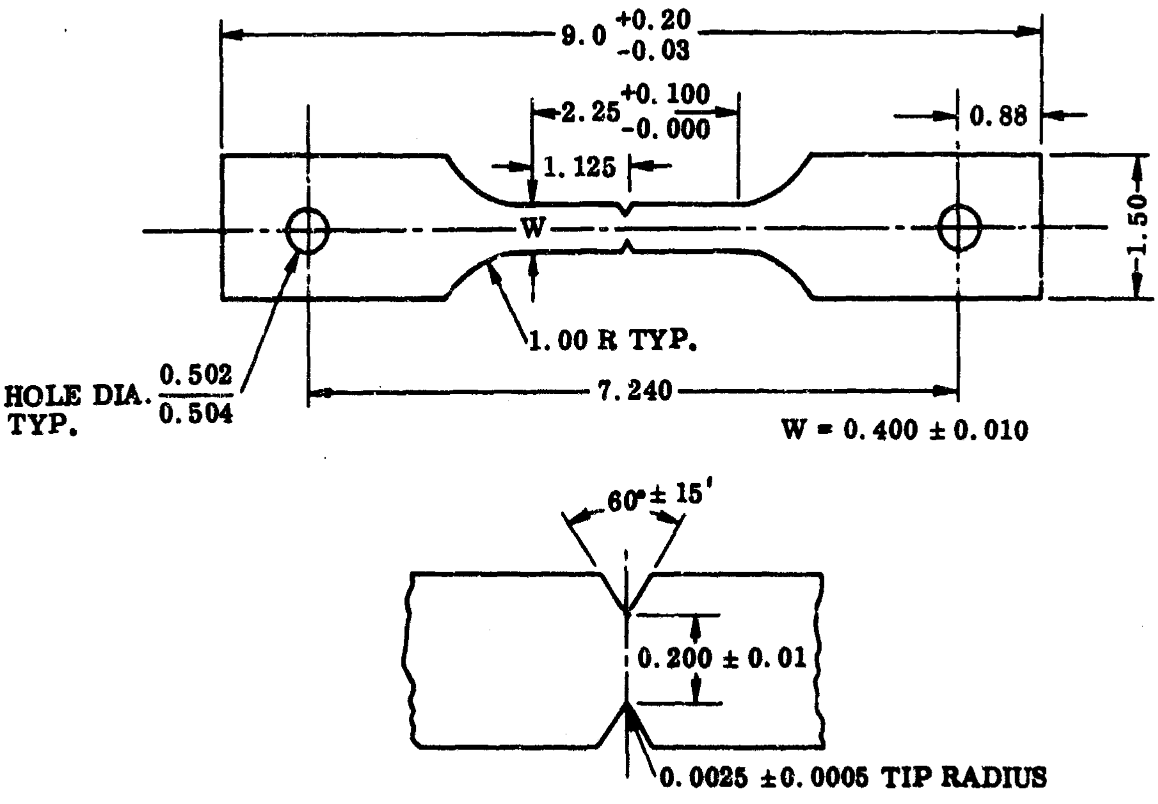

NOTCH DETAIL

Figure 2. Notched Tensile Specimen

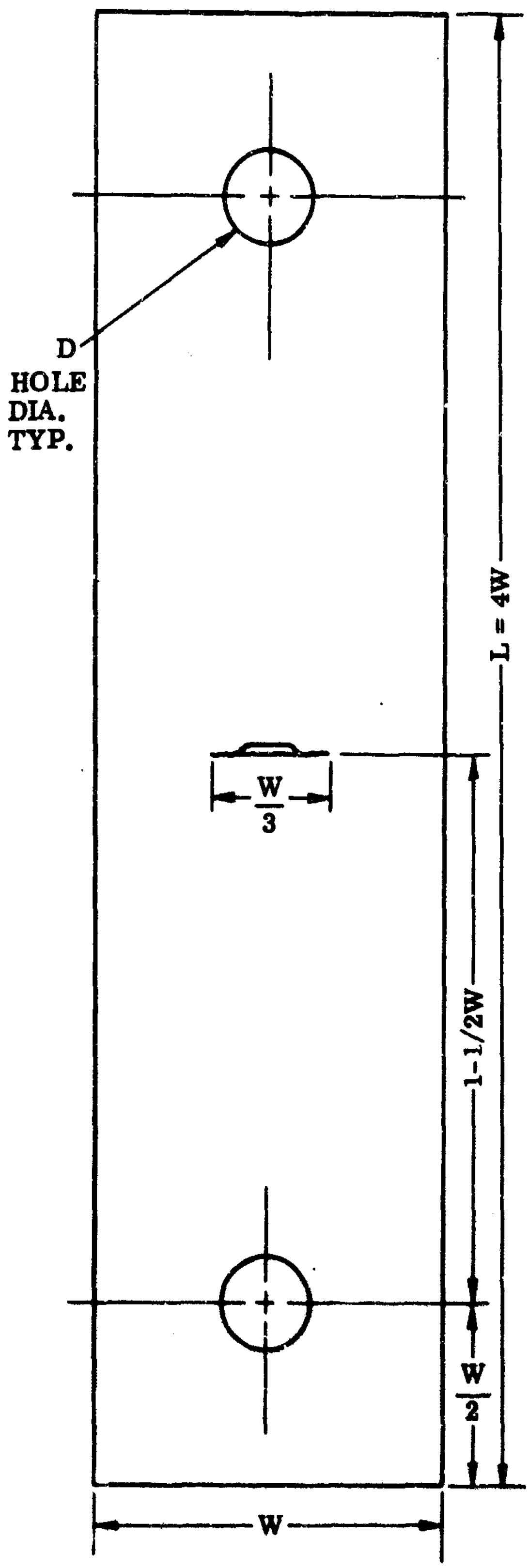

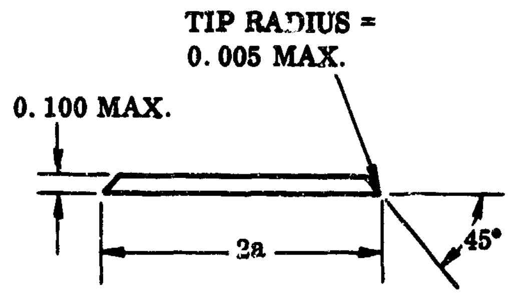

-1 NOTCH DETAIL

NOTE: ALL DIMENSIONS IN INCHES.

W	L	2a	D	W/2	1-1/2W
3.00	12.0	0.75	1.002 1.004	1.50	4.50

Figure 3. Center Notched Specimen

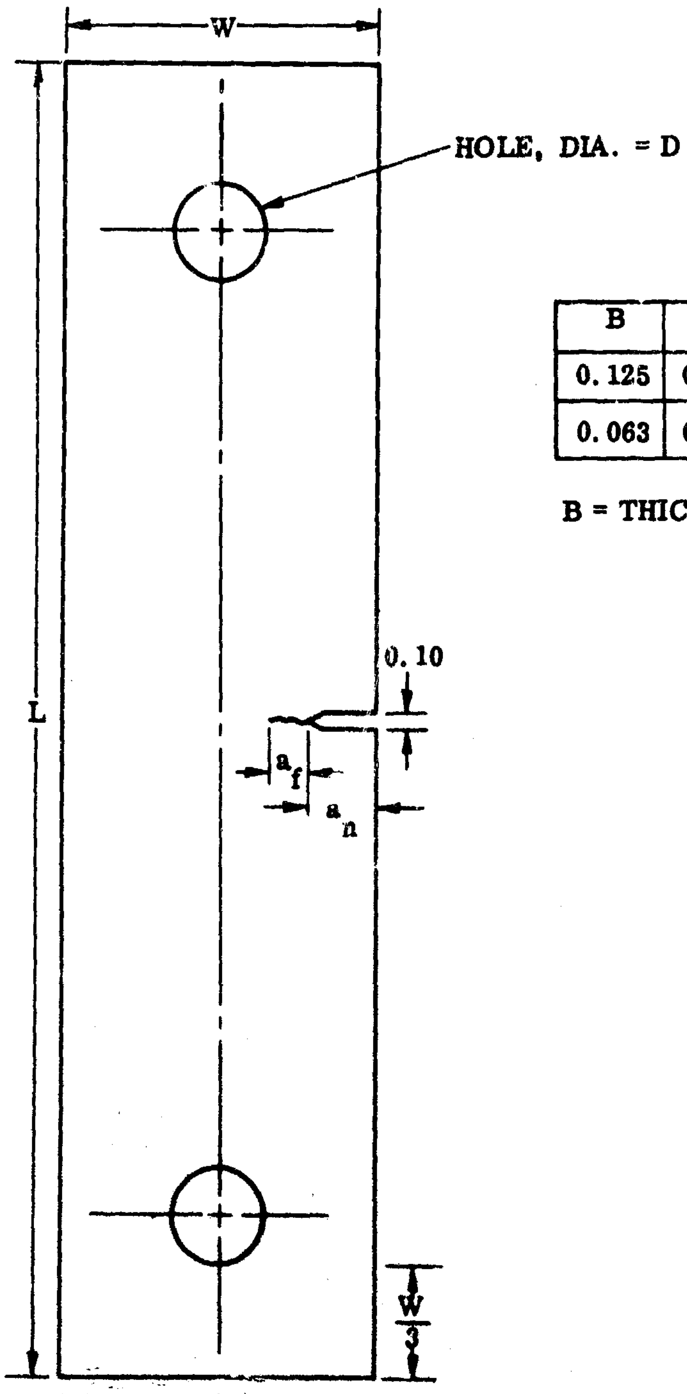

B	W	L	a_f	a_n	D
0.125	0.50	4.0	0.1	0.1	0.187
0.063	0.50	4.0	0.1	0.1	0.187

B = THICKNESS

Figure 4. Single Edge Notch (SEN) Specimen

Figure 5. Titanium Center Notched Fracture Mechanics Specimen

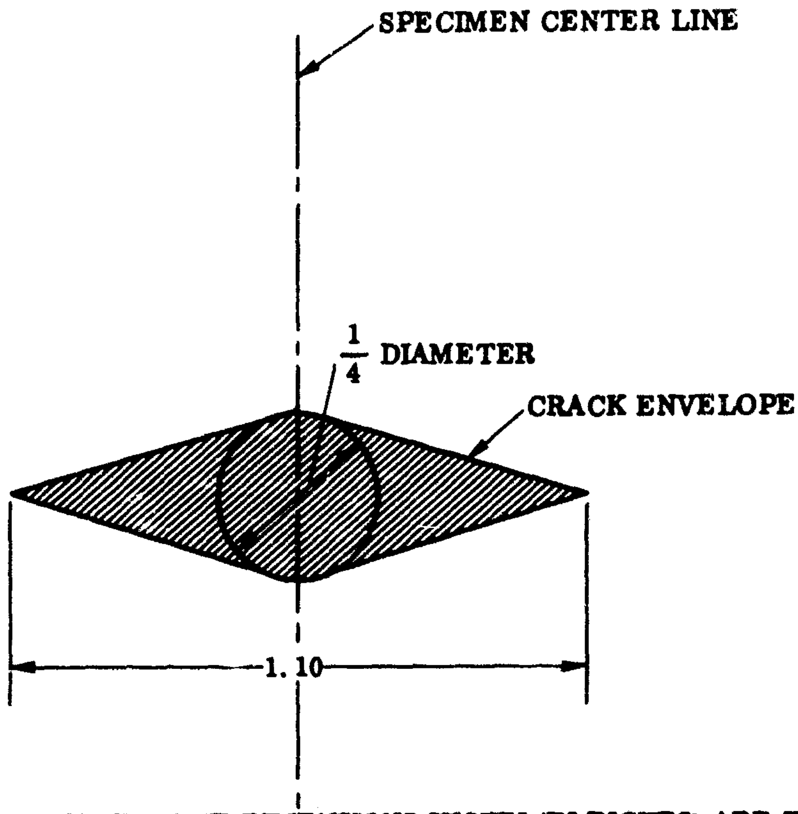

NOTE: THE DIMENSIONS SHOWN (IN INCHES) ARE FOR A 3-INCH-WIDE SPECIMEN. ENVELOPES FOR OTHER SIZE SPECIMENS ARE ADJUSTED USING THESE PROPORTIONS.

Figure 6. ASTM Recommended Acceptable Center Crack Envelope (Reference 1)

Aside from theoretical considerations, there are advantages to using a larger crack length as far as testing is concerned. For example, a larger crack minimizes the changes that the specimen will fail in the pin hole or grip section. As a consequence, an attempt was made to obtain a crack length that approached 40 percent of the specimen width.

3. $\underline{K_{Ic}}$ TEST SPECIMENS. The most logical specimen for determination of K_{Ic} in thin sheet materials is the single edge notch (SEN) tensile specimen. Actually no specimen configuration can meet all the requirements of the various organizations (e.g. ASTM) or investigators as far as plane strain of sheet materials is concerned. Obviously, round notched tensile specimens cannot be fabricated from 0.063-inch thick sheet. Notch bend specimens are also quite difficult to fabricate from such thin materials. As far as the surface flaw specimens are concerned. it is extremely difficult to induce a tiny perfectly shaped semielliptical flaw in the surface of the thin materials investigated under this program.

According to Brown and Srawley (Reference 4), the minimum thickness for adequate K_{Ic} testing is obtained by the equation:

$$B = 2.5\left(\frac{K_{1c}}{\sigma_{ys}}\right)^2$$

where

B = specimen thickness (inches)

K_{1c} = plane strain fracture toughness

σ_{ys} = tensile yield strength

Where the K_{Ic} approaches the yield strength, the required thickness is 2.5 inches. Such a requirement almost automatically rules out the possibility of testing sheet materials under conditions of plane strain. Prior work by Srawley and Brown (Reference 1) placed no such restriction on SEN specimens, but merely set limits on its width-to-thickness ratio. They suggested:

$$4 < \frac{W}{B} < 8$$

For a 1/8-inch thick material the specimen width would vary from 1/2 to 1 inch and for a thickness of 0.063 inch, the specimen would be wider than 1/4 but narrower than 1/2 inch.

With these values in mind, a specimen width of 1/2 inch was selected for all alloys and thicknesses. Hanna and Steigerwald (Reference 5) widen the range somewhat (2 to 12), so that such a specimen would be acceptable under their criteria.

The same general comments about notch lengths apply to the SEN specimens as well as the center notched specimens. In this case, the machine notch was limited to a depth of 0.1 inch and the fatigue crack was extended to about 40 percent of the width. To facilitate cracking, it was convenient to make a "chevron" cut, 45 degrees to the edge of the specimen on both sides of the sheet. The resultant triangular crack front caused the crack to start growing after only a few cycles.

SECTION III

MATERIALS

Alloys for this program were selected in two thicknesses, namely 0.063 and 0.125 inch. In general, the higher strength materials were obtained in the thinner sheets. Except for the X2021-T8 E31 alloy, the aluminum alloys were 0.125-inch-thick. The following materials were tested:

- Titanium 6Al-4V ELI, B = 0.063 inch
- Titanium 5Al-2.5Sn ELI, B = 0.063 inch
- INCO 718 Nickel Base Alloy, B = 0.063 inch
- X2021-T8 E31 Aluminum, B = 0.063 inch
- 2219-T81 Aluminum, B = 0.125 inch
- 7039-T64 Aluminum, B = 0.125 inch

Chemical compositions for these alloys are listed in Table I.

Both of the titanium alloys were tested in the annealed condition. However, due to the unavailability of annealed material in the 0.063-inch thickness, the Ti 6Al-4V ELI alloy was annealed by Convair division using the following procedure, recommended by TMCA:

a. Material was placed in a vacuum retort (10^{-3} torr).

b. Retort with parts were heated to 1350 ± 25°F.

c. Parts were held at temperature for 4 hours.

d. Parts were slow cooled (30°F/hr) to 1050°F.

e. Parts were air cooled.

After annealing, the material was given a light pickle (hydrofluoric-nitric acid) to remove a scale that was formed during the thermal treatment. The resultant material was in the dead annealed condition when tested. Although titanium alloys are frequently obtained in the mill annealed condition (as was the Ti 5Al-2.5Sn, ELI), the sheets are usually worked slightly by the mill to obtain the required flatness. It is the experience of Convair division that mill annealed titanium is slightly stronger than the dead annealed material. Both of the alloys were obtained in the Extra Low Interstitial (ELI) grade.

The nickel base alloy INCO 718 supposedly was supplied in the 20-percent cold rolled and aged condition. After tensile specimens were fabricated and tested at -423°F, (no room temperature tests were supposed to be made according to the original work

PRECEDING PAGE BLANK

Table I. History and Chemical Analysis of Test Materials

	TITANIUM		INCO	ALUMINUM		
Alloy	6Al-4V ELI	5Al-2.5Sn ELI	718	X2021	2219	7039
Temper	Annealed*	Mill Annealed	Aged*	T8 E31	T81	T64
Gauge	0.063 in.	0.063 in.	0.063 in.	0.063 in.	0.125 in.	0.125 in.
Supplier	TMCA	TMCA		Alcoa	Alcoa	Kaiser
Heat No.	D-9890	D-9453	7758 EV	Lot 106-597		Lot 182261
[illegible]ecification	MIL-T-9046D		RBO 170-039E		MIL-A-8920	
Hardness (15 N)	76.0	76.1	82.0	54.0	54.7	52.7
Chemistry (Wt. %)						
Al	6.0	5.0	0.60	BAL	BAL	BAL
B			0.006			
C	0.023	0.026	0.07			
Co			0.05			
Cd				0.05-0.20		
Cu			0.01	5.8-6.8	5.8-6.8	0.1 max
Cr			19.53			0.15-0.25
Fe	0.07	0.15	BAL	0.30 max.	0.30 max.	0.4 max.
H	0.007	0.008				
Mg		0.007		0.02 max.	0.02 max.	2.3-3.3
Mn			0.[illegible]	0.20-0.40	0.20-0.40 max.	0.1-0.4
Mo			3.05			
N		0.012				
Ni			52.07			
O	0.12	0.09				
P			0.001			
S			0.007			
Si			0.24	0.20 max.	0.20 max.	0.30 max.
Sn		2.3		0.03-0.08		
Ti	BAL	BAL	0.94	0.02-0.10		0.1 max.
V	3.9			0.05-0.15		
Zn				0.10 max.		3.5-4.5
Zr				0.10-0.25		
Cb + Ta			[illegible].32			
Other				0.15 max. (Total)		0.15 max. (Total)

*Thermal treatment by Convair division.

statement), it became obvious that the material was not processed as reported, but was in the annealed condition. At that point, two alternatives were possible, namely: 1) cold roll the remainder of the sheet and age it afterward, or 2) age the remainder of the specimens and the sheet. The first possibility was rejected since it was of value to keep the thickness of the sheet the same as the titanium alloys. Furthermore, the existing tensile specimens could still be utilized after aging. Therefore, the INCO 718 was aged in accordance with the following schedule:

a. Heat to 1350°F.

b. Hold at 1350 ± 25°F for 8 hours.

c. Furnace cool to 1200°F.

d. Hold at 1200°F until 18 hours elapsed (at or below 1350° F since attaining 1350° F).

The X2021-T8 E31 alloy was designed primarily as a cryogenic material (Reference 6). It is very similar to 2219 alloy, modified by the addition of 0.15 percent Cd and 0.05 percent Zn. Precipitation of the Al-Cu transition phase provides the basic hardening. The nucleation of this phase is assisted by the presence of cadmium and tin. Manganese provides both grain size control and supplemental strengthening but is limited to 0.02 percent maximum to avoid the undesirable insoluble Mg_2Sn phase that inhibits nucleation of the precipitate.

The alloy is solution heat treated at 980°F followed by rapid quenching in cold water. Prior to flattening, the material is pre-aged at 300°F. After flattening, the alloy is aged at 325°F for 10 hours.

The medium strength, weldable 7039 aluminum alloy was obtained in the T64 temper since T6 was not available in the 0.125-inch gauge. The T64 temper is an aging-stress relieving process specifically designed for ballistic usage.

Weldability and toughness of 2219-T81 aluminum alloy have made this material a promising candidate for use as a cryogenic tank material (Reference 7). Two popular tempers are T81 and T87. The T81, which is slightly weaker and more tough, is heat treated and stretched by the manufacturer, then aged 18 hours at 350°F.

SECTION IV

TEST PROCEDURE

1. GENERAL. All alloys were tested at -423°F. Two materials, X2021 aluminum and INCO 718, were tested at four test temperatures, namely: room temperature, -110°F, -320°F, and -423°F. Tests at -423°F were conducted while the specimens were totally immersed in liquid hydrogen (Figure 7). Tests at -320°F were performed in liquid nitrogen while those at -110°F were conducted in a bath of an alcohol-dry ice mixture.

2. TENSILE TESTS. Tensile tests were performed on flat specimens 9 inches long with a 1/2-inch-wide test section (Figure 1). All tests were performed in accordance with Federal Test Method Standard Number 151a and good engineering judgment. A class B-1 extensometer was used for obtaining stress-strain curves over a 2-inch gage length. The specimens were pulled at a strain rate of 0.005 inch/inch/minute up to the yield point and at a head travel rate of 0.15 inch per minute thereafter.

The procedure for testing smooth and notched tensile specimens is as follows.

1. Measure specimen width and thickness for all specimens. Measure notch radius and distance between notches for notched specimens. Record all data. Lay out gage marks on smooth specimens (G.L. = 2.0 inches).

2. Attach gage blocks to tensile specimens.

3. Install specimen in clevises (in cryostat, for cryogenic testing).

4. Attach extensometer to gage blocks (smooth tensiles only). For cryogenic testing using a remote extensometer, rod and tube must fit through cap of cryostat before cap is fastened down. If no cap is used, transducer of extensometer must be suspended over the top of cryostat (Figure 8).

5. For cryogenic testing, attach cap of cryostat (if needed).

6. Wire extensometer to recorder. Rough zero recorder (smooth tensiles only).

7. Remove slack from loading system.

8. For cryogenic testing, fill cryostat with fluid and stabilize temperature. Monitor load on test machine.

9. When temperature has stabilized, adjust recorder and test machine to proper zero.

10. Load smooth tensile specimen at a strain rate of 0.005 in./in./min to yield and a head travel rate of 0.15 in./min thereafter.

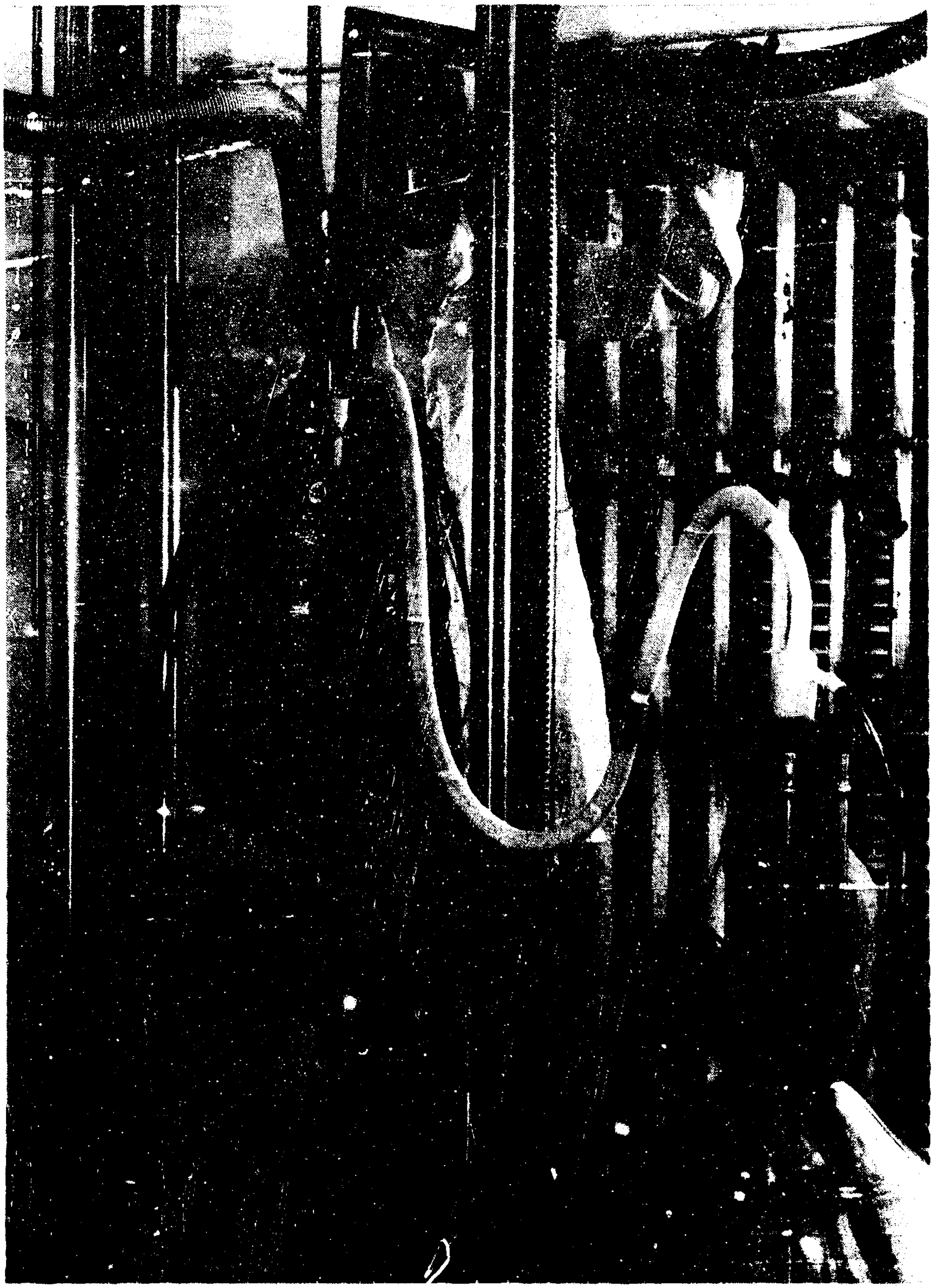

Figure 7. Liquid Hydrogen Cryostat in Tensile Test Machine

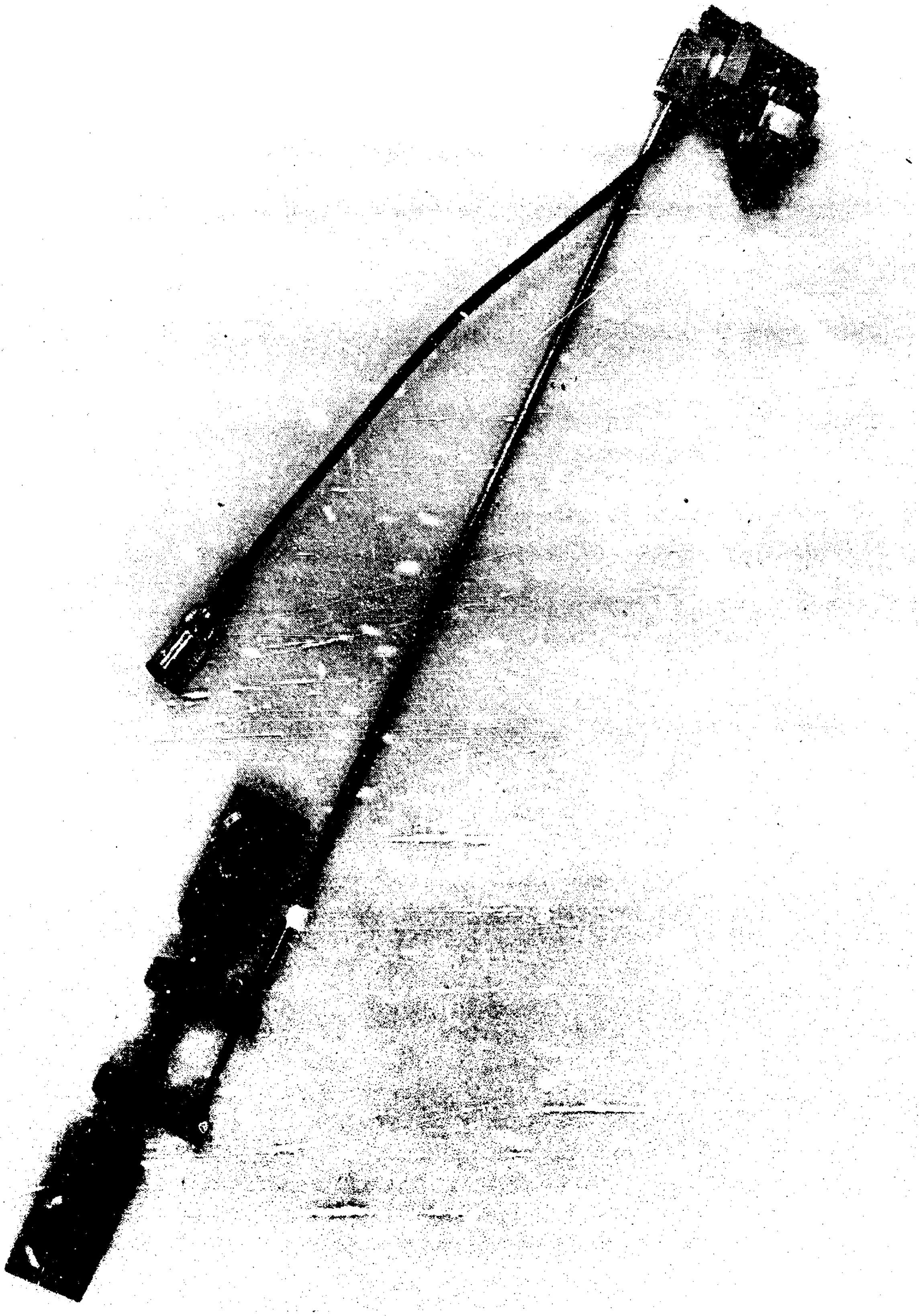

Figure 8. Tensile Specimen With Remote Cryogenic Extensometer ..tached

11. Load notched tensile specimen at a head travel rate of 0.05 in./min.

12. After failure, remove fractured specimen from machine.

13. Observe fracture surface and record unusual appearance.

14. Lay parts of smooth specimens together on a flat surface. Carefully measure distance between gage marks for elongation purposes. Record.

15. Remove stress strain curve from recorder (smooth tensiles) and record ordinates, specimen identification, specimen dimensions, date, test temperature, and operator's initials.

16. Determine yield and ultimate strengths, elongation, and modulus of elasticity for smooth tensiles. Record on stress-strain curve.

17. Determine notched tensile strengths for notched tensile tests.

3. CENTER NOTCHED SPECIMENS. Usually, dimensions of the center notched specimens were measured prior to fatigue notch sharpening. Nevertheless, width, thickness, and total crack length were measured accurately before commencing with static fracture tests.

The brackets for containing the compliance gage were carefully attached making sure that the clamps were parallel. Mechanical doublers, designed to provide clamping pressure as well as to serve as clevises (Figure 9), were fastened to the ends of the specimens. At this time the compliance gage was installed into the brackets (Figure 10). For room temperature tests it is not necessary to install the gage until after the specimen is installed in the tensile machine. However, since such a procedure is practically impossible at cryogenic temperatures, and since uniformity of procedure was desirable, cryogenic procedures were used at room temperature.

After the gage was installed on the specimen, the gage was wired to a Moselly X-Y plotter (Figure 11). The load cell of the tensile test machine also was connected to the plotter. A predetermined power input was impressed on the gage, and the instrument was zeroed. (Note: Compliance gages were calibrated at each temperature for various impressed voltages. The calibration fixture is shown in Figure 12. Such calibrations provide an idea as to the scale factor on the plotter to provide a suitable load deflection curve. Often, the larger voltages for tests at -423° will heat the strain gages to the extent that the liquid hydrogen boils with such vigor that a wiggly curve results. Under these conditions, some compromise must be made between gage output and the noise due to hydrogen boiling. Convair division found that a proper input could be found to provide a more-than-adequate gage output.)

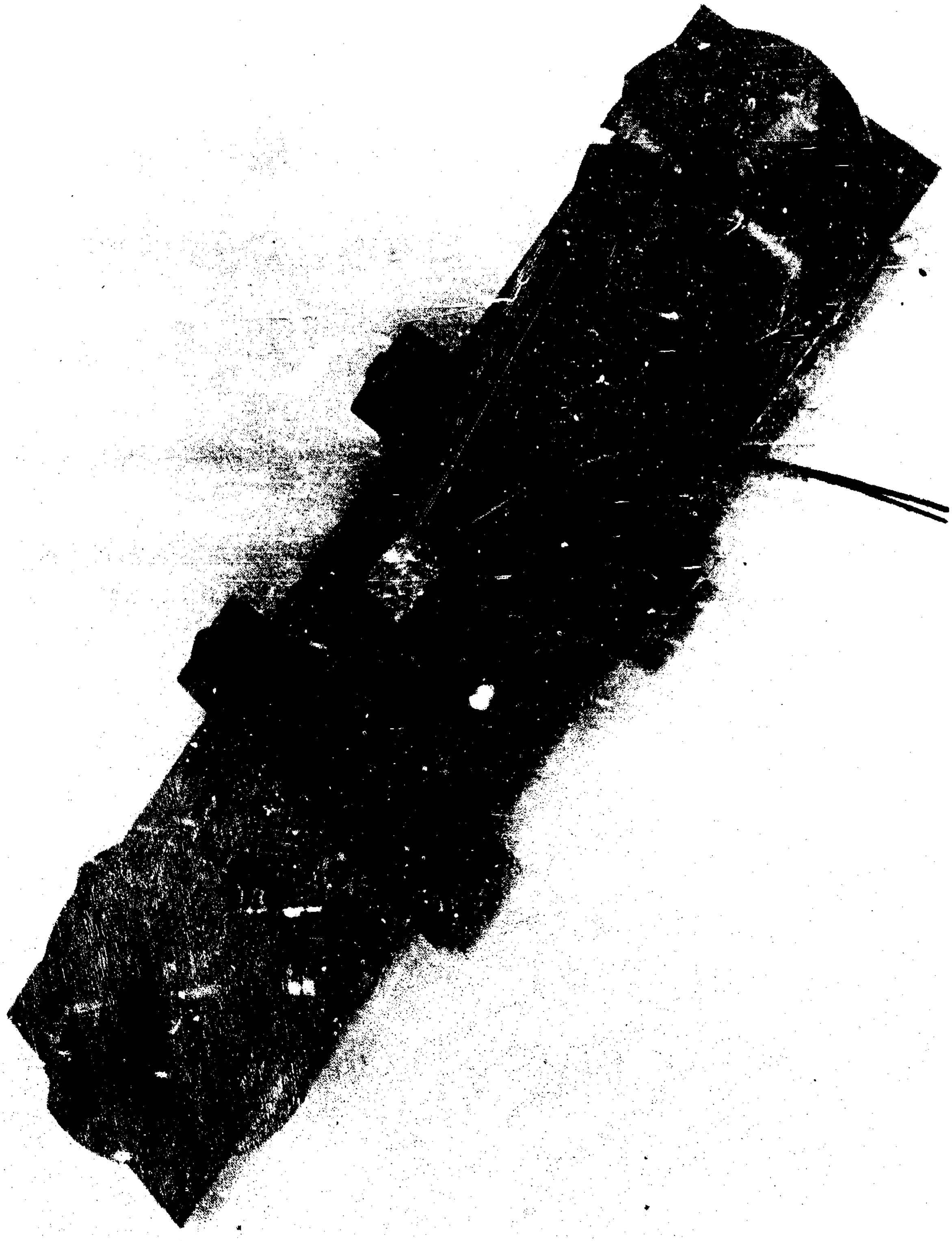

Figure 9. Center Nc'ched Specimen Witu Original Compliance Gage Installed

Figure 10. Center Notched Specim... With Mechanical Doublers and Improved Compliance Gage Attached

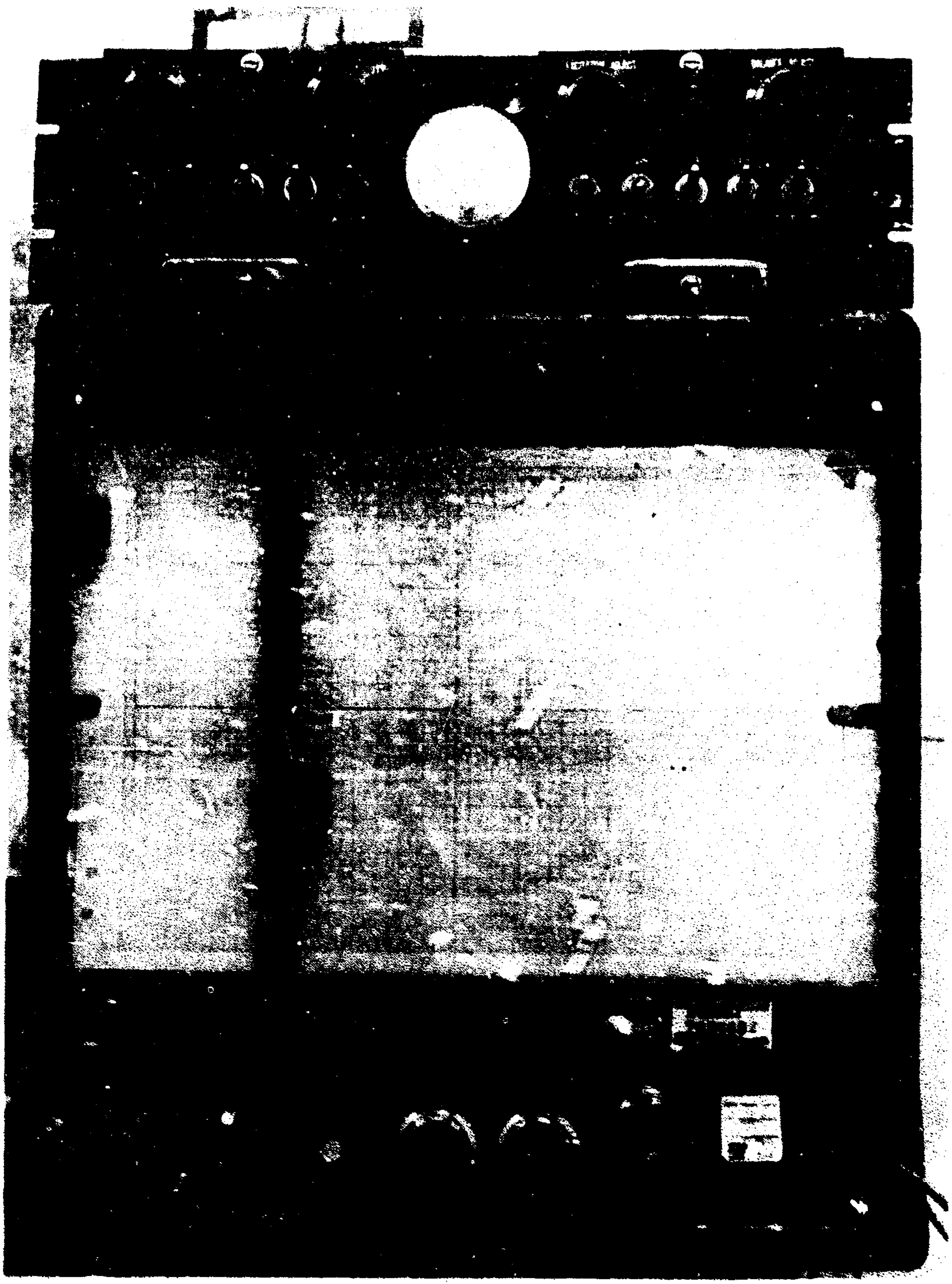

Figure 11. Typical X-Y Plotter

Figure 12. Convair division Developed Cryogenic Gage Calibrator

The specimen, with gage attached, was then installed in the tensile machine. After installation, the X-Y plotter was re-zeroed as required.

After the gage output was verified, an increasing tensile load was applied to the specimen until failure occurred. If any sounds were detected during loading, an appropriate note was made on the load-deflection curve. After the specimen failed, the X-Y plotter was switched off and the fractured pieces removed from the machine. For tests in liquid hydrogen, it was necessary to boil off all hydrogen prior to removal of the specimen. For tests at -320°F and -110°F, it was possible to remove the fractured specimen from the cryogenic fluid without removing the fluid from the container. Upon removal from the cryostat, the specimen was warmed and the fractured surface was examined to determine critical crack growth.

4. SINGLE EDGE NOTCH (SEN) TESTS. Inasmuch as it was necessary to obtain K_{Ic} for both center notched and single edge notch (SEN) specimens, the procedures were virtually the same. The only differences were of accessory equipment (clevises, compliance gage clamps) and treatment of crack growth.

5. INSTRUMENTATION

a. Extensometer. As has been reported, all tensile tests were performed using a Convair division developed cryogenic extensometer (Figure 8). The basic elements of this instrument are a rod-in-tube device that is inserted through the cap of the cryostat to attach to the clamps on the specimen, and a standard tensile machine transducer that is wired directly to the drum recorder of the machine.

Although an extensometer of this nature is quite satisfactory, submerged strain gaged instruments can also be used for this task.

b. Compliance Gage. Convair division has used a band type compliance gage fitted with strain gages (Figure 9) for previous studies. However, just prior to testing on this program, an improved strain gaged instrument was perfected (Figure 10) that has greater stability at -423°F and better output at all test temperatures. These gages were calibrated at each test temperature using the following procedure:

1. Wire the gage into a Wheatstone bridge circuit (similar to that shown in Figure 13). It is convenient to use a recorder that is to be used during actual testing in order to observe the best scale factor setting.

2. Fit the gage into a calibration device (as in Figure 12) that permits adjustment of the gage deflection remotely, along with a suitable linear readout instrument. (A dial gage is quite satisfactory.)

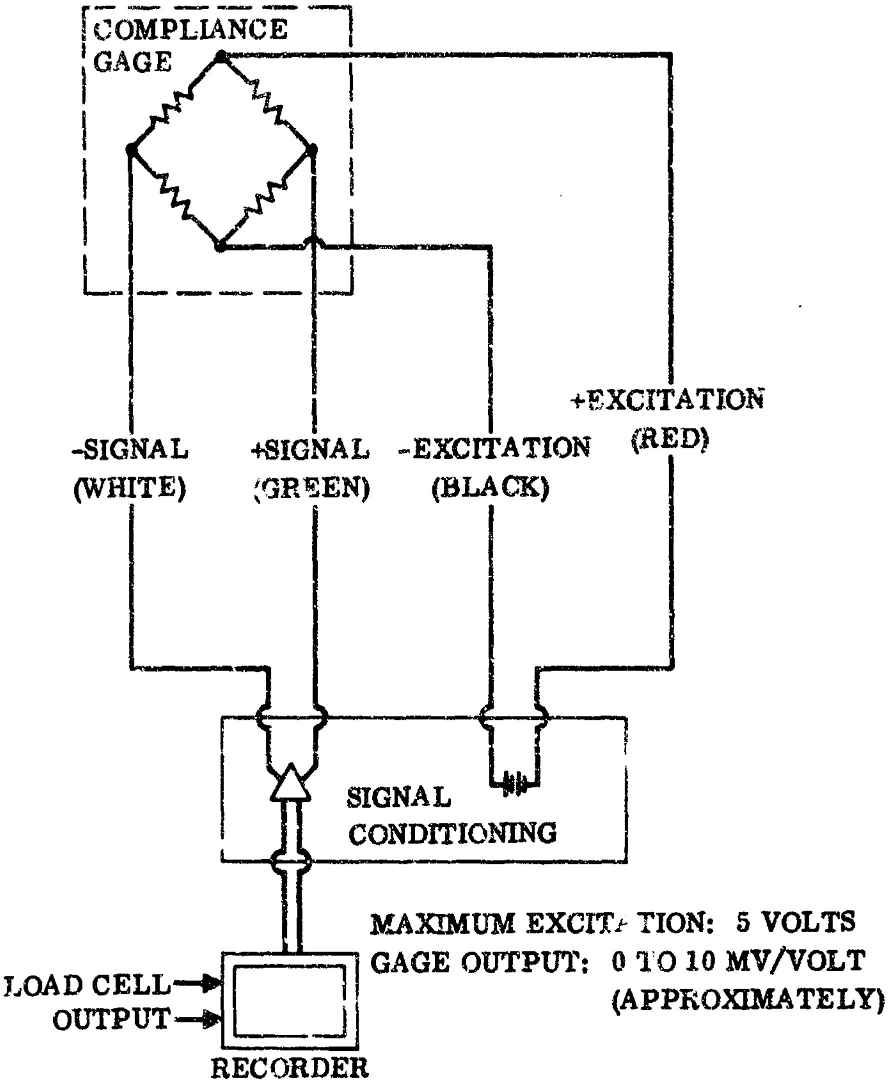

Figure 13. Compliance Gage Circuit

3. Select an excitation voltage (less than 5 volts) on the power supply and zero the recorder.

4. Insert the compliance gage end of the fixture in the test temperature fluid.

5. Reset the recorder at a convenient zero point.

6. Deflect the compliance gage so that the dial gage reads an even increment of deflection and observe the corresponding change on the recorder.

7. Repeat Step 6 until five or six points are observed.

8. Reverse the direction of deflection in the same increments until the original dial gage reading is obtained. (Slight slippage in the mechanical linkage can cause

errors in calibration. It is prudent to average out these errors.)

9. Adjust the excitation voltage up or down depending on the desired recorder output and the noise in the output.

10. Repeat the calibration (Steps 5 through 8) for the new excitation voltage.

11. Adjust the excitation voltage for optimum operation and repeat.

Acutally such a calibration is unnecessary for determination of pop-in for K_{Ic} testing. However, if it is desired to obtain a plot of compliance variation with crack length, such a calibration is useful. Even if a compliance-crack length plot is not needed, it is helpful to determine the optimum excitation voltage before testing commences.

SECTION V

REDUCTION OF DATA

1. MECHANICAL PROPERTIES. The following properties were obtained from tensile test data: ultimate tensile strength (F_{tu}), 0.2-percent offset yield strength (F_{ty}), percent elongation for a 2-inch gage length (e), and modulus of elasticity (E). From the notched tensile tests, notched tensile strength (ultimate) was obtained.

Tensile strength was obtained by dividing the maximum tensile load by the original minimum net test section area of the smooth or notched specimen.

Modulus of elasticity was determined by measuring the slope of a line drawn tangent to the elastic portion of the stress-strain curve. After the tangent line was established, a second line was drawn parallel to it at a scale distance of 0.002 inch/inch from the zero point of the stress-strain curve. The intersection between the stress-strain curve and the offset line was established as the yield point and the corresponding stress was the yield stress.

Upon completion of a tensile test, the two fractured pieces of the specimen were carefully fitted together and the distance between the gage marks was measured. This value, less the original value, was divided by the original gage length to determine percent elongation.

Notched tensile strength is a function of the notch acuity. The specimens used in this program contained a "medium" notch identified by the notch factor K_t as follows:

$$K_t = \sqrt{\frac{a}{r}}$$

where

a = one-half the distance between notches

r = the radius at the tip of the notch

(See Figure 2 for specimen configuration.)

For example, if

$$a = \frac{0.22}{2} = 0.11$$

and

$$r = 0.00225$$

$$K_t = \sqrt{\frac{0.11}{0.00225}} \approx 7.0$$

2. FRACTURE MECHANICS TESTS

a. Center Notched (CN). The experimental approach for the center notched tensile specimens was an exploratory one. An attempt was made to determine both plane strain (K_{Ic}) and plane stress (K_c) fracture toughness from a single test specimen. Without examining the theoretical analysis supporting plane strain and plane stress, it would appear that K_{Ic} could be determined at pop-in and K_c could be measured at critical crack length or maximum load. To obtain such values, a number of other values must be obtained first. Various experimenters have set up criteria for acceptance (Reference 3) of fracture toughness, but the other supplementary values (such as gross stress) are usually unchallenged. Therefore, all of the following values were calculated and are shown in this report as follows:

Gross stress, pop-in $\left(\sigma_p = \frac{P_p}{BW}\right)$

Net stress, pop-in $\left(\sigma_{pN} = \frac{P_p}{B(W-2a)}\right)$

Maximum gross stress $\left(\sigma_G = \frac{P}{BW}\right)$

Maximum net stress $\left(\sigma_N = \frac{P}{B(W-2a_c)}\right)$

where

P_p = pop-in load (see Page 50 for determination of P_p)

B = specimen thickness

W = specimen width

$2a$ = initial crack length

P = maximum load

$2a_c$ = critical crack length (crack length at onset of rapid propagation) (determined by observation of fractured surface)

With these values available, it follows that K_c and K_{Ic} can be calculated as follows:

$$K_{Ic} = \sigma_p \sqrt{\left(W \tan \frac{\pi a}{W}\right)\left(\frac{1}{1 - \mu^2}\right)}$$

and

$$K_c = \sigma_G \sqrt{W \tan \frac{\pi a_c}{W}}$$

where

K_{Ic} = plane strain fracture toughness

K_c = plane stress fracture toughness

μ = Poisson's ratio

(Note: Occasionally the term "crack intensity factor" is substituted for "fracture toughness.")

These equations assume elastic conditions at the tip of the crack. Since such conditions are impossible in reality, a correction must be applied. The plastic zone correction simply assumes that the crack length extends to the ends of the plastic zone. The corrected fracture toughness is calculated by substituting the corrected crack length for the original lengths.

The plastic zone corrections are calculated as follows:

Plane Strain

$$a_1 = a + \frac{K_{Ic}^2}{6\pi \sigma_{ys}^2}$$

Plane Stress

$$a_{c1} = a_c + \frac{K_c^2}{2\pi \sigma_{ys}^2}$$

Since crack length is a function of K_x and since K_x is a function of the plastic zone correction, it appears that the solution to these equations is an iterative process. However, it is customary to use the uncorrected K_x value for solution of the plastic zone correction only once. The resultant plastic zone correction is substituted back into the

K_x equation to obtain the corrected fracture toughness. Both corrected and uncorrected values are shown in the tables in this report.

b. Single Edge Notch (SEN). The calculations for determination of plane strain are somewhat similar to those of the center notched specimens. Prior to calculation of K_{Ic}, it is useful to determine gross stress and net stress at pop-in as follows:

$$\sigma_G = \frac{P}{BW}$$

$$\sigma_N = \frac{P}{B\,(W - a)}$$

where

P = load at pop-in

W = specimen width

B = specimen thickness

a = initial crack length

Using these values, K_{Ic} is determined using the polynomial equation:

$$K_{Ic}^{\,2} = \left(\frac{P}{B}\right)^2 \frac{1}{W}\left[7.59\,\frac{a}{W} - 32\left(\frac{a}{W}\right)^2 + 117\left(\frac{a}{W}\right)^3\right]\frac{1}{1 - \mu^2}$$

where

μ = Poisson's ratio

In like manner, the plastic zone correction is:

$$a = a_0 + \frac{K_{Ic}^{\,2}}{6\pi\,\sigma_{ys}^{\,2}}$$

where

a_0 = initial crack length

σ_{ys} = yield strength of the material

All of the preceding solutions have been reduced to digital computer programs, which were used for this study. After debugging, results were spot checked manually before tabulating.

SECTION VI

RESULTS AND DISCUSSION

1. SMOOTH AND NOTCHED TENSILE TESTS. Mechanical properties obtained from these tests are shown in Tables II through VIII. Variation of strength with temperature is shown for X2021-T8 E31 aluminum alloy in Figures 14 and 15 and for INCO 718 (Aged) in Figures 16 and 17.

The INCO 718 in its aged condition had an ultimate tensile strength of about 193 ksi at room temperature that increased continuously as the test temperature decreased to -423°F (Table 2, Figure 16). Published data on Type 718 Nickel Alloy (e.g., Reference 8) in the 30-percent cold rolled and aged condition show an increase of about 40 ksi over the aged (but not cold rolled) material at all test temperatures. The notch-unnotch tensile ratio is good for all test temperatures, the least desirable being 0.97 at -423°F. Table III presents properties of INCO 718 in the annealed condition at -423°F.

The new X2021-T8 E31 aluminum alloy which has a room temperature ultimate strength of 67 ksi shows a continuing increase in strength to a maximum of 100 ksi at -423°F (Table IV, Figure 14). The notch-unnotch ratio is quite consistent over all four of the temperatures tested with the lowest value of 0.93 at -423°F. Elongation also shows a smooth increase as temperature decreases. There is no apparent variation in tensile properties with grain direction.

The other four alloys tested are more difficult to evaluate since tests were performed at -423°F only. The titanium 5Al-2.5Sn (ELI) had a yield strength of about 210 ksi and an ultimate strength of 233 ksi at -423°F (Table V). Good elongation (more than 13 percent) and notch-unnotch ratio (0.91 minimum) suggest a fairly tough material at this test temperature.

Although both ultimate and yield strength of the titanium 6Al-4V (ELI) were higher than the other titanium alloy (Table VI), the notch tensile strength was significantly lower, resulting in an unsatisfactory notch-unnotch ratio in both grain directions (0.75 - 0.77). Very low elongation at -423°F strengthens the contention that this alloy is brittle at that temperature.

The two aluminum alloys tested in the 0.125-inch thickness were 2219-T81 (Table VII) and 7039-T64 (Table VIII).

The 2219 alloy was stronger than the 7039 at -423°F. The longitudinal ultimate tensile strength was about 5 percent less than the transverse strength, but yield strength, longation, and notch strength were about the same. It follows that the notch-unnotch ratio (0.91) of the longitudinal material was higher than the corresponding value of the transverse material. Again the elongation remained good (10 to 15 percent).

Table II
Mechanical Properties of INCO 718 (Aged)

Specimen Number	Test Direction	Test Temperature (°F)	Width (in.)	Thickness (in.)	F_{tu} (ksi)	(0.2%) F_{ty} (ksi)	(2.0 in.) Elongation (%)	Elastic Modulus ($\times 10^6$ psi)	Notch/Unnotched Ratio
IL6	Longitudinal Unnotched	-423	0.5090	0.0627	274	212	22.5	***	
IL8	Longitudinal Unnotched	-423	0.5093	0.0634	275	207	25.5	29.0	
IL13	Longitudinal Unnotched	-423	0.4968	0.0638	271	206	*18.0	29.3	
IL17	Longitudinal Unnotched	-423	0.4977	0.0635	280	206	24.0	31.5	
		Average			275	208	22.5	29.9	
IL4	†Longitudinal Notched	-423	0.1960	0.0632	277				
IL12	Longitudinal Notched	-423	0.2036	0.0641	249				
IL16	Longitudinal Notched	-423	0.1916	0.0632	273				
IL18	Longitudinal Notched	-423	0.2025	0.0619	263				
		Average			266				
									0.97
IT6	Transverse Unnotched	-423	0.4986	0.0636	268	218	*13.5	***	
IT11	Transverse Unnotched	-423	0.5028	0.0653	258	197	*21.0	32.0	
IT13	Transverse Unnotched	-423	0.4922	0.0635	270	208	18.5	***	
IT18	Transverse Unnotched	-423	0.4998	0.0623	271	206	*20.0	30.6	
		Average			267	207	18.3		
IT4	†Transverse Notched	-423	0.2035	0.0629	260				
IT9	Transverse Notched	-423	0.2029	0.0642	259				
IT15	Transverse Notched	-423	0.1926	0.0633	260				
IT17	Transverse Notched	-423	0.1929	0.0621	259				
		Average			260				
									0.97

Table II
Mechanical Properties of INCO 718 (Aged), Contd

Specimen Number	Test Direction	Test Temperature (°F)	Width (in.)	Thickness (in.)	F_{tu} (ksi)	(0.2%) F_{ty} (ksi)	(2.0 in.) Elongation (%)	Elastic Modulus (x 10^6 psi)	Notch/ Unnotched Ratio
IL3	Longitudinal Unnotched	-320	0.5092	0.0638	248	191	30.0	29.5	
IL10	Longitudinal Unnotched	-320	0.4998	0.0634	246	193	19.0	31.1	
IL12	Longitudinal Unnotched	-320	0.5004	0.0624	240	193	**15.0		
IL19	Longitudinal Unnotched	-320	0.5000	0.0628	248	197	25.5	34.9	
		Average			246	194	22.4	31.8	
ILN2	*Longitudinal Notched	-320	0.1950	0.0636	253				
ILN6	Longitudinal Notched	-320	0.1990	0.0634	253				
ILN11	Longitudinal Notched	-320	0.2032	0.0642	252				
ILN14	Longitudinal Notched	-320	0.1993	0.0639	259				
		Average			254				
									1.03
IT2	Transverse Unnotched	-320	0.4993	0.0643	244	193	20.5	***	
IT7	Transverse Unnotched	-320	0.5050	0.0636	240	193	**16.0	34.3	
IT10	Transverse Unnotched	-320	0.5049	0.0625	245	191	22.0	***	
IT16	Transverse Unnotched	-320	0.4952	0.0633	249	192	25.5	***	
		Average			245	192	21.0	34.3	
ITN2	*Transverse Notched	-320	0.2038	0.0628	250				
ITN5	Transverse Notched	-320	0.2041	0.0635	248				
ITN11	Transverse Notched	-320	0.1915	0.0640	251				
ITN14	Transverse Notched	-320	0.1934	0.0632	250				
		Average			250				
									1.02

Table II
Mechanical Properties of INCO 718 (Aged), Contd

Specimen Number	Test Direction	Test Temperature (°F)	Width (in.)	Thickness (in.)	F_{tu} (ksi)	(0.2%) F_{ty} (ksi)	(2.0 in.) Elongation (%)	Elastic Modulus (x 10^6 psi)	Notch/ Unnotched Ratio
IL18	Longitudinal Unnotched	-110	0.4989	0.0635	214	173	30.0	31.9	
IL14	Longitudinal Unnotched	-110	0.4973	0.0638	211	173	28.5	30.7	
		Average			213	173	29.0	31.0	
ILN7	†Longitudinal Notched	-110	0.2051	0.0639	228				
ILN14	Longitudinal Notched	-110	0.1993	0.0635	233				
ILN17	Longitudinal Notched	-110	0.2041	0.0623	228				
		Average			230				
									1.08
IT5	Transverse Unnotched	-110	0.5036	0.0634	207	169	28.5	29.0	
IT9	Transverse Unnotched	-110	0.5097	0.0648	211	172	27.5	29.4	
IT17	Transverse Unnotched	-110	0.4989	0.0621	209	171	30.5	32.3	
		Average			209	171	29.0	30.2	
ITN7	†Transverse Notched	-110	0.2035	0.0639	226				
ITN16	Transverse Notched	-110	0.1929	0.0634	227				
ITN18	Transverse Notched	-110	0.1929	0.0624	224				
		Average			226				
									1.08

Table II
Mechanical Properties of INCO 718 (Aged), Contd

Specimen Number	Test Direction	Test Temperature (° F)	Width (in.)	Thickness (in.)	F_{tu} (ksi)	(0.2%) F_{ty} (ksi)	(2.0 in.) Elongation (%)	Elastic Modulus (x 10^6 psi)	Notch/ Unnotched Ratio
IL4	Longitudinal Unnotched	+75	0.5093	0.0636	192	***148	25.0		
IL11	Longitudinal Unnotched	+75	0.5002	0.0631	191	160	25.5	***	
IL2	Longitudinal Unnotched	+75	0.4995	0.0632	192	162	24.5	31.0	
IL7	Longitudinal Unnotched	+75	0.4999	0.0635	192	162	23.5	30.8	
		Average			192	158	24.6	31.0	
ILN3	†Longitudinal Notched	+75	0.1945	0.0634	215				
ILN8	Longitudinal Notched	+75	0.1988	0.0637	213				
ILN15	Longitudinal Notched	+75	0.2015	0.0633	219				
ILN20	Longitudinal Notched	+75	0.2013	0.0621	214				
		Average			215				1.12
IT3	Transverse Unnotched	+75	0.5042	0.0641	192	163	23.5	31.[illegible]	
IT15	Transverse Unnotched	+75	0.4935	0.0638	196	165	23.5	31.3	
IT10	Transverse Unnotched	+75	0.5099	0.0648	195	164	22.5	31.0	
IT4	Transverse Unnotched	+75	0.4970	0.0628	192	162	21.5	30.5	
		Average			194	164	22.8	31.0	
ITN3	†Transverse Notched	+75	0.2033	0.0628	216				
ITN6	Transverse Notched	+75	0.2042	0.0638	211				
ITN12	Transverse Notched	+75	0.1925	0.0638	214				
ITN19	Transverse Notched	+75	0.1930	0.0624	213				
		Average			214				1.10

*Broke outside gage area.
**Broke on gage area mark.
***Estimated value, elastic region erratic.
† K_t = 6.3

Table III

Mechanical Properties of INCO 718 (Annealed) at -423°F

Specimen Number	Test Direction	Width (in.)	Thickness (in.)	F_{tu} (ksi)	(0.2%) F_{ty} (ksi)	(2.0 in.) Elongation (%)	Notch/ Unnotched Ratio
IL1	Longitudinal Unnotched	0.4990	0.0636	178	89.9	71.0	
IL5	Longitudinal Unnotched	0.5040	0.0620	175	91.0	*52.0	
IL9	Longitudinal Unnotched	0.4965	0.0644	180	89.8	69.0	
IL15	Longitudinal Unnotched	0.4978	0.0637	174	91.2	*46.5	
IL20	Longitudinal Unnotched	0.4990	0.0631	181	95.2	*66.0	
		Average		178	91.4	61.0	
ILN1	†Longitudinal Notched	0.2002	0.0638	160			
ILN5	Longitudinal Notched	0.2003	0.0[illegible]8	160			
ILN10	Longitudinal Notched	0.1940	0.0641	167			
ILN13	Longitudinal Notched	0.2000	0.0636	167			
ILN19	Longitudinal Notched	0.2004	0.0621	166			
		Average		164			0.92
IT1	Transverse Unnotched	0.4957	0.0643	167	89.3	47.0	
IT8	Transverse Unnotched	0.4941	0.0638	165	84.1	*47.0	
IT12	Transverse Unnotched	0.4968	0.0642	179	93.3	*50.0	
IT14	Transverse Unnotched	0.5036	0.0637	181	87.5	67.0	
IT20	Transverse Unnotched	0.4967	0.0622	180	95.5	66.0	
		Average		174	89.9	55.4	
ITN1	†Transverse Notched	0.2003	0.0634	156			
ITN8	Transverse Notched	0.2140	0.0638	142			
ITN10	Transverse Notched	0.2005	0.0643	155			
ITN13	Transverse Notched	0.1894	0.0634	164			
ITN20	Transverse Notched	0.1950	0.0624	161			
		Average		156			0.90

* Broke outside gage area marks.

† $Kt \approx 6.3$

Table IV
Mechanical Properties of X2021-T8 E31 Aluminum Alloy

Specimen Number	Test Direction	Test Temperature (°F)	Width (in.)	Thickness (in.)	F_{tu} (ksi)	(0.2%) F_{ty} (ksi)	(2.0 in.) Elongation (%)	Elastic Modulus ($\times 10^6$ psi)	Notch/ Unnotched Ratio
XL1	Longitudinal Unnotched	-423	0.4986	0.0626	100	72.1	14.0	10.8	
XL6	Longitudinal Unnotched	-423	0.4992	0.0620	101	72.6	14.5	11.4	
XL11	Longitudinal Unnotched	-423	0.4977	0.0625	102	75.6	14.5		
XL16	Longitudinal Unnotched	-423	0.4989	0.0620	102	76.1	11.0		
XL20	Longitudinal Unnotched	-423	0.5000	0.0631	100	72.8	14.5	13.8	
		Average			101	73.8	14.0	12.0	
XLN1	† Longitudinal Notched	-423	0.1978	0.0631	95.7				
XLN4	Longitudinal Notched	-423	0.1977	0.0630	95.6				
XLN9	Longitudinal Notched	-423	0.1959	0.0628	90.2				
XLN14	Longitudinal Notched	-423	0.1947	0.0627	90.2				
XLN19	Longitudinal Notched	-423	0.1931	0.0627	93.1				
		Average			93.0				0.92
XT1	Transverse Unnotched	-423	0.5004	0.0620	100	71.1	14.5	11.6	
XT6	Transverse Unnotched	-423	0.5028	0.0621	99.4	68.9	16.0	11.3	
XT11	Transverse Unnotched	-423	0.5032	0.0631	100	70.8	15.5	13.3	
XT16	Transverse Unnotched	-423	0.5033	0.0630	99.1	71.1	16.0	12.3	
XT20	Transverse Unnotched	-423	0.5026	0.0630	98.6	69.4	15.0	11.4	
		Average			99.4	70.3	15.0	12.0	
XTN4	† Transverse Notched	-423	0.1933	0.0628	89.0				
XTN9	Transverse Notched	-423	0.1943	0.0627	90.3				
XTN14	Transverse Notched	-423	0.1970	0.0620	93.4				
XTN19	Transverse Notched	-423	0.1970	0.0626	97.3				
XTN1	Transverse Notched	-423	0.1937	0.0627	92.7				
		Average			92.5				0.93

Table IV
Mechanical Properties of X2021-T8 Aluminum Alloy, Contd

Specimen Number	Test Direction	Test Temperature (°F)	Width (in.)	Thickness (in.)	F_{tu} (ksi)	(0.2%) F_{ty} (ksi)	(2.0 in.) Elongation (%)	Elastic Modulus (x 10^6 psi)	Notch/ Unnotched Ratio
XL24	Longitudinal Unnotched	-320	0.5055	0.0630	84.9	64.4	12.0	10.2	
XL25	Longitudinal Unnotched	-320	0.5057	0.0630	85.4	66.4	12.0	9.8	
XL26	Longitudinal Unnotched	-320	0.5057	0.0631	85.2	66.6	13.5	11.3	
		Average			85.2	65.8	12.5	10.4	
XLN27	†Longitudinal Notched	-320	0.1994	0.0628	81.6				
XLN28	Longitudinal Notched	-320	0.2002	0.0626	81.4				
XLN29	Longitudinal Notched	-320	0.2004	0.0625	81.0				
		Average			81.3				0.95
XT24	Transverse Unnotched	-320	0.5027	0.0631	84.2	64.6	13.0	10.2	
XT25	Transverse Unnotched	-320	0.5029	0.0629	84.7	64.9	12.5	12.1	
XT26	Transverse Unnotched	-320	0.5032	0.0629	84.7	64.5	13.5	10.5	
		Average			84.5	64.7	13.0	10.9	
XTN27	†Transverse Notched	-320	0.1970	0.0623	77.0				
XTN28	Transverse Notched	-320	0.1978	0.0623	79.9				
XTN29	Transverse Notched	-320	0.1968	0.0624	80.0				
		Average			79.0				0.93

Table IV
Mechanical Properties of X2021-T8 Aluminum Alloy, Contd

Specimen Number	Test Direction	Test Temperature (°F)	Width (in.)	Thickness (in.)	F_{tu} (ksi)	(0.2%) F_{ty} (ksi)	(2.0 in.) Elongation (%)	Elastic Modulus ($\times 10^6$ psi)	Notch/ Unnotched Ratio
XL27	Longitudinal Unnotched	-110	0.5054	0.0633	71.9	58.5	11.0	10.5	
XL28	Longitudinal Unnotched	-110	0.5051	0.0632	72.2	56.7	11.0	11.4	
XL29	Longitudinal Unnotched	-110	0.5031	0.0632	72.2	59.3	11.0	8.6	
		Average			72.1	58.2	11.0	10.2	
XLN21	†Longitudinal Notched	-110	0.1995	0.0633	71.3				
XLN22	Longitudinal Notched	-110	0.2003	0.0632	69.9				
XLN23	Longitudinal Notched	-110	0.2002	0.0630	69.2				
		Average			70.1				0.97
XT27	Transverse Unnotched	-110	0.5032	0.0632	71.9	58.5	11.0	10.0	
XT28	Transverse Unnotched	-110	0.5032	0.0631	71.8	57.5	10.0	10.7	
XT29	Transverse Unnotched	-110	0.5025	0.0630	72.0	58.3	11.0	13.0	
		Average			71.9	58.1	11.0	11.2	
XTN21	†Transverse Notched	-110	0.1965	0.0627	67.8				
XTN22	Transverse Notched	-110	0.1956	0.0627	70.7				
XTN23	Transverse Notched	-110	0.1969	0.0622	70.0				
		Average			69.5				0.97

Table IV

Mechanical Properties of X2021-T8 E31 Aluminum Alloy, Contd

Specimen Number	Test Direction	Test Temperature (°F)	Width (in.)	Thickness (in.)	F_{tu} (ksi)	(0.2%) F_{ty} (ksi)	(2.0 in.) Elongation (%)	Elastic Modulus ($\times 10^6$ psi)	Notch/ Unnotched Ratio
XL21	Longitudinal Unnotched	+75	0.5033	0.0633	66.7	54.5	10.0	11.4	
XL22	Longitudinal Unnotched	+75	0.5040	0.9632	67.2	4.7	10.0	12.2	
XL23	Longitudinal Unnotched	+75	0.5044	0.0633	67.2	54.6	9.5	11.1	
		Average			67.0	54.6	9.8	11.6	
XLN24	†Longitudinal Notched	+75	0.2001	0.0631	64.8				
XLN25	Longitudinal Notched	+75	0.1996	0.0630	66.4				
XLN26	Longitudinal Notched	+75	0.2003	0.0629	64.6				
		Average			65.3				
									0.97
XT21	Transverse Unnotched	+75	0.5003	0.0633	67.3	54.3	9.0	10.6	
XT22	Transverse Unnotched	+75	0.5016	0.0631	67.5	54.3	9.5	12.1	
XT23	Transverse Unnotched	+75	0.5021	0.0631	67.6	54.8	10.0	10.7	
		Average			67.5	54.5	9.5	11.1	
XTN24	†Transverse Notched	+75	0.1964	0.0621	65.1				
XTN25	Transverse Notched	+75	0.1965	0.0621	65.2				
XTN26	Transverse Notched	+75	0.1967	0.0621	64.7				
		Average			65.0				
									0.96

† $K_t \approx 6.3$

Table V
Mechanical Properties of Titanium 6Al-4V (ELI) at -423°F

Specimen Number	Test Direction	Width (in.)	Thickness (in.)	F_{tu} (ksi)	(0.2%) F_{ty} (ksi)	(2.0 in.) Elongation (%)	Elastic Modulus ($\times 10^6$ psi)	Notch/ Unnotched Ratio
5L4	Longitudinal Unnotched	0.4975	0.0594	236	215	12.0	20.0	
5L6	Longitudinal Unnotched	0.4973	0.0594	*	214	*	17.8	
5L10	Longitudinal Unnotched	0.4982	0.0612	233	212	11.0	20.8	
5L13	Longitudinal Unnotched	0.5002	0.0621	235	210	15.5	19.5	
5L17	Longitudinal Unnotched	0.4969	0.0597	236	212	15.5	18.7	
		Average		235	213	13.5	19.4	
5LN3	†Longitudinal Notched	0.2002	0.0609	223				
5LN4	Longitudinal Notched	0.1996	0.0608	233				
5LN8	Longitudinal Notched	0.2005	0.0612	228				
5LN10	Longitudinal Notched	0.1995	0.0617	229				
5LN15	Longitudinal Notched	0.1999	0.0604	233				
		Average		229				
								0.97
5T8	Transverse Unnotched	0.4934	0.0616	231	210	17.0	20.6	
5T11	Transverse Unnotched	0.5045	0.0592	234	208	17.5	19.2	
5T13	Transverse Unnotched	0.4974	0.0592	233	209	18.0	16.5	
5T17	Transverse Unnotched	0.5073	0.0590	234	211	16.0	19.4	
5T19	Transverse Unnotched	0.4975	0.0591	233	211	19.5	19.3	
		Average		233	210	17.6	19.0	
5TN2	†Transverse Notched	0.2137	0.0609	210				
5TN6	Transverse Notched	0.1940	0.0600	216				
5TN9	Transverse Notched	0.2106	0.0616	209				
5TN10	Transverse Notched	0.2009	0.0617	213				
5TN19	Transverse Notched	0.2125	0.0613	211				
		Average		212				
								0.91

* Fractured shortly after yield. † $K_t \approx 6.3$

Table VI

Mechanical Properties of Titanium 6Al-4V (ELI) at -423° F

Specimen Number	Test Direction	Width (in.)	Thickness (in.)	F_{tu} (ksi)	(0.2%) F_{ty} (ksi)	(2.0 in.) Elongation (%)	Elastic Modulus ($\times 10^6$ psi)	Notch/Unnotched Ratio
6L1	Longitudinal Unnotched	0.4980	0.0638	250	243	2.0	19.1	
6L7	Longitudinal Unnotched	0.4980	0.0613	268	252	9.5	20.9	
6L10	Longitudinal Unnotched	0.4946	0.0626	253	242	2.0	20.6	
6L14	Longitudinal Unnotched	0.5035	0.0627	255	248	2.0	18.6	
6L19	Longitudinal Unnotched	0.5025	0.0619	256	246	2.0	20.9	
		Average		256	246	3.5	20.0	
6LN15	†Longitudinal Notched	0.2005	0.0616	194				
6LN16	Longitudinal Notched	0.1950	0.0609	200				
6LN17	Longitudinal Notched	0.2005	0.0613	197				
6LN18	Longitudinal Notched	0.2010	0.0620	197				
6LN19	Longitudinal Notched	0.2000	0.0620	201				
		Average		198				0.77
6T1	Transverse Unnotched	0.4970	0.0630	256	249	2.0	20.6	
6T6	Transverse Unnotched	0.5013	0.0591	253	251	1.0	18.4	
6T10	Transverse Unnotched	0.5022	0.0579	253	248	2.0	19.1	
6T14	Transverse Unnotched	0.5025	0.0615	255	248	3.0	19.2	
6T20	Transverse Unnotched	0.5048	0.0607	255	250	2.0	20.6	
		Average		254	249	2.0	19.6	
6TN2	†Transverse Notched	0.1957	0.0622	196				
6TN5	Transverse Notched	0.1955	0.0636	185				
6TN11	Transverse Notched	0.1980	0.0618	201				
6TN13	Transverse Notched	0.1973	0.0642	185				
6TN18	Transverse Notched	0.2015	0.0631	185				
		Average		190				0.75

† $K_t \approx 6.3$

Table VII

Mechanical Properties of 2219-T81 Aluminum Alloy at -423°F

Specimen Number	Test Direction	Width (in.)	Thickness (in.)	F_{tu} (ksi)	(0.2%) F_{ty} (ksi)	(2.0 in.) Elongation (%)	Elastic Modulus ($\times 10^6$ psi)	Notch/ Unnotched Ratio
9L1	Longitudinal Unnotched	0.4985	0.1231	94.5	67.8	16.0	15.0	
9L6	Longitudinal Unnotched	0.4992	0.1229	94.5	67.5	16.5		
9L9	Longitudinal Unnotched	0.4995	0.1228	94.9	67.3	16.5	11.6	
9L13	Longitudinal Unnotched	0.4952	0.1228	95.4	67.8	15.0	9.7	
9L20	Longitudinal Unnotched	0.5007	0.1227	93.6	66.4	15.5	11.3	
		Average		94.6	67.4	15.9	11.9	
9LN1	†Longitudinal Notched	0.1938	0.1225	86.9				
9LN6	Longitudinal Notched	0.1935	0.1223	85.7				
9LN13	Longitudinal Notched	0.1990	0.1220	87.7				
9LN17	Longitudinal Notched	0.2005	0.1228	84.6				
9LN20	Longitudinal Notched	0.2015	0.1228	86.3				
		Average		86.2				
								0.91
9T1	Transverse Unnotched	0.4988	0.1236	100	68.1	18.0	14.5	
9T6	Transverse Unnotched	0.4978	0.1234	100	67.2	15.0	13.2	
9T9	Transverse Unnotched	0.4985	0.1234	100	67.4	16.0	12.4	
9T13	Transverse Unnotched	0.4962	0.1238	101	67.4	14.5	12.4	
9T20	Transverse Unnotched	0.4978	0.1223	98.9	65.7	14.0	13.7	
		Average		100	67.2	15.5	13.2	
9TN1	†Transverse Notched	0.20[illegible]0	0.1222	84.0				
9TN6	Transverse Notched	0.1935	0.1221	83.9				
9TN13	Transverse Notched	0.1970	0.1225	86.7				
9TN17	Transverse Notched	0.1986	0.1225	85.0				
9TN20	Transverse Notched	0.2000	0.1231	87.4				
		Average		85.4				0.85

† $K_t \approx 6.3$

Table VIII
Mechanical Properties of 7039-T64 Aluminum Alloy at -423°F

Specimen Number	Test Direction	Width (in.)	Thickness (in.)	F_{tu} (ksi)	(0.2%) F_{ty} (ksi)	(2.0 in.) Elongation (%)	Elastic Modulus ($\times 10^6$ psi)	Notch/Unnotched Ratio
3L1	Longitudinal Unnotched	0.5015	0.1234	89.7	62.5	22.5	9.8	
3L6	Longitudinal Unnotched	0.5020	0.1224	89.6	61.6	23.0	8.9	
3L9	Longitudinal Unnotched	0.4996	0.1219	90.1	63.1	21.5	11.5	
3L13	Longitudinal Unnotched	0.5012	0.1220	89.2	61.6	19.5	9.6	
3L20	Longitudinal Unnotched	0.5005	0.1223	89.2	62.2	20.0	10.8	
		Average		89.6	62.2	21.0	10.1	
3LN1	† Longitudinal Notched	0.2068	0.1232	79.2				
3LN4	Longitudinal Notched	0.2063	0.1232	82.1				
3LN6	Longitudinal Notched	0.2057	0.1219	80.7				
3LN17	Longitudinal Notched	0.2086	0.1218	81.5				
3LN19	Longitudinal Notched	0.2087	0.1217	84.3				
		Average		81.6				
								0.91
3T1	Transverse Unnotched	0.4988	0.1232	93.3	63.3	16.5	9.5	
3T6	Transverse Unnotched	0.5017	0.1221	95.0	65.3	13.5	10.8	
3T9	Transverse Unnotched	.5004	0.1223	93.1	63.9	17.5		
3T13	Transverse Unnotched	0.5002	0.1218	93.0	65.5	18.5		
3T20	Transverse Unnotched	0.4990	0.1220	92.8	63.9	20.0	12.8	
		Average		93.4	64.4	17.0	11.0	
3TN1	† Transverse Notched	0.2052	0.1236	84.8				
3TN4	Transverse Notched	0.2057	0.1221	83.6				
3TN9	Transverse Notched	0.2077	0.1225	[illegible]				
3TN14	Transverse Notched	0.2045	0.1214	82.2				
3TN19	Transverse Notched	0.2085	0.1214	83.6				
		Average		82.6				
								.88

† $K_t \approx 6.3$

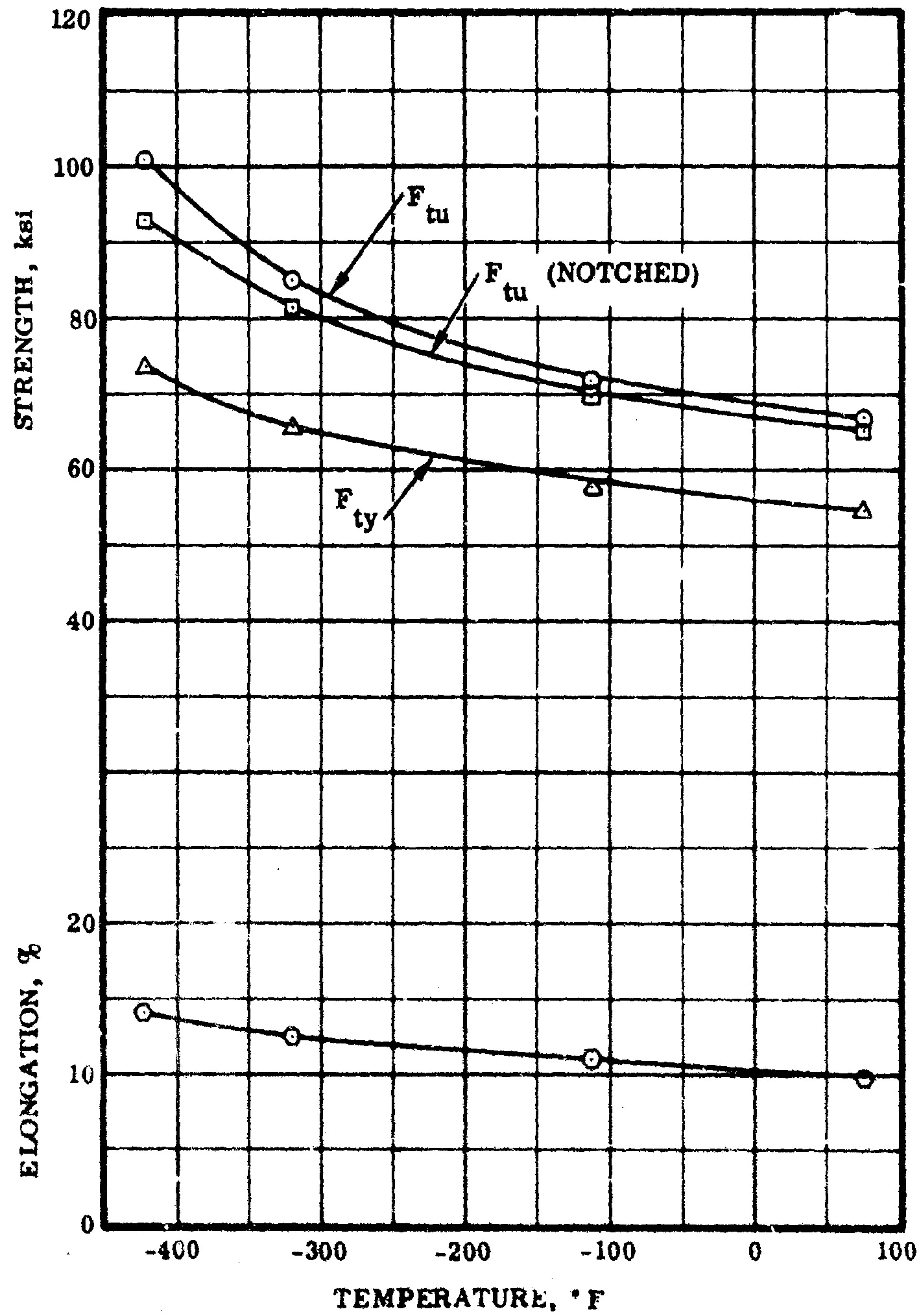

Figure 14. Variation of Mechanical Properties With Temperature for X2021-T8 E31 Aluminum Alloy (Longitudinal)

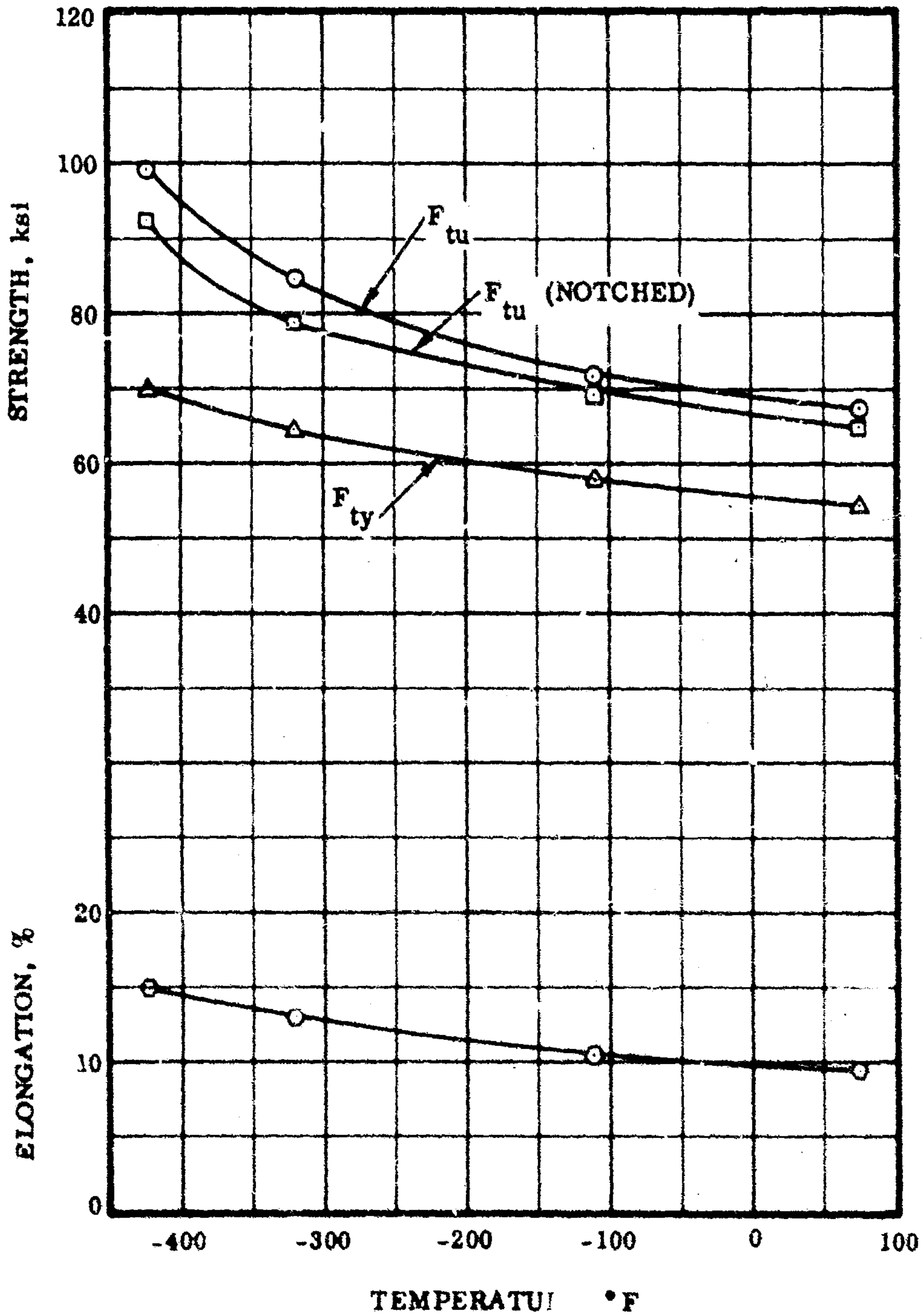

Figure 15 Variation of Mechanical Properties With Temperature for X2021-T8 E31 Aluminum Alloy (Transverse)

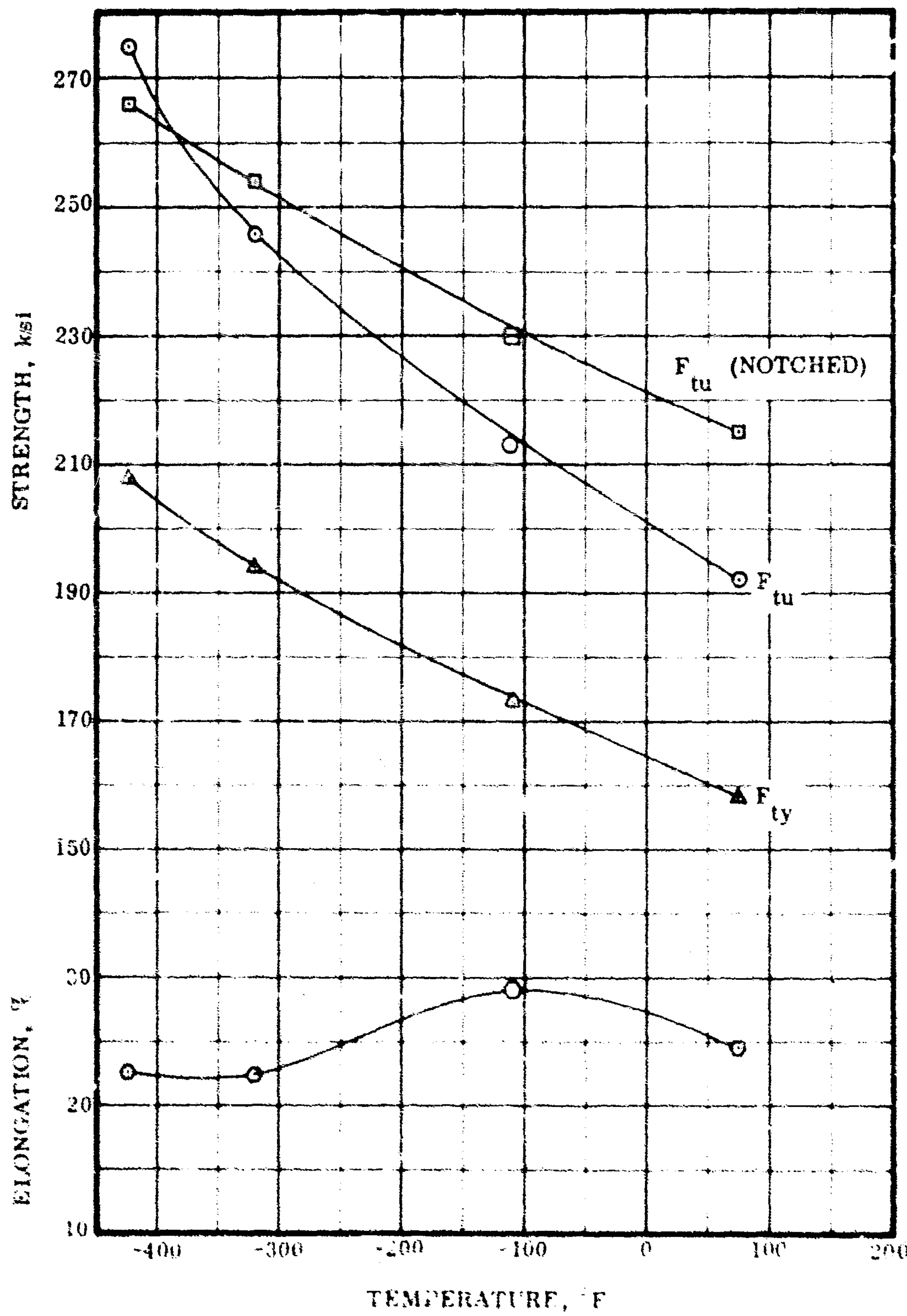

Figure 16. Variation of Mechanical Properties With Temperature for INCO 718 (Aged) (Longitudinal)

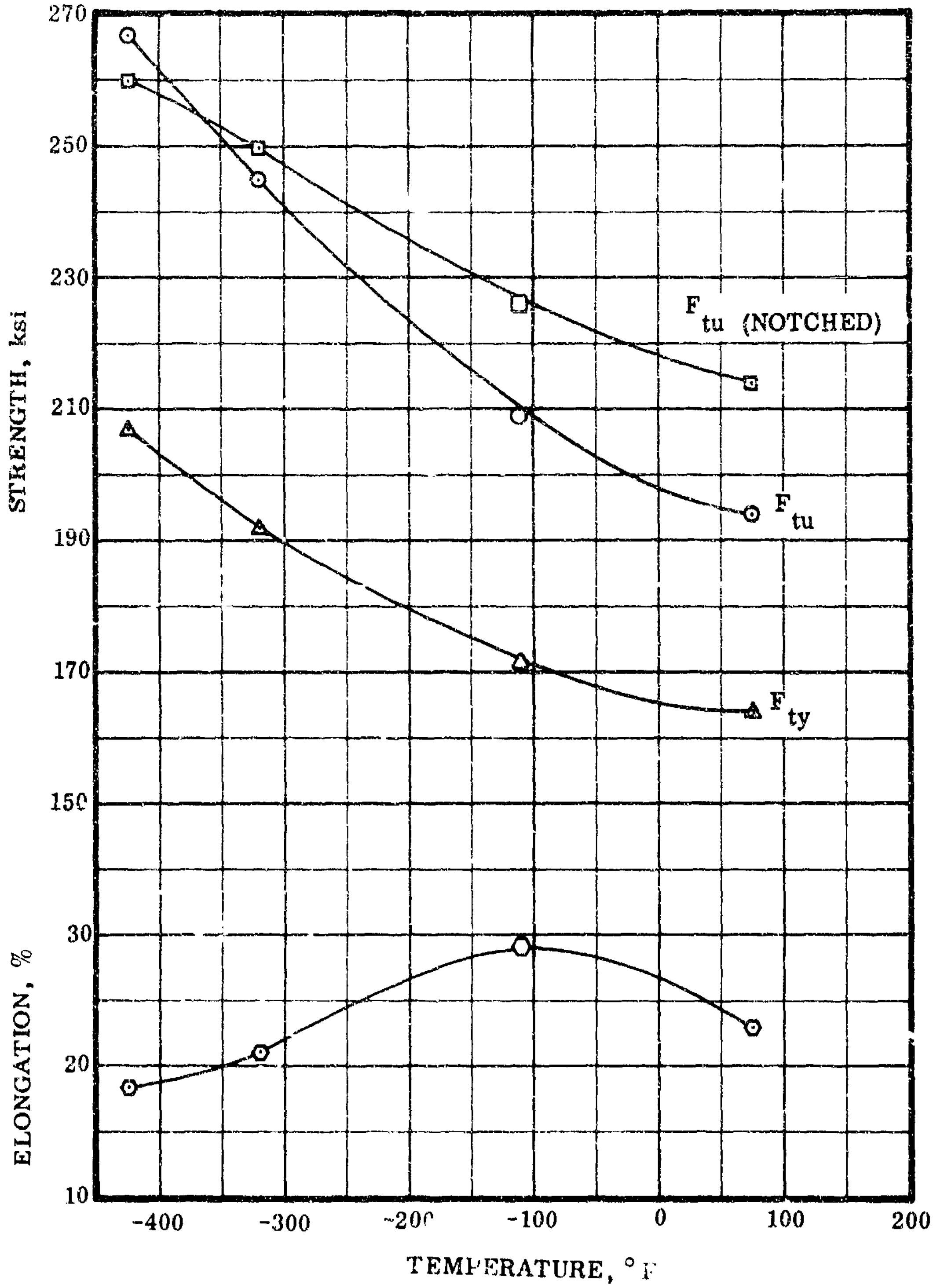

Figure 17. Variation of Mechanical Properties With Temperature for INCO 718 (Aged) (Transverse)

In similar manner, the longitudinal grain direction of the 7039-T64 was slightly weaker than the transverse. For this material, the yield strength and notch strength were also slightly higher for the transverse direction. However, the notch-unnotch ratio for the longitudinal direction was higher (0.91 versus 0.88) due to the larger differences in ultimate strengths. Again, the elongation was a good 10 to 11 percent.

This material appears to be slightly weaker and slightly more tough than the 7039-T6 reported by Christian, Yang, and Witzell (Reference 8).

2. FRACTURE MECHANICS. One of the basic objectives of this program was to determine if both K_{Ic} and K_c could be obtained from a single test specimen. At first glance, such a situation is impossible, since pure plane strain is a condition that excludes all plane stress and vice versa. However, it is conceivable that a material could be subject to pure plane strain as an initial condition, and then be acted upon by external forces that would cause a mixed mode (plane stress and plane strain). Assuming that a continually increasing load would cause redistribution of stresses by some reasonable phenomenon (such as orderly slow crack growth), it is then possible that plane stress could exist. There is little doubt that such a situation is improbable. Nevertheless, thin sheet materials are used quite frequently at cryogenic temperatures in the aerospace industry, and fracture data are critically needed. Meeting the exact requirements of various agencies (References 3, 5, and 9) is difficult in some cases and impossible in others. For example, if the recent criteria of Brown and Srawley (Reference 4) were used, the thicknesses shown below would be required for K_{Ic} test specimens.

For purposes of discussion, consider the results of this program with respect to the formula:

$$B = 2.5\left(\frac{K_{Ic}}{\sigma_{ys}}\right)^2$$

For the alloys in this program at -423°F:

	YIELD STRENGTH (ksi)	K_{Ic} (ksi $\sqrt{in.}$)	$\frac{K_{Ic}}{\sigma_{ys}}$	$\left(\frac{K_{Ic}}{\sigma_{ys}}\right)^2$	B (in.)
Titanium 5Al-2.5Sn	210	62	0.295	0.087	0.22
Titanium 6Al-4V	246	55	0.223	0.050	0.125
INCO 718	207	95	0.46	0.212	0.53
2021 Aluminum	73.8	36	0.487	0.237	0.59
2219 Aluminum	67.2	37.2	0.552	0.305	0.76
7039 Aluminum	64.4	31.6	0.49	0.24	0.60

The values shown were selected in such a manner as to provide a minimum value of the thickness (B). Even so, no material in this program approaches being acceptable according to these criteria. It is conceivable that it would be possible to test the titanium 6Al-4V ELI in 1/8-inch-thick material, but all the rest of the alloys would not qualify as sheet material, even if such thicknesses were useful in cryogenic pressure vessels.

In a recently published article (Reference 10) Brown and Srawley have added the requirement that the final crack length must also be greater than the thickness as calculated with the preceding equation. They have also suggested a method of determination of the load that is used for calculation of K_{Ic} that is cumbersome, but is systematic and seems consistent.

The determination of pop-in for the present program was derived by observation of the continuous load-deflection curve (see Figure 18). The criteria used were:

Determine if there is a definite jog in the load-deflection curve. Use the load value corresponding to this pop-in for calculation of plane strain fracture roughness. If the jog is substantially below the proportional limit, it is probably a false indication and the proportional limit should be used.

If there is no distinct pop-in, use the proportional limit for the plane strain fracture toughness calculation.

The vast majority of cases will be covered by these criteria. However, there are several other situations which can occur. All of these require some degree of engineering judgement. Infrequently, a load-deflection curve will be linear until failure occurs, in which case the ultimate load must be used. Occasionally, the proportional limit will be ill defined. In this case it is convenient to use an arbitrary offset line that is parallel to the lower portion of the curve or to use the secant method proposed by Brown and Srawley. In this program, engineering judgement was used to identify the proportional limit. Critical crack length was determined by measurement of the fractured surface after failure.

A few curves will deviate to both the left and right of the linear portion, making selection of pop-in or proportional limit extremely difficult. In these cases, it is prudent to examine the instrumentation for malfunctions and the fractured specimen for unusual fracture modes. After such examinations are exhausted without significant discoveries, it is necessary to evaluate the specific load-deflection curves with respect to other specimens of the same alloy tested under identical conditions. If such evaluation is fruitless, the test should be discarded.

a. Center Notched Tests. The fracture toughness of all alloys was examined using center notched (machine cut and fatigue pre-cracked) tensile specimens. Five each, longitudinal and transverse grain directions, were tested at -423° F for all alloys. In addition, five longitudinal and five transverse tests each were performed on

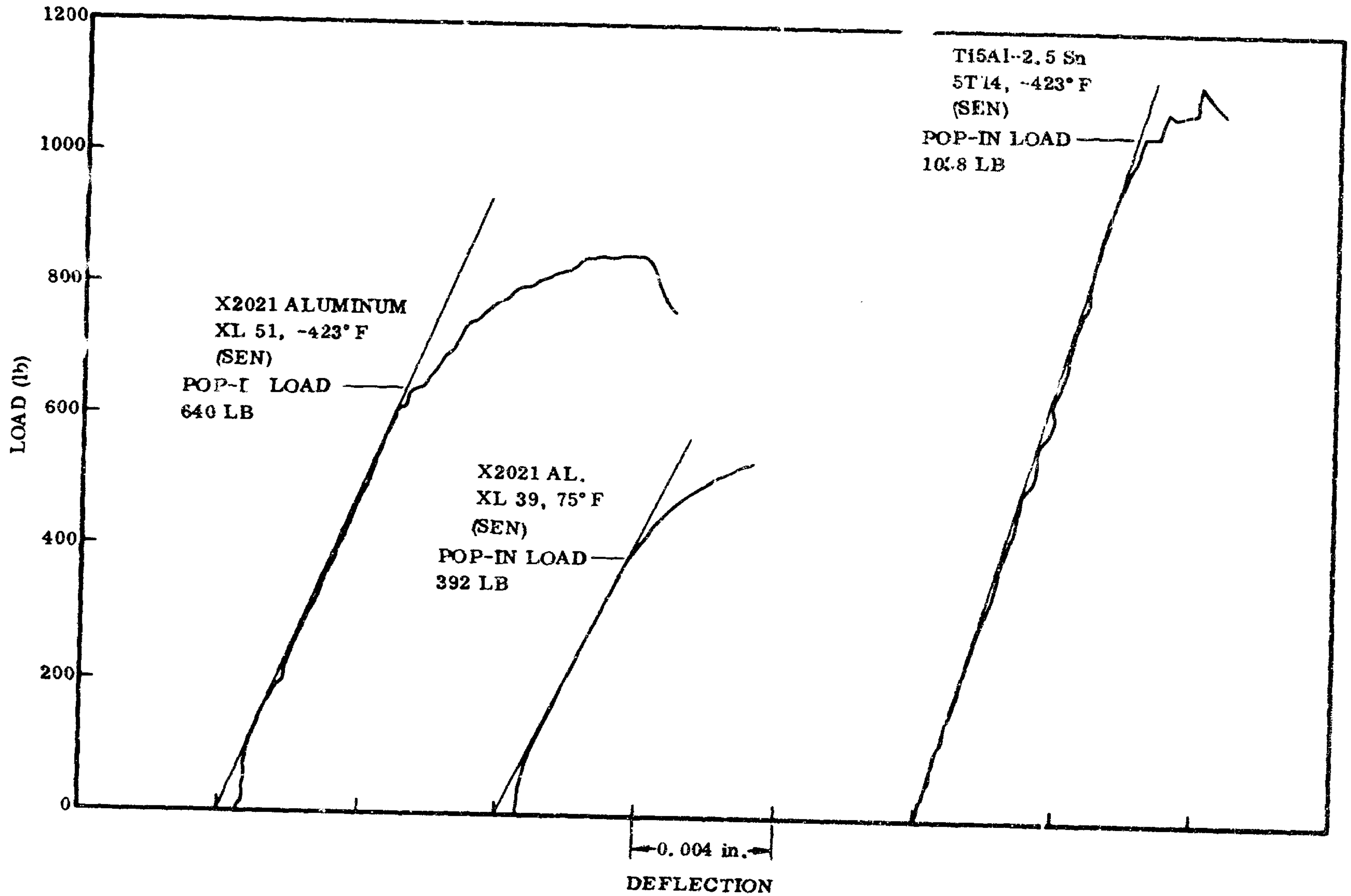

Figure 18. Representative Load-Deflection Curves

INCO 718 alloy at room temperature, -110°F, and -320°F. Three longitudinal and three transverse each of X2021 aluminum alloy specimens were tested at room temperature, -110°F, and -320°F for purposes of providing comparable values for the AFML testing program. As in the mechanical properties portion of this program, the other four alloys were tested at -423°F only.

Center notched data for INCO 718 are shown in Table IX. In some cases, center notched specimens failed through the loading pin hole (rather than through the center notch). In these tests, K_{Ic} was calculated but K_c was not, since no critical crack length was obtained.

Since the calculated K_{Ic} and K_c are both shown in a single table, some care must be used in selection of data. For example, the original crack length (including fatigue crack extension) is shown under the column designated "2a," while the final critical crack length is "$2a_c$." The pop-in load is designated as "P_p" and stresses associated with this load contain the subscript "p." The load at critical crack length is designated "P" but the gross stress and net fracture stress corresponding to this load are σ_G and σ_N respectively. The column headings K_{Ic}' and K_c' represent the uncorrected plane strain and plane stress respectively. Plastic zone corrections are a_1 and a_{c1} for plane strain and plane stress, respectively. Finally, corrected plane strain fracture toughness is designated K_{Ic} and corrected plane stress fracture toughness is K_c. (Refer to Section V for discussion of calculations.)

In all cases, the net stress at fracture for the INCO 718 center notch specimens exceeds the yield strength of the material. This would suggest that the specimen width is too small and that the K_c values are not valid. However, in all cases, the net stress at pop-in is significantly less than yield strength, which suggests valid plane strain fracture toughness data. For both plane stress and plane strain, however, the fracture toughness increases continuously with a decrease in temperature. In fact, the percentage increase in fracture toughness from room temperature to -423°F is about the same for K_c and K_{Ic} (Figures 19 and 20). (Notice that the curves for fracture toughness indicate the range of data points by horizontal bars superimposed on the average value curve.)

Test results indicate a large range of data (scatter) for INCO 718 at several test temperature points. The fact that the K_c values are not theoretically valid for the 3-inch-wide specimen was not unexpected for the INCO 718 material. Test results as reported previously (Reference 8) indicated that K_c values were not considered valid in a 4-inch-wide specimen tested at room temperature, -320°F, and -423°F. In that study, the net fracture stresses were somewhat lower for all test temperatures than the current studies. However, in all cases, the gross stresses for the 3-inch specimens tested in the current program were lower than those reported for the 4-inch specimens in the prior program. Uncorrected K_c' values were similar for the two programs.

Table IX

Plane Stress (K_c) and Plane Strain (K_{Ic}) Fracture Toughness for INCO 718 (Aged) Using Center Notched Specimens

Specimen Number	Test Direction	Test Temp. (°F)	Thickness, B (in.)	2a (in.)	Pop-in Load, P_p (k)	Yield Strength, σ_{ys} (ksi)	Max. Load, P (k)	$2a_c$ (in.)	K_{Ic}' (ksi $\sqrt{in.}$)	Pop-in Stress, σ_p (ksi)	Net Stress, σ_{pN} (ksi)	a_1 (Corrected) (in.)	K_{Ic} (Corrected) (ksi $\sqrt{in.}$)	K_c' (ksi $\sqrt{in.}$)	Gross Stress, σ_G (ksi)	Net Stress, σ_N (ksi)	a_{c1} (Corrected) (in.)	K_c (Corrected) (ksi $\sqrt{in}$)
ILC19	Long.	-423	0.0628	1.45	18.00	208.0	19.50	1.70	169.0	95.54	184.9	0.7607	175.5	199.2	103.5	238.9	0.9996	235.9
ILC17	Long.	-423	0.0600	1.46	17.00	208.0	19.175	1.67	167.9	94.44	184.0	0.7652	174.2	201.8	106.5	240.3	0.9896	239.4
ILC04	Long.	-423	0.0632	1.46	17.28	208.0	19.50	1.60	162.0	91.14	177.5	0.7628	167.5	187.7	102.8	220.4	0.9329	216.7
ILC12	Long.	-423	0.0645	1.43	17.76	208.0	20.20	*	157.4	90.28	170.0	0.7460	162.5		102.6			
ITC04	Trans.	-423	0.0638	1.52	15.12	207.0	18.20	1.80	145.6	79.26	161.2	0.7862	149.6	194.2	95.41	239.7	1.0409	229.6
ITC15	Trans.	-423	0.0635	1.46	15.60	207.0	19.60	1.65	145.6	81.89	159.5	0.7562	149.7	192.8	102.9	228.6	0.9638	224.7
ITC12	Trans.	-423	0.0640	1.50	15.75	207.0	19.68	1.70	148.9	82.03	164.1	0.7774	153.3	197.3	102.5	236.5	0.9954	232.5
ITC01	Trans.	-423	0.0635	1.45	16.40	207.0	18.96	1.66	152.3	86.09	166.9	0.7537	156.9	187.5	99.53	222.8	0.9613	216.7
ITC16	Trans.	-423	0.0639	1.49	15.36	207.0	19.30	1.72	144.7	80.13	159.2	0.7709	148.7	195.9	100.68	236.0	1.0033	230.56
ILC05	Long.	-320	0.0620	1.47	13.9	194.0	18.1	1.67	134.7	75.23	148.5	0.8117	146.1	186.1	97.96	222.9	0.9814	219.4
ILC01	Long.	-320	0.0636	1.48	15.5	194.0	18.6	1.70	146.0	81.24	160.3	0.8301	160.5	187.6	97.48	225.0	0.9989	221.9
ILC15	Long.	-320	0.0635	1.45	14.8	194.0	19.1	1.67	138.0	77.93	151.3	0.8055	150.2	190.8	100.6	227.9	0.9889	226.8
ILC03	Long.	-320	0.0635	1.48	13.0	194.0	18.6	1.67	122.6	68.24	134.7	0.8036	131.1	184.9	97.64	220.2	0.9796	217.2
ILC10	Long.	-320	0.0638	1.47	13.0	194.0	18.9	1.66	127.0	71.06	139.3	0.8032	136.4	186.1	98.75	221.1	0.9764	218.8
ITC19	Trans.	-320	0.0618	1.46	14.2	192.0	18.1	1.68	136.2	76.59	149.2	0.8101	148.1	185.9	97.63	221.9	0.9892	219.7
ITC03	Trans.	-320	0.0633	1.47	14.0	192.0	17.9	1.63	132.9	74.22	146.5	0.8113	144.1	176.4	94.89	209.5	0.9493	204.6
ITC07	Trans.	-320	0.0631	1.46	14.0	192.0	18.45	1.68	131.5	73.96	144.1	0.8047	142.2	185.6	97.46	221.5	0.9887	219.2
ITC04	Trans.	-320	0.0640	1.47	13.7	192.0	18.7	1.70	127.5	71.35	139.9	0.8052	137.3	187.5	97.40	224.8	1.0017	222.5
ITC11	Trans.	-320	0.0637	1.46	14.5	192.0	18.9	1.66	134.9	75.88	147.8	0.8086	146.5	186.3	98.90	221.4	0.9799	220.1
ILC14	Long.	-110	0.0639	1.47	13.5	173.0	17.8	1.56	126.4	70.66	139.0	0.8200	139.3	166.7	93.16	194.8	0.9278	195.6
ILC04	Long.	-110	0.0638	1.46	14.7	173.0	18.0	1.57	137.1	77.06	150.6	0.8300	152.4	169.7	94.36	198.7	0.9362	200.5
ILC18	Long.	-110	0.0623	1.48	14.2	173.0	17.3	1.60	136.5	75.98	150.0	0.8391	151.5	169.0	92.56	198.3	0.9518	199.4
ILC16	Long.	-110	0.0636	1.47	14.5	173.0	18.0	1.56	133.0	74.75	144.3	0.8291	146.6	165.0	92.79	189.9	0.9248	192.2
ILCD1	Long.	-110	0.0632	1.44	14.8	173.0	17.7	1.60	139.5	78.58	152.1	0.8220	154.3	171.9	93.98	202.9	0.9572	204.5
ITC10	Trans.	-110	0.0639	1.49	11.5	171.0	17.5	1.66	108.4	59.99	119.2	0.8089	115.9	172.0	91.29	204.4	0.9910	205.9
ITC14	Trans.	-110	0.0640	1.49	12.5	171.0	17.5	1.66	117.6	65.10	129.3	0.8203	127.3	171.7	91.15	204.1	0.9905	205.4
ITC20	Trans.	-110	0.0621	1.50	13.6	171.0	16.65	1.60	132.5	73.00	146.0	0.8456	146.6	163.1	89.37	191.5	0.9448	191.0
ITCD1	Trans.	-110	0.0642	1.40	14.6	171.0	18.9	1.56	130.6	75.80	142.1	0.7928	144.0	175.4	98.13	204.4	0.9474	210.3
ITCD2	Trans.	-110	0.0635	1.40	15.3	171.0	19.3	1.47	138.4	80.32	150.6	0.8042	154.4	172.7	101.3	198.7	0.8974	205.3
ILC08	Long.	+75	0.0633	1.44	11.4	160.0	17.1	1.50	103.5	59.05	111.9	0.7866	110.8	152.7	88.57	174.3	0.8950	177.6
ILCD2	Long.	+75	0.0639	1.50	12.5	160.0	16.65	1.55	118.9	65.42	131.3	0.8379	130.5	155.1	87.14	180.9	0.9246	182.3
ILC02	Long.	+75	0.0639	1.36	12.0	160.0	17.25	1.42	106.0	62.81	115.2	0.7499	114.1	150.1	90.29	171.9	0.8500	174.0
ILCD3	Long.	+75	0.0629	1.45	11.4	160.0	16.2	1.50	107.3	60.62	117.7	0.7966	115.7	149.3	86.14	172.9	0.8887	173.1
ILCD4	Long.	+75	0.0634	1.43	12.6	160.0	17.0	1.48	115.9	66.25	126.6	0.7986	126.6	153.2	89.38	176.4	0.8659	178.8
ITC08	Trans.	+75	0.0633	1.46	12.0	164.0	16.4	1.50	113.3	63.62	124.7	0.8060	122.8	150.9	86.94	175.1	0.8847	174.3
ITCD3	Trans.	+75	0.0620	1.47	11.25	164.0	16.2	1.52	108.1	60.48	118.6	0.8042	116.2	152.4	87.10	176.5	0.8975	176.5
ITCD4	Trans.	+75	0.0632	1.42	12.6	164.0	16.65	1.48	116.2	66.68	127.0	0.7899	126.4	151.2	98.11	174.5	0.8752	174.5
ITCD5	Trans.	+75	0.0622	1.43	12.3	164.0	16.35	1.48	115.4	65.92	126.0	0.7938	125.3	150.2	87.62	172.9	0.8735	173.0
ITCD6	Trans.	+75	0.0632	1.43	12.5	164.0	16.475	1.48	115.4	65.93	126.0	0.7938	125.3	148.9	86.89	171.5	0.8713	171.1

*Fractured thru pin hole.

Note: All K_{Ic} values shown in this table were obtained from nonstandard ASTM specimens.

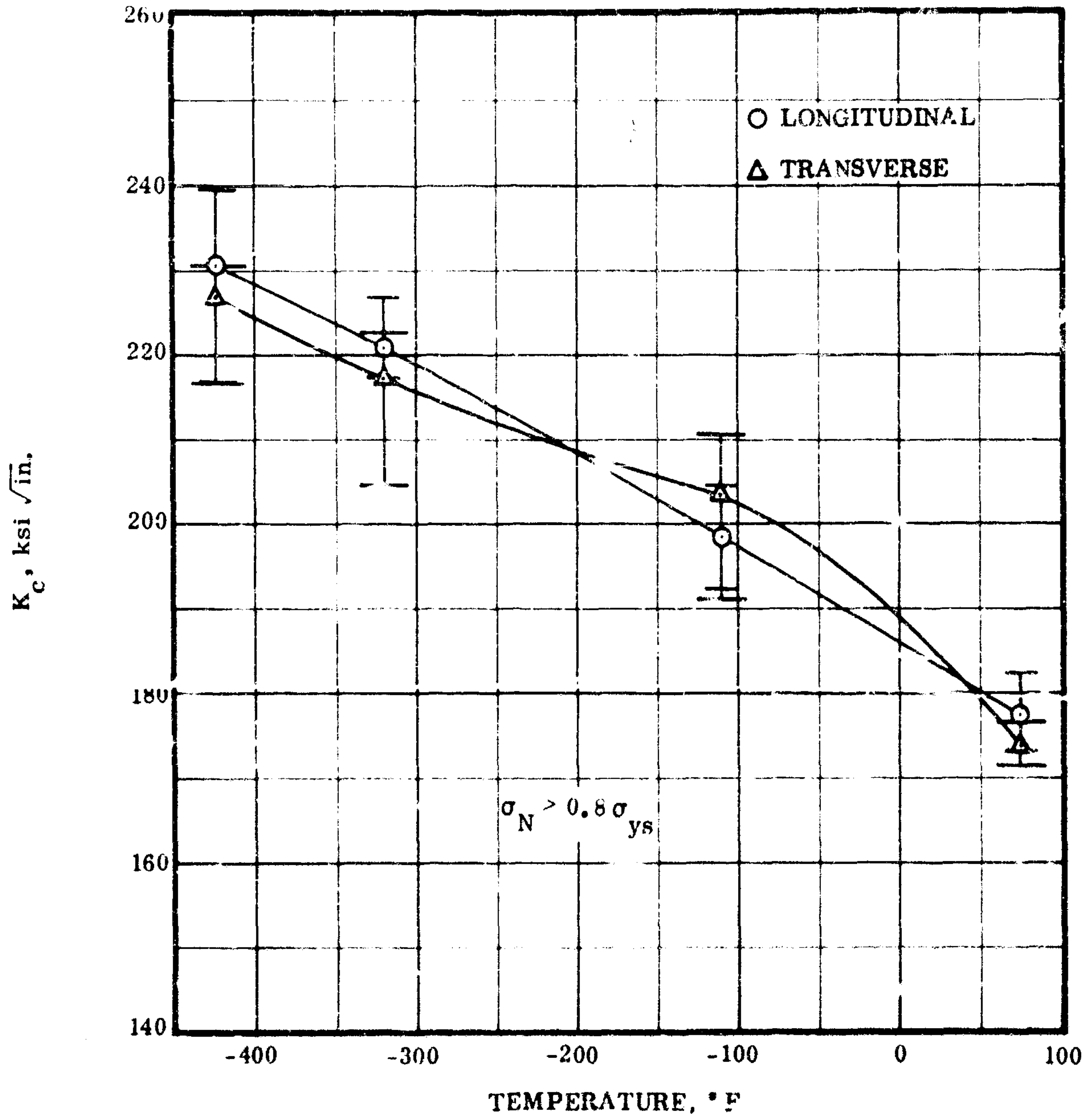

Figure 19. Variation of Plane Stress Fracture Toughness (K_c) With Temperature for INCO 718 (Aged) Using Center Notched (CN) Specimens

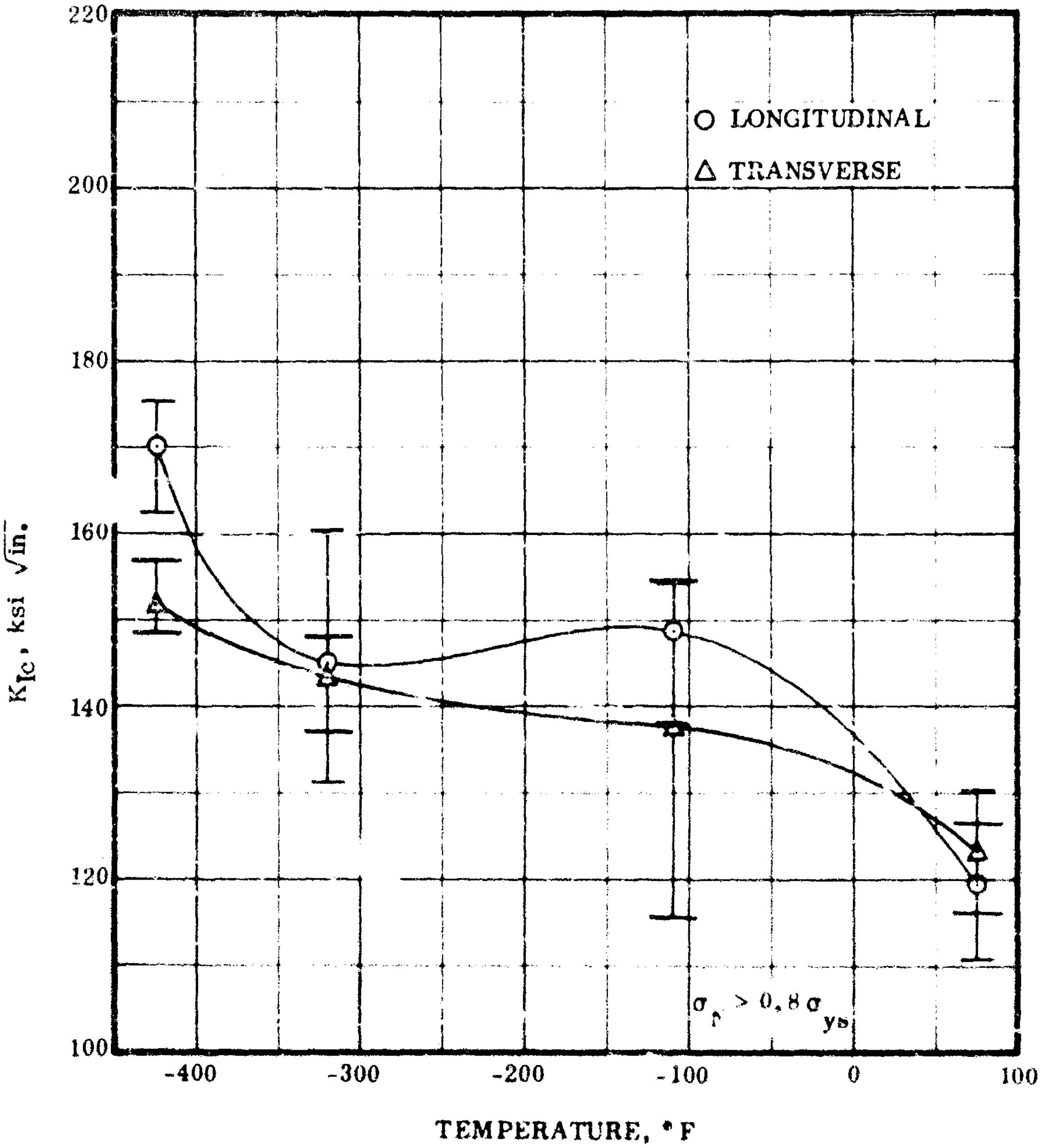

Figure 20. Variation of Pl·ne Strain Fracture Toughness (K_{1c}) With Temperature i.. INCO 718 (Aged) Using Center Notched (CN) Specimens

It appears that a 3-inch-wide specimen is not wide enough for acceptable plane stress fracture toughness values. From a net strength to yield strength relationship, however, it appears that acceptable plane strain fracture toughness data can be obtained from such a specimen. (Note that only four longitudinal specimens were tested at -423°F. Two other specimens failed through the pin holes during fatigue crack extension.)

The maximum net fracture stress for X2021-T8 E31 ranges from 82 to 102 percent of yield strength (average values) for the same size specimen. This ratio increases continuously from room temperature to -423° F (Table X). At the same time, all other values (net and gross stress, K_c) increase as the temperature decreases. A fairly large amount of scatter in K_c was observed at -110°F for this material due to differences in the maximum load (Figure 21). (It should be remembered that only three specimens were tested at each test temperature — and grain direction — except at -423°F where five specimens — each — were tested.) (See Figure 22.)

Again, as in the case of INCO 718, the net stress at pop-in is well below the yield strength of the material. At -423°F, the transverse K_c is greater than the longitudinal due to large critical crack length. However the K_{Ic} values are reversed at this temperature. Again the data scatter is fairly large and since only three specimens were tested at most temperatures, it is risky to make use of average values.

Scatter in fracture data is not uncommon. In the round robin testing performed for the ASTM and reported by Heyer (Reference 3), various laboratories reported scatter in notched strength (both edge notched and center notched tests) that frequently exceeded 25 percent. In view of such widespread scatter, the data presented in this program appear to be better than the majority of the data obtained in the ASTM program.

As in the tensile testing program, the rest of the alloys were tested at -423° F only, which made evaluation quite difficult. Nevertheless, it is possible to consider the relative merits of plane stress and plane strain for each alloy at one temperature.

As in the other alloys, the net fracture stress of the 2219-T81 aluminum was greater than the yield strength at -423° F (Table XI). Again, the net stress at pop-in was below the yield strength of the material. Eitman and Rawe of Douglas report plane stress fracture toughness for 2219-T87 aluminum alloy (transverse) 0.063-inch-thick, 16-inch-wide center cracked specimens of about 90 ksi $\sqrt{in.}$ and net fracture stresses of about 42 ksi. At the same time, the gross stress reported (26 ksi) was also somewhat less than the gross stress observed in the 3-inch-wide specimens of the current program. Others (Reference 5) report uncorrected K_c values of 65 ksi $\sqrt{in.}$ for 0.063-inch sheet at -423° F.

The corrected K_{Ic} values average between 50 and 55 ksi $\sqrt{in.}$ with about a 10-percent scatter. It should be noted here that one each longitudinal and transverse specimens (No. 9LC-14 and 9TC) are designated as calibration specimens. These tests (and

Table X

Plane Stress (K_c) and Plane Strain (K_{Ic}) Fracture Toughness for X2021-T8 E31 Aluminum Alloy Using Center Notched (CN) Specimens

Specimen Number	Test Direction	Test Temp. (°F)	Thickness, B (in.)	2a (in.)	Pop-in Load, P_p (k)	Yield Strength, σ_{ys} (ksi)	Max. Load, P (k)	$2a_c$ (in.)	K_{Ic}' (ksi$\sqrt{in.}$)	Pop-in Stress, σ_p (ksi)	Net Stress, σ_{pN} (ksi)	a_1 (Corrected) (in.)	K_{Ic} (Corrected) (ksi$\sqrt{in.}$)	K_c' (ksi$\sqrt{in.}$)	Gross Stress, σ_G (ksi)	Net Stress, σ_N (ksi)	a_{c1} (Corrected) (in.)	K_c (Corrected) (ksi$\sqrt{in.}$)
XLC20	Long.	-423	0.0623	1.33	4.6	73.80	6.88	1.36	40.70	24.53	43.95	0.7134	42.83	59.00	36.69	66.93	0.7317	63.62
XLC16	Long.	-423	0.0630	1.43	4.00	73.80	7.000	1.55	37.04	21.16	40.44	0.7551	38.63	65.65	37.04	76.63	0.9017	73.40
XLC17	Long.	-423	0.0628	1.34	4.80	73.80	6.500	1.40	42.53	25.49	46.04	0.7228	44.96	56.70	34.50	64.60	0.7940	62.58
XLC11	Long.	-423	0.0627	1.30	5.15	73.80	6.890	1.40	44.73	27.38	48.32	0.7085	47.59	60.20	36.63	68.68	0.8659	67.25
XLC14	Long.	-423	0.0638	1.30	4.60	73.80	7.000	1.40	39.27	24.03	42.41	0.6651	41.19	60.11	36.57	68.57	0.8056	67.15
XTC16	Trans.	-423	0.0630	1.44	4.135	70.30	6.360	1.62	38.66	21.95	42.35	0.7681	40.66	62.36	33.76	73.69	0.9352	71.49
XTC07	Trans.	-423	0.0632	1.36	4.02	70.30	6.700	1.63	35.62	21.13	38.53	0.7209	37.18	65.93	35.22	77.95	0.9650	76.86
XTC17	Trans.	-423	0.0633	1.42	4.20	70.30	6.400	1.70	38.67	22.19	42.26	0.7582	40.68	65.17	33.81	78.38	0.9868	76.04
XTC14	Trans.	-423	0.0628	1.32	4.40	70.30	6.500	1.47	38.72	23.43	41.95	0.7083	40.76	59.08	34.62	69.09	0.8474	66.53
XTC13	Trans.	-423	0.0655	1.34	4.55	70.30	6.450	1.45	38.96	23.31	42.36	0.7189	41.04	55.85	33.04	64.36	0.8255	62.12
XLC25	Long.	-320	0.0633	1.36	4.51	65.8	6.080	1.41	40.23	23.83	43.71	0.7395	42.93	53.12	32.12	60.79	0.8057	59.25
XLC22	Long.	-320	0.0634	1.39	4.10	65.8	5.96	1.47	36.94	21.56	40.17	0.7452	38.94	53.43	31.34	61.44	0.8399	59.67
XLC29	Long.	-320	0.0629	1.35	4.30	65.8	6.11	1.42	38.39	22.86	41.68	0.7292	40.65	54.27	32.65	62.18	0.8183	60.83
XTC21	Trans.	-320	0.0630	1.34	4.41	64.7	5.85	1.40	38.95	23.33	42.17	0.7277	41.39	50.8	30.95	58.04	0.7981	56.40
XTC22	Trans.	-320	0.0632	1.35	4.32	64.7	6.00	1.42	38.23	22.78	41.43	0.7306	40.54	52.56	31.65	60.09	0.8150	58.69
XTC23	Trans.	-320	0.0632	1.35	3.65	64.7	5.750	1.42	32.43	19.32	35.22	0.7150	33.84	50.58	30.43	57.95	0.8073	56.04
XLC23	Long.	-110	0.0622	1.36	4.50	58.2	5.425	1.41	40.46	23.97	43.96	0.7569	43.87	47.77	28.89	54.57	0.8122	53.49
XLC24	Long.	-110	0.0624	1.39	4.25	58.2	5.125	1.42	38.30	22.34	41.64	0.7639	41.17	44.75	26.95	51.16	0.8041	49.40
XLC26	Long.	-110	0.0631	1.36	4.25	58.2	5.050	1.40	38.03	22.53	41.32	0.7479	40.85	44.03	26.77	50.33	0.7911	48.46
XTC24	Trans.	-110	0.0632	1.31	3.65	58.1	5.22	1.36	31.62	19.25	34.17	0.7021	33.24	44.30	27.53	50.36	0.7725	48.83
XTC25	Trans.	-110	0.0632	1.35	3.75	58.1	5.2	1.40	33.32	19.84	36.18	0.7274	35.22	45.26	27.32	51.75	0.7966	50.11
XTC26	Trans.	-110	0.0628	1.30	4.35	58.1	5.55	1.32	37.58	23.01	40.51	0.7166	40.31	46.22	29.36	52.29	0.7607	51.38
XLC	Long.	+75	0.0633	1.27	3.67	54.6	4.99	1.39	31.20	19.39	33.71	0.6870	32.98	41.12	26.36	46.65	0.7403	45.24
XLC30	Long.	+75	0.0629	1.27	3.85	54.6	4.7	1.41	32.93	20.47	35.59	0.6929	35.03	41.32	24.99	47.29	0.7962	45.48
XLC40	Long.	+75	0.0629	1.36	3.25	54.6	4.88	1.40	28.77	17.15	31.30	0.6911	29.58	38.92	25.75	48.14	0.7810	45.80
XTC29	Trans.	+75	0.0624	1.32	3.70	54.5	4.675	1.35	32.51	19.70	35.09	0.7166	34.51	39.81	24.89	45.13	0.7599	43.52
XTC23	Trans.	+75	0.0638	1.35	3.65	54.5	4.65	1.37	31.87	19.01	34.46	0.7294	33.74	39.14	24.21	44.44	0.7671	42.65
XTC30	Trans.	+75	0.0622	1.39	3.75	54.5	4.42	1.42	34.44	20.10	37.45	0.7586	36.82	39.34	23.89	44.98	0.7929	42.92

Note: All K_{Ic} values shown in this table were obtained from nonstandard ASTM specimens.

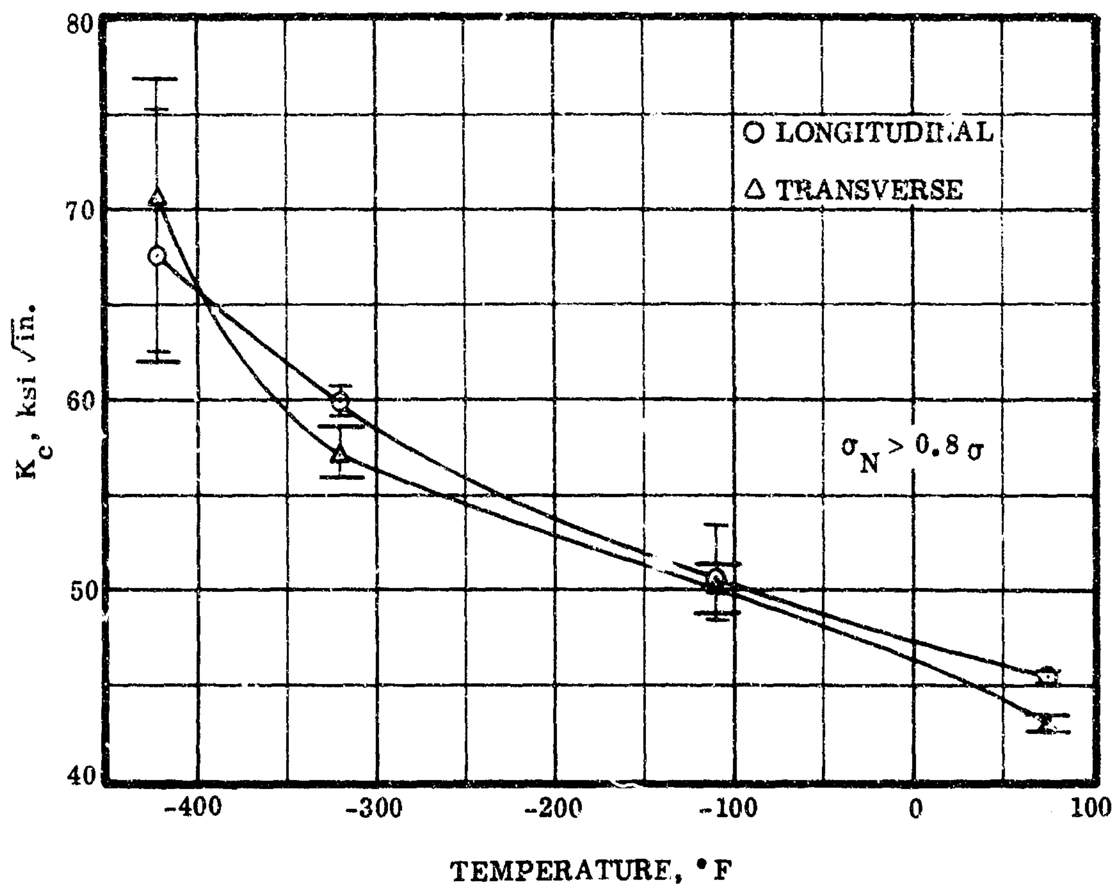

Figure 21. Variation of Plane Stress Fracture Toughness (K_c) With Temperature for X2021-T8 E31 Aluminum Alloy Using Center Notched (CN) Specimens

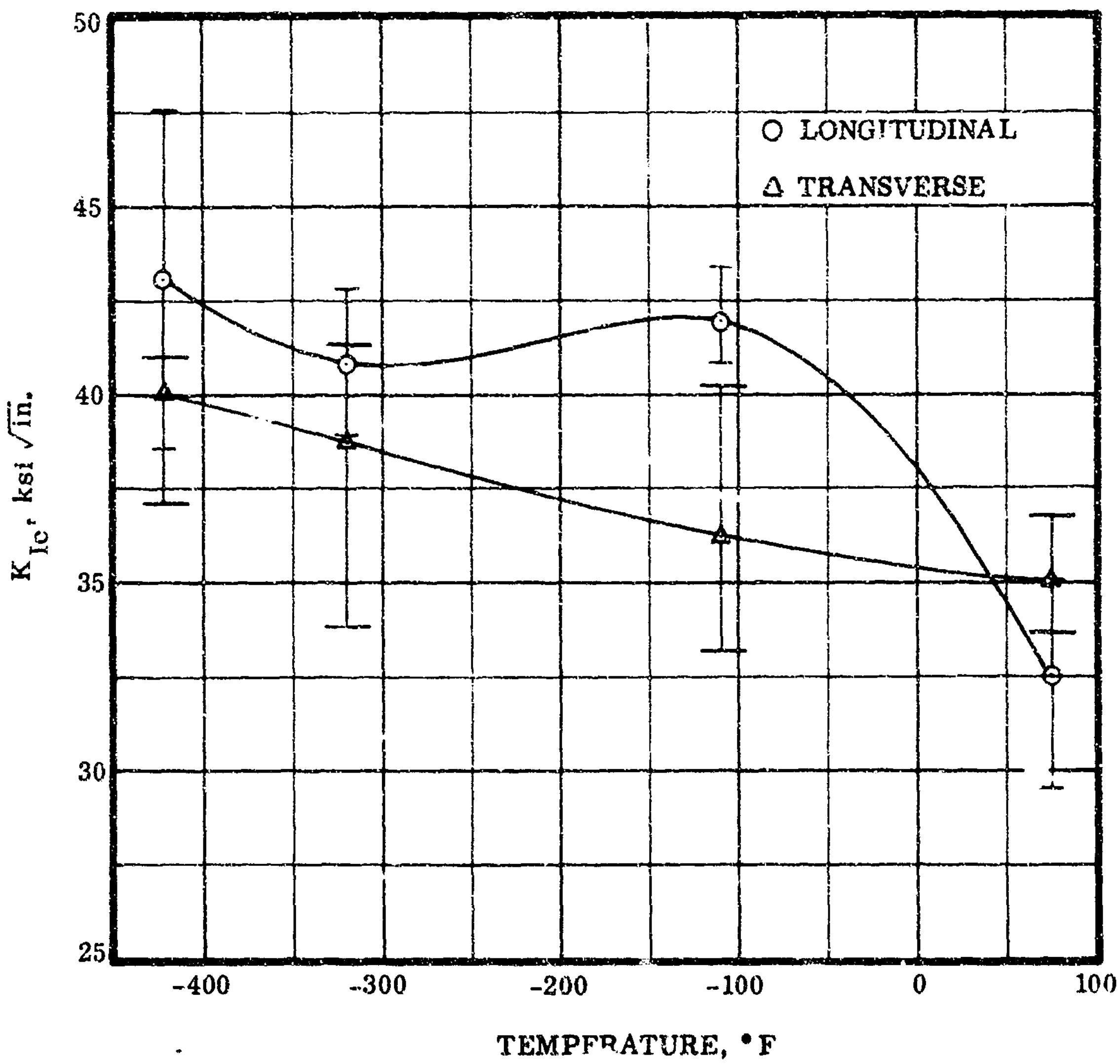

Figure 22. Variation of Plane Strain Fracture Toughness (K_{Ic}) With Temperature for X2021-T8 E31 Aluminum Alloy Using Center Notched (CN) Specimens

others for the titanium and 7039 aluminum alloys) were handled somewhat differently with regard to center notch preparation. The calibration specimens were not fatigue cracked prior to test. Instead, the electrical discharge notch was cut to a shorter original length. A given static load was applied to the specimen and a load-deflection trace was obtained. The specimen was then removed from the test machine and the notch length was increased by electrical discharge machining. The specimen was returned to the test machine, the previous load was applied, and a new load-deflection curve was obtained. This procedure was repeated until three curves were obtained. At that point, the machine notch was extended one more time and the specimen was tested to failure as in the other center notched tests. Consequently, four curves were obtained that reflected compliance variation with notch length. In most cases, the final K_{Ic} and K_c values obtained from the machine notched specimens are greater than those obtained from the fatigue crack extended specimens. It must be concluded that machine notching provides an artificially high fracture toughness value and either: 1) should be discarded, or 2) K_{Ic} should be modified downward to avoid unconservative answers.

Furthermore, at -423°F such a calibration is no simple task. At least one test to failure must be performed prior to calibrating in order to establish a suitable load. If the selected load is too low, the output of the compliance gage will be so small that large errors are highly probable. If the load is too large, premature crack extension or even failure can result.

Prior to embarking on the fracture mechanics testing in this program, Convair division made a number of pilot tests on similar materials (same alloys but different heats and/or thicknesses) to study the calibration problem. In order to overcome the problem of comparing a machine notched calibration curve to a fatigue cracked static specimen, a slightly different technique was used. Center notched (and several SEN) specimens were prepared with a short electrical discharge machined notch that was extended by fatigue cracking. At this point, the regular calibration technique was followed except that subsequent crack enlargement was performed by fatigue cycling (at room temperature) instead of machine notching. The results were quite erratic. The compliance of a fatigue cracked specimen was less than for a machine notched specimen, resulting in a difficult measurement problem. Frequently it appeared that the compliance with a larger crack length was less than the shorter crack length (but not consistently so). Two possible explanations for this anomaly are: 1) the noise in the instrumentation exceeded the output due to compliance, and 2) the material changed due to fatigue cycling. Another difficulty resulted from the problems associated with detection and characterization of the fatigue crack itself. It was not possible to be absolutely sure of the visually detected crack length until after fracture of the specimen. Even then, only the final fatigue growth could be determined with accuracy. Electron microscopy was used to evaluate the fatigue growth with some success, but determination of sequential crack lengths was impossible. (Typical electron fractographs are shown in Appendix II of this report.)

Although this experiment was not totally successful, the possibility of adequate fatigue crack growth calibration should not be abandoned. The machine notch calibration technique is incompatible with fatigue crack extended specimens. Subsequent to these experiments, Convair division has achieved some success with determination of crack lengths utilizing sophisticated nondestructive testing equipment. This technique is expensive and time consuming but does offer a glimmer of hope for the future.

The net fracture stress of the 7039-T64 aluminum alloy exceeded the yield strength of the material in virtually all tests (Table XI). As in all other materials tested, the net stress at pop-in was well below the yield strength of the material at -423° F. Again the calibration test specimens (3LC-04, 3TC-03) provided significantly higher plane strain fracture toughness values although the K_c values were somewhat lower than the average.

The plane strain fracture toughness values are in general agreement with D'Annessa (Reference 11) who tested 7039-T6, 0.160-inch plate at liquid helium temperature.

Others have reported values of less than 50 ksi $\sqrt{in.}$ (uncorrected for plastic zone) at -423°F (Reference 8), using a 4-inch-wide center notched specimen. The same report showed that K_c increases with an increase in specimen width up to 18 inches at room temperature. If these data may be extrapolated to -423° F, the 3-inch-wide specimen should show a lower K_c. Since it did not, it appears that the T64 temper is tougher than T6.

The two titanium alloys were the only materials tested in the center notched program whose net fracture stresses were significantly below yield strength at -423°F (Table XI). Nevertheless, the calibration test specimens provided higher fracture toughness values than the other specimens in the groups. The Ti 5Al-2.5Sn (ELI) material shows higher K_c and K_{Ic} values than does the Ti 6Al-4V (ELI) at this test temperature.

Eitman and Rawe report comparable K_c values (from 89 to 102 ksi $\sqrt{in.}$) for 0.020-inch-thick, 16-inch-wide Ti 5Al-2.5Sn (ELI) sheet at -423° F.

b. Single Edge Notch (SEN) Tests. SEN tests were performed at the same test temperatures as were the center notched and mechanical properties tests as follows:

(1) INCO 718 (aged). Room temperature, -110° F, -320° F, -423° F. Five each, longitudinal and transverse at each temperature.

(2) X2021-T8 E31 Aluminum Alloy. Room temperature, -110° F, -320° F, -423° F. Three each longitudinal and transverse at each temperature.

(3) All Other Alloys. -423°F only. Five each longitudinal and transverse at one temperature.

Table XI

Plane Strain (K_{Ic}) and Plane Stress (K_c) Fracture Toughness for Center Notched (CN) Specimens at -423° F

Specimen Number	Test Direction	Thickness, B (in.)	2a (in.)	Pop-in Load, P_p (k)	Yield Strength, σ_{ys} (ksi)	Max. Load, P (k)	$2a_c$ (in.)	K_{Ic}' (ksi $\sqrt{in.}$)	Pop-in Stress, σ_p (ksi)	Net Stress, σ_{pN} (ksi)	a_1 Corrected (in.)	K_{Ic} Corrected (ksi $\sqrt{in.}$)	K_c' (ksi $\sqrt{in.}$)	Gross Stress, σ_G (ksi)	Net Stress, σ_N (ksi)	a_{c1} Corrected (in.)	K_c Corrected (ksi $\sqrt{in.}$)
2219-T81 Aluminum Alloy																	
9LC11	Long.	0.1220	1.32	10.50	67.4	13.25	1.65	46.27	28.13	49.46	0.7350	50.01	66.04	35.49	77.03	0.9778	77.81
9LC13	Long.	0.1220	1.39	10.50	67.4	12.40	1.66	49.17	28.69	53.46	0.7797	53.74	63.83	33.83	75.85	0.9728	74.77
* 9LC14	Long.	0.1220	1.43	11.475	67.4	13.20	1.67	55.11	31.46	60.29	0.8214	61.64	68.63	36.19	81.97	1.000	82.69
9LC15	Long.	0.1220	1.40	9.30	67.4	12.05	1.66	43.78	25.41	47.64	0.7671	46.97	62.03	32.92	73.71	0.9648	71.98
9LC20	Long.	0.1222	1.40	11.40	67.4	12.70		53.58	31.10	58.31	0.8006	59.54		34.64			
9TC06	Trans.	0.1250	1.40	9.60	67.2	11.60	1.70	44.11	25.60	46.00	0.7686	47.39	59.54	30.93	71.38	0.9749	68.4
9TC07	Trans.	0.1225	1.38	10.30	67.2	11.90	1.68	47.78	28.03	51.90	0.7705	51.99	61.66	32.38	73.59	0.9740	71.56
* 9TC10	Trans.	0.1230	1.43	11.25	67.2	12.00	1.70	53.36	30.49	58.26	0.8154	59.29	62.59	32.52	75.05	0.9881	73.08
9TC11	Trans.	0.1218	1.27	11.35	67.2	13.00	1.66	49.26	30.70	52.80	0.7205	53.89	65.97	35.17	77.62	0.9834	77.99
9TC20	Trans.	0.1220	1.45	9.40	67.2	10.80	1.70	45.43	25.68	49.71	0.7977	49.03	56.80	29.51	68.10	0.9637	64.43
7039-T64 Aluminum Alloy																	
3LC01	Long.	0.1220	1.37	9.55	62.20	11.40	1.75	44.25	26.09	48.02	0.7655	48.15	61.58	31.15	74.75	1.031	73.77
* 3LC04	Long.	0.1224	1.43	11.10	62.20	12.20	1.80	52.91	30.23	57.76	0.8302	59.72	67.51	33.22	83.06	1.098	84.76
3LC05	Long.	0.1220	1.34	9.60	62.20	9.60	1.67	43.78	26.23	47.40	0.7488	47.57	49.68	26.23	59.16	0.9365	55.52
3LC09	Long.	0.1210	1.34	9.65	62.20	11.25	1.74	44.37	26.58	48.04	0.7510	48.32	60.95	30.99	73.79	1.023	72.65
3LC15	Long.	0.1215	1.18	11.35	62.20	12.70	1.77	47.66	31.14	51.33	0.6835	52.72	69.65	34.84	84.98	1.085	88.52
3TC01	Trans.	0.1222	1.38	9.35	64.40	10.90	1.90	43.48	25.51	47.23	0.7626	46.92	63.91	29.73	81.09	1.107	77.92
3TC02	Trans.	0.1221	1.35	10.00	64.40	11.30	1.95	45.81	27.30	49.64	0.7555	49.86	68.26	30.85	88.14	1.1[illegible]4	86.76
* 3TC03	Trans.	0.1228	1.43	10.60	64.40	12.00	1.62	50.36	28.77	54.98	0.8123	55.78	60.09	32.57	70.81	0.9486	69.89
3TC05	Trans.	0.1228	1.36	9.30	64.40	11.40	1.88	42.98	25.53	46.32	0.7509	46.27	64.74	30.64	80.73	1.101	78.81
3TC06	Trans.	0.1218	1.19	11.00	64.40	12.00	1.90	46.53	30.10	49.90	0.6774	50.64	70.59	32.84	89.57	1.141	90.56
Titanium 5 Al-2.5Sn (ELI)																	
5LC01	Long.	0.0602	1.25	9.90	213.00	10.400	1.50	87.19	54.82	93.97	0.6517	89.73	99.74	57.59	115.2	0.7849	103.5
5LC04	Long	0.0612	1.18	9.30	213.00	10.600	1.55	77.53	50.65	83.49	0.6111	79.35	102.7	57.73	119.5	0.8120	106.7
5LC12	Long.	0.0604	1.19	9.25	213.00	9.750	1.50	78.57	51.05	84.61	0.6167	80.46	93.20	53.81	107.6	0.7805	96.22
* 5LC06	Long.	0.0615	1.46	9.45	213.00	13.25	1.60	91.07	51.22	99.78	0.7591	93.89	131.1	71.82	153.9	0.8603	139.8
5LC18	Long.	0.0610	1.20	9.10	213.00	9.35	1.45	76.96	49.73	82.88	0.6208	78.73	96.21	51.09	98.89	0.7511	88.59
5TC01	Trans.	0.0610	1.20	8.50	210.00	10.10	1.45	71.89	46.45	77.41	0.6186	73.37	83.74	55.19	94.4	0.6503	86.03
5TC05	Trans.	0.0612	1.19	8.85	210.00	10.30	1.19	74.19	48.20	79.89	0.6149	75.83	82.37	56.10	92.98	0.8195	84.61
* 5TC05	Trans.	0.0600	1.46	9.00	210.00	12.50	1.60	89.28	50.17	98.04	0.7588	92.02	127.5	69.68	140.9	0.8565	135.5
5TC14	Trans.	0.0610	1.18	9.00	210.00	10.20	1.60	75.28	49.18	81.07	0.6105	76.99	101.7	55.74	119.4	0.8374	105.8
5TC16	Trans.	0.0602	1.18	9.05	210.00	10.00	1.60	76.70	50.11	82.60	0.6112	78.51	101.1	55.37	118.7	0.8369	105.1
Titanium 6 Al-4V (ELI)																	
* 6LC04	Long.	0.0614	1.45	8.28	246.00	10.60	1.55	79.51	44.95	87.00	0.7416	80.90	96.53	54.29	112.3	0.7995	99.04
6LC02	Long.	0.0585	1.34	7.10	246.00	9.200	1.70	67.53	40.46	73.11	0.6820	68.39	100.9	52.42	121.0	0.8768	103.9
6LC16	Long.	0.0611	1.40	7.25	246.00	9.500	1.65	67.31	39.16	72.80	0.7119	69.16	95.82	51.31	112.67	0.8191	98.28
6LC01	Long.	0.0615	1.38	6.90	246.00	9.200	1.46	63.76	37.40	69.26	0.7007	64.48	84.58	49.86	97.14	0.7488	88.26
6LC14	Long.	0.0618	1.37	8.15	246.00	9.[illegible]	1.58	74.55	43.96	80.91	0.6996	75.71	91.58	50.70	107.1	0.8121	93.73
* 6TC04	Trans.	0.0609	1.45	7.00	249.00	10.00	1.52	67.77	38.31	74.16	0.7368	68.61	95.80	54.73	110.9	0.7836	96.20
6TC10	Trans.	0.0618	1.39	6.70	249.00	9.015	1.53	61.93	36.14	67.34	0.7048	62.58	85.55	48.62	99.43	0.7638	87.26
6TC20	Trans.	0.0621	1.37	6.00	249.00	8.200	1.47	63.27	36.19	74.32	0.6953	64.05	87.52	49.46	110.0	0.7543	89.60
6TC13	Trans.	0.0615	1.36	6.30	249.00	8.150	1.53	65.42	37.80	75.88	0.6910	[illegible]	89.16	48.90	112.3	0.7854	91.35
6TC15	Trans.	0.0633	1.35	7.40	249.00	9.800	1.55	65.39	38.97	70.85	0.6860	66.15	96.72	51.61	114.7	0.8490	99.22

* Calibration Values

Note: All K_{Ic} values shown in this table were obtained from nonstandard ASTM specimens.

The test technique and determination of pop-in were identical to the center notched pro-tram except that plane strain fracture toughness only was obtained. As before, gross stress and net stress were calculated at pop-in, prior to determination of K_{Ic}' (Tables XII to XIV). A plastic zone correction was calculated and was used to obtain a corrected plane strain fracture toughness, K_{Ic}. (Unless stated otherwise, the term "plane strain fracture toughness" will refer to K_{Ic}.)

For INCO 718 (aged) as for all other alloys tested, the net stress at pop-in was substantially below the yield strength of the material (e.g., at -423° F, a longitudinal net stress of 108 ksi compared to the yield strength of 208 ksi) at all test temperatures. Generally, $\sigma_N < 0.5\sigma_{ys}$ for virtually all tests.

Load-deflection traces for the INCO 718 (aged) were the most erratic of all curves obtained under this program. In fact, the plane strain fracture toughness of this material showed so much scatter at -423° F (range of 116 to 143 ksi $\sqrt{in.}$, compared to the CN average of 164) that two extra specimens were tested to verify the other results. The results of all seven tests are shown in Table XII.

Nevertheless, the variation of plane strain fracture toughness with temperature is in agreement with the trend demonstrated by the center notched tests; the fracture toughness of INCO 718 (aged) increases with a decrease in temperature. Again, the scatter should be noted (Figure 23). Longitudinal K_{Ic} varies from 125 at -423° F to 77 at 75° F.

The X2021-T8 E31 aluminum alloy shows the same sort of trends noted in the INCO 718, except that scatter was somewhat more favorable (Table XIII). Again, the unmistakable trend is that the plane strain fracture toughness of this material increases with a decrease in temperature (Figure 24). The net stress at pop-in was slightly less than 50 percent of yield stress for all test temperatures.

Plane strain fracture toughness values obtained for the 2219 and 7039 aluminum alloys are quite similar (Table XIV). However, evaluation of the 7039 load-deflection curves was somewhat more difficult than evaluation of the 2219 curves. Net stresses and gross stresses of these two aluminum alloys also show marked similarity at -423°F.

The net stress at pop-in for both of the titanium alloys is less than 30 percent of the yield strength at -423°F (Table XIV). However the net stress, gross stress, and plane strain fracture toughness of the Ti 5Al-2.5 (ELI) are higher than the correspondir values of the Ti 6Al-4V (ELI). Despite this difference, there is nothing to indicate that the Ti 6Al-4V (ELI) is brittle at -423° F, despite the fact that poor notch-unnotch tensile ratios were observed during mechanical properties tests.

Tiffany (Reference 12) reports slightly lower values (45 to 58 ksi $\sqrt{in.}$) for Ti 5Al-2.5Sn (ELI) in center notched sheet specimens, 0.188-inch thick by 14 inches wide.

Table XII

Plane Strain Fracture Tougness (K_{Ic}) for INCO 718 (Aged) Using Single Edge Notch (SEN) Specimens

Specimen Number	Test Direction	Test Temp. (°F)	Thick-ness, B (in.)	Width (in.)	a_0 (in.)	Pop Load, P (k)	Yield Strength, σ_{ys} (ksi)	K_{Ic}' (ksi $\sqrt{in.}$)	Gross Stress, σ_G (ksi)	Net Stress, σ_N (ksi)	Corrected a (in.)	Corrected K_{Ic} (ksi $\sqrt{in.}$)
IL62	Long.	-423	0.0636	0.500	0.210	2.010	208.0	117.36	63.21	108.98	0.2269	131.40
IL20	Long.	-423	0.0616	0.510	0.190	2.130	208.0	107.44	67.80	108.06	0.2042	118.71
IL22	Long.	-423	0.0621	0.510	0.190	2.100	208.0	105.08	66.31	105.68	0.2035	115.60
IL66	Long.	-423	0.0613	0.500	0.200	2.220	208.0	125.44	72.43	120.72	0.2193	143.21
IL54	Long.	-423	0.0624	0.500	0.210	1.830	208.0	108.90	58.65	101.13	0.2245	120.[illegible]8
IL65	Long.	-423	0.0614	0.500	0.210	1.890	208.0	114.30	61.56	106.14	0.2260	127.[illegible]
IL53	Long.	-423	0.0628	0.500	0.200	2.160	208.0	119.13	68.79	111.65	0.2174	134.30
IT12	Trans.	-423	0.0628	0.520	0.210	1.665	207.0	91.28	50.99	85.53	0.2203	97.76
IT57	Trans.	-423	0.0635	0.510	0.190	1.725	207.0	84.41	53.27	84.89	0.1988	89.86
IT61	Trans.	-423	0.06[illegible]	0.500	0.220	[illegible]10	207.0	[illegible]7.95	44.27	[illegible]9.05	0.22[illegible]6	93.66
IT01	Trans.	-423	0.0625	0.5[illegible]0	0.220	1.670	207.0	98.32	51.[illegible]8	[illegible]9.07	0.2320	106.23
IT05	Trans.	-423	0.0628	0.520	0.190	1.770	207.0	84.48	54.20	85.[illegible]	0.1988	89.89
IL02	Long.	-320	0.0624	0.520	0.210	1.500	194.0	82.76	46.23	[illegible]7.54	0.2197	88.26
IL10	Long.	-320	0.0624	0.510	0.210	1.770	194.0	101.37	55.62	[illegible]4.55	0.2245	111.65
IL57	Long.	-320	0.0629	0.500	0.200	1.530	194.0	84.25	43.65	[illegible]1.08	0.2100	90.33
IL58	Long.	-320	0.0630	0.500	0.190	1.610	194.0	82.40	51.11	82.44	[illegible]996	88.25
IL64	Long.	-320	0.0635	0.500	0.200	1.500	194.0	81.82	47.24	78.74	[illegible]094	87.38
IL60	Long.	-320	0.0639	0.500	0.200	1.500	194.0	81.31	46.95	[illegible] 25	0.2093	86.76
IT54	Trans.	-320	0.0630	0.510	0.210	1.140	192.0	64.67	35.48	[illegible]2	0.2160	67.3[illegible]
IT53	Trans.	-320	0.0630	0.500	0.[illegible]0	2.100	192.0	79.40	66.[illegible]7	95.24	0.1591	85.21
IT04	Trans.	-320	0.0628	[illegible]530	0.200	1.800	192.0	88.91	5[illegible]8	86.86	0.2114	96.03
IT52	Trans.	-320	0.063[illegible]	0.500	0.200	1.500	192.0	82.34	47.54	79.24	0.2098	88.13
IT66	Trans.	-320	0.062[illegible]	0.510	0.200	1.470	192.0	78.95	46.[illegible]	76.36	[illegible] 2090	84.00

Note: All K_{Ic} values shown in this table were obtained from nonstandard ASTM specimens.

Table XII
Plane Strain Fracture Toughness (K_{Ic}) for INCO 718 (Aged) Using Single Edge Notch (SEN) Specimens, Contd

Specimen Number	Test Direction	Test Temp. (°F)	Thickness, B (in.)	Width (in.)	a_0 (in.)	Pop-in Load, P (k)	Yield Strength, σ_{ys} (ksi)	K_{Ic}' (ksi $\sqrt{in.}$)	Gross Stress, σ_G (ksi)	Net Stress, σ_N (ksi)	Corrected a (in.)	Corrected K_{Ic} (ksi $\sqrt{in.}$)
IL05	Long.	-110	0.0628	0.500	0.200	1.320	173.0	72.80	42.04	70.06	0.2094	77.73
IL55	Long.	-110	0.0620	0.500	0.210	1.320	173.0	79.06	42.58	73.41	0.2211	85.20
IL51	Long.	-110	0.0629	0.500	0.210	1.440	173.0	85.01	45.79	78.94	0.2228	92.67
IL09	Long.	-110	0.0618	0.510	0.190	1.440	173.0	72.40	45.69	72.82	0.1993	77.33
IL61	Long.	-110	0.0639	0.500	0.210	1.170	173.0	67.99	36.62	63.14	0.2182	71.88
IT58	Trans.	-110	0.0634	0.500	0.210	1.230	171.0	72.04	38.80	66.90	0.2194	76.78
IT67	Trans.	-110	0.0613	0.510	0.200	1.260	171.0	67.89	39.91	65.66	0.2084	71.94
IT03	Trans.	-110	0.0625	0.520	0.220	1.350	171.0	79.48	41.54	72.00	0.2315	85.60
IT55	Trans.	-110	0.0634	0.510	0.230	1.230	171.0	79.14	38.04	69.29	0.2414	85.03
IT51	Trans.	-110	0.0632	0.500	0.220	1.230	171.0	77.33	38.92	69.51	0.2308	83.03
IL25	Long.	+75	0.0614	0.510	0.200	1.270	160.0	68.99	40.56	66.72	0.2039	73.85
IL18	Long.	+75	0.0629	0.500	0.200	1.390	160.0	76.54	44.20	73.66	0.2121	83.27
IL24	Long.	+75	0.0616	0.500	0.190	1.380	160.0	72.24	44.81	72.27	0.2006	78.04
IL04	Long.	+75	0.0617	0.501	0.200	1.260	160.0	70.73	40.84	68.07	0.2104	76.02
IL03	Long.	+75	0.0621	0.500	0.200	1.260	160.0	70.28	40.58	67.63	0.2102	75.47
IT59	Trans.	+75	0.0636	0.510	0.200	1.260	164.0	66.08	38.85	63.91	0.2086	70.13
IT02	Trans.	+75	0.0625	0.510	0.210	1.290	164.0	73.76	40.47	68.80	0.2207	79.27
IT64	Trans.	+75	0.0639	0.510	0.200	1.380	164.0	72.03	42.35	69.67	0.2102	77.30
IT09	Trans.	+75	0.0625	0.520	0.210	1.410	164.0	77.67	43.38	72.77	0.2219	84.06
IT56	Trans.	+75	0.0636	0.500	0.260	1.110	164.0	89.12	34.91	72.72	0.2757	97.53

Note: All K_{Ic} values shown in this table were obtained from nonstandard ASTM specimens.

Table XIII
Plane Strain Fracture Toughness (K_{Ic}) for X2021-T8 E31 Aluminum Alloy Using Single Edge Notch (SEN) Specimens

Specimen Number	Test Direction	Test Temp. (°F)	Thickness, B (in.)	Width (in.)	a_0 (in.)	Pop-in Load, P (k)	Yield Strength, σ_{ys} (ksi)	K_{Ic}' (ksi $\sqrt{in.}$)	Gross Stress, σ_G (ksi)	Net Stress, σ_N (ksi)	Corrected a (in.)	Corrected K_{Ic} (ksi $\sqrt{in.}$)
XL51	Long.	-423	0.0631	0.510	0.190	0.640	73.8	31.52	19.[illegible]	31.70	0.200	33.75
XL52	Long.	-423	0.0630	0.510	0.190	0.650	73.8	32.06	20.13	32.24	0.200	34.42
XL53	Long.	-423	0.0633	0.500	0.180	0.692	73.8	32.76	21.06	34.16	0.191	35.37
XLP3	Long.	-423	0.0621	0.490	0.220	0.520	73.8	34.62	17.09	31.01	0.232	37.39
XL54	Long.	-423	0.0629	0.510	0.200	0.660	73.8	35.00	20.57	33.85	0.212	37.99
XT51	Trans.	-423	0.0631	0.510	0.[illegible]00	0.652	70.3	34.46	20.[illegible]6	33.33	0.213	37.62
XT52	Trans.	-423	0.0630	0.510	0.200	0.667	70.3	35.31	20.76	34.15	0.215	38.71
XT53	Trans.	-423	0.0629	0.510	0.200	0.662	70.3	35.10	20.64	33.95	0.213	38.44
XTP1	Trans.	-423	0.0624	0.490	0.150	0.740	70.3	29.23	24.[illegible]0	34.89	0.159	31.42
XTP2	Trans.	-423	0.0623	0.480	0.180	0.615	70.3	31.90	20.57	32.91	0.191	34.62
XL06	Long.	-320	0.0619	0.550	0.200	0.588	65.8	27.51	17.27	27.14	0.209	29.26
XL18	Long.	-320	0.0623	0.480	0.160	0.546	65.8	24.24	18.26	27.39	0.167	25.66
XL20	Long.	-320	0.0623	0.500	0.200	0.552	65.8	30.69	17.72	29.53	0.212	33.25
XT22	Trans.	-320	0.0619	0.480	0.140	0.725	64.7	27.56	24.40	34.45	0.150	29.81
XT03	Trans.	-320	0.0621	0.490	0.170	0.672	64.7	31.19	22.08	33.82	0.182	34.25
XT14	Trans.	-320	0.0620	0.480	0.140	0.692	64.7	26.26	23.25	32.83	0.149	28.20
XL08	Long.	-110	0.0616	0.530	0.200	0.565	58.2	28.45	17.31	27.79	0.213	31.00
XL38	Long.	-110	0.0628	0.490	0.190	0.445	58.2	23.74	14.46	23.62	0.199	25.30
XL37	Long.	-110	0.0619	0.490	0.200	0.380	58.2	22.10	12.53	21.17	0.208	23.33
XT04	Trans.	-110	0.0618	0.500	0.200	0.435	58.1	24.38	14.08	23.46	0.209	26.02
XT05	Trans.	-110	0619	0.500	0.150	0.485	58.1	18.66	15.67	22.39	0.156	19.48
XT36	Trans.	-110	0.0625	0.500	0.200	0.370	58.1	20.50	11.84	19.73	0.207	21.47
XL36	Long.	+75	0.0623	0.490	0.170	0.398	54.6	18.41	13.04	19.9[illegible]	0.176	19.28
XL39	Long.	+75	0.0626	0.490	0.190	0.392	54.6	20.98	12.78	20.87	0.198	22.20
XL48	Long.	+75	0.0624	0.500	0.180	0.397	54.6	19.06	12.72	19.88	0.187	19.99
XT37	Trans.	+75	0.0624	0.500	0.200	0.330	54.5	18.32	10.58	17.63	0.200	19.10
XT40	Trans.	+75	0.0623	0.510	0.190	0.425	54.5	21.20	13.38	21.32	0.198	22.44
XT41	Trans.	+75	0.0623	0.510	0.190	0.397	54.5	19.80	12.19	19.91	0.197	20.81

Note: All K_{Ic} values shown in this table were obtained from nonstandard ASTM specimens.

Table XIV
Plane Strain (K_{Ic}) Fracture Toughness for Single Edge Notch (SEN) Specimens at -423°F

Specimen Number	Test Direction	Thickness, B (in.)	Width (in.)	a_0 (in.)	Pop-in Load, P (k)	Yield Strength, σ_{ys} (ksi)	K_{Ic}' (ksi $\sqrt{in.}$)	Gross Stress, σ_G (ksi)	Net Stress, σ_N (ksi)	Corrected a (in.)	Corrected K_{Ic} (ksi $\sqrt{in.}$)
					2219-T81 Aluminum Alloy						
9L21	Long.	0.1227	0.490	0.200	1.152	67.40	33.80	19.16	32.375	0.2133	37.11
9L18	Long.	0.1227	0.480	0.190	1.170	67.40	33.215	19.[illegible]	32.88	0.2029	36.47
9L01	Long.	0.1226	0.500	0.210	1.118	67.40	33.66	18.[illegible]4	31.45	0.2234	37.06
9L03	Long.	0.1224	0.500	0.190	1.180	67.40	31.09	19.28	31.10	[illegible]	33.70
[illegible]	[illegible]	[illegible]	[illegible]	0.200	1.140	[illegible]	[illegible]	16.57	30.94	0.2121	34.97
9T16	Trans.	0.1222	0.500	0.240	0.810	67.20	29.97	13.26	25.49	0.2506	31.99
9T20	Trans.	0.1222	0.480	0.200	1.258	67.20	38.57	21.45	36.77	0.2175	43.59
9T14	Trans.	0.12[illegible]	0.480	0.180	1.310	67.20	34.62	22.32	35.70	0.1941	38.45
9T15	Trans.	0.1220	0.500	0.170	1.362	67.20	31.[illegible]	22.33	33.83	0.1813	33.78
9T11	Trans.	0.1226	0.500	0.210	1.140	67.20	34.53	18.60	32.06	0.2240	37.94
					7039-T64 Aluminum Alloy						
3L07	Long.	0.1213	0.480	0.200	1.068	62.20	32.99	18.34	31.45	0.2149	36.63
3L10	Long.	0.1212	0.490	0.180	1.121	62.20	28.77	18.88	29.84	0.1913	31.29
3L13	Long.	0.1212	0.500	0.190	1.201	62.20	31.95	19.82	31.97	0.2040	35.30
3L24	Long.	0.1212	0.480	0.190	1.130	62.20	32.48	19.42	32.15	0.2045	36.06
3L09	Long.	0.1212	0.480	0.200	1.214	62.20	37.53	20.87	35.77	0.2193	42.94
3T05	Trans.	0.1212	0.500	0.210	1.100	64.40	33.70	18.15	31.30	0.2245	37.16
3T14	Trans.	0.1215	0.500	0.200	1.020	64.40	22.08	16.79	27.98	0.2108	31.35
3T07	Trans.	0.1213	0.490	0.220	0.840	64.40	28.63	14.13	25.65	0.2306	30.68
3T17	Trans.	0.1214	0.490	0.200	0.999	64.40	29.63	16.79	28.38	0.2112	32.05
3T10	Trans.	0.1214	0.500	0.100	1.906	64.40	25.35	31.40	39.25	0.1082	26.98
					Titanium 5 Al-2.5Sn (ELI)						
5L01	Long.	0.0592	0.510	0.210	0.962	213.0	58.07	31.86	54.17	0.2139	[illegible]
5L09	Long.	0.0591	0.490	0.210	1.020	213.0	65.66	35.22	61.64	0.2152	69.08
5L11	Long.	0.0593	0.480	0.200	0.950	213.0	60.02	33.38	57.22	0.2042	61.[illegible]
5L15	Long.	0.0590	0.480	0.200	1.00	213.0	63.50	35.31	[illegible]0.53	0.20[illegible]	[illegible].68
5L21	Long.	0.0592	0.480	0.190	1.060	213.0	62.37	37.30	61.74	0.194[illegible]	64.49
5T03	Trans.	0.0642	0.500	0.200	1.070	210.0	57.73	33.33	55.56	0.204	59.38
5T10	Trans.	0.0642	0.500	0.200	1.160	210.0	62.58	36.14	60.23	0.2047	64.69
5T12	Trans.	0.065[illegible]	0.500	0.200	1.060	210.0	57.11	32.98	54.96	0.2039	[illegible].71
5T14	Trans.	0.0654	0.500	0.220	1.038	210.0	63.06	31.74	56.68	0.2248	65.09
5T22	Trans.	0.0647	0.490	0.200	1.090	210.0	60.66	34.38	58.09	0.2044	62.59
					Titanium 6Al-4V (ELI)						
6L05	Long.	0.0622	0.4[illegible]	0.200	0.923	246.0	53.37	30.25	51.11	0.203	54.33
6L10	Long.	0.0632	0.500	0.150	0.958	246.0	36.11	30.32	43.31	0.151	36.43
3L12	Long.	0.0635	0.500	0.200	0.950	246.0	51.82	29.92	49.87	0.202	52.69
6L24	Long.	0.0626	0.500	0.200	0.960	246.0	53.12	30.67	51.12	0.202	54.05
6L25	Long.	0.0629	0.500	0.200	0.912	246.0	50.22	29.00	4[illegible].33	0.202	51.01
6T27	Trans.	0.0614	0.500	0.200	0.925	249.0	52.18	30.13	50.22	0.202	53.04
6T26	Trans.	0.0622	0.500	0.200	0.960	249.0	53.46	30.87	51.45	0.202	54.39
6T07	Trans.	0.0622	0.490	0.190	0.973	249.0	52.40	31.92	52.14	0.192	53.30
6T23	Trans.	0.0618	0.500	0.200	0.920	249.0	51.56	29.77	49.62	0.202	52.40
6T09	Trans.	0.0632	0.500	0.210	0.987	249.[illegible]	57.99	31.23	53.[illegible]	0.213	59.14

Note: All K_{Ic} values shown in this table were obtained from nonstandard ASTM specimens.

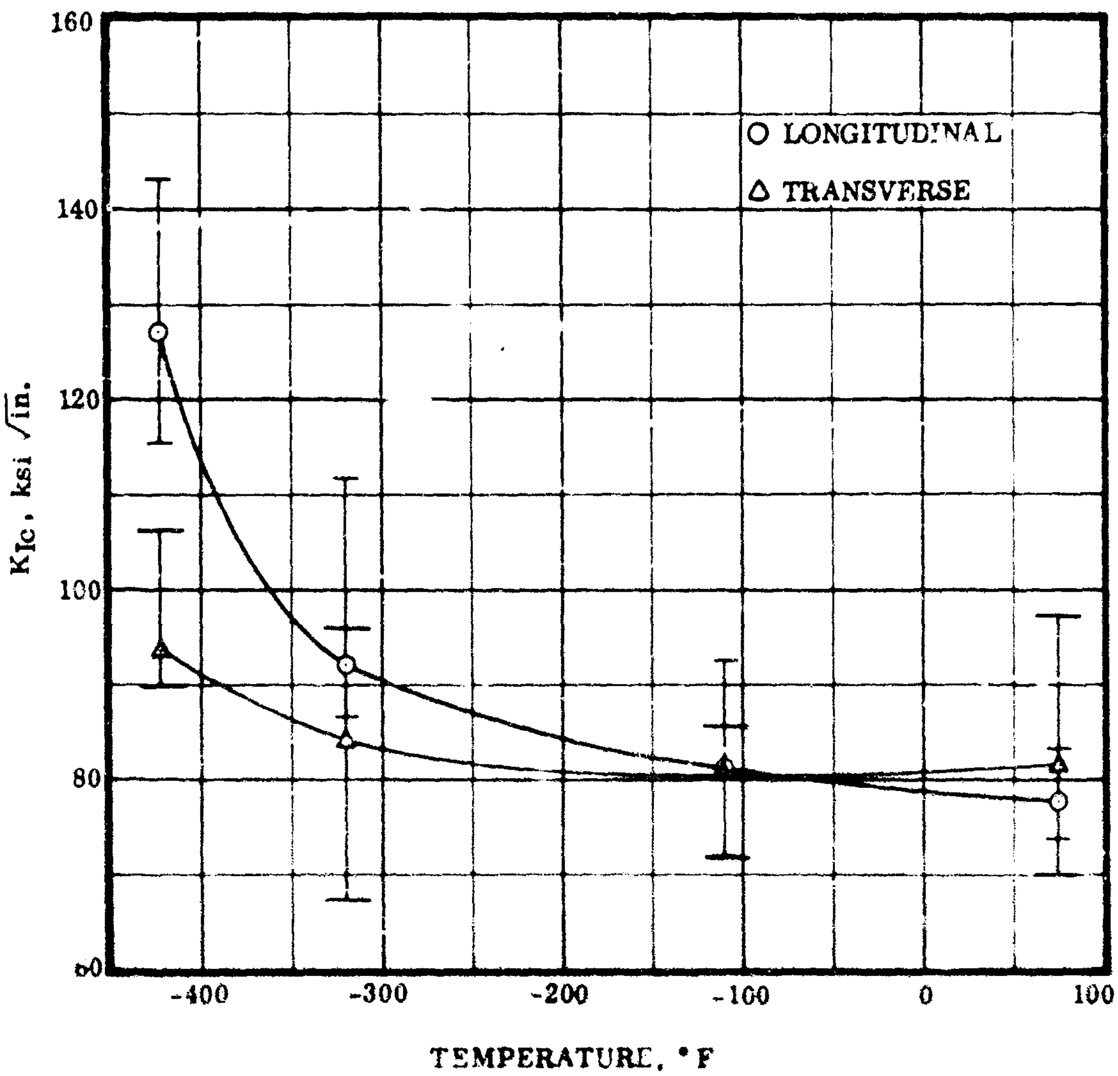

Figure 23. Variation of Plane Strain Fracture Toughness (K_{Ic}) With Temperature for INCO 718 (Aged) Using Single Edge Notch (SEN) Specimens

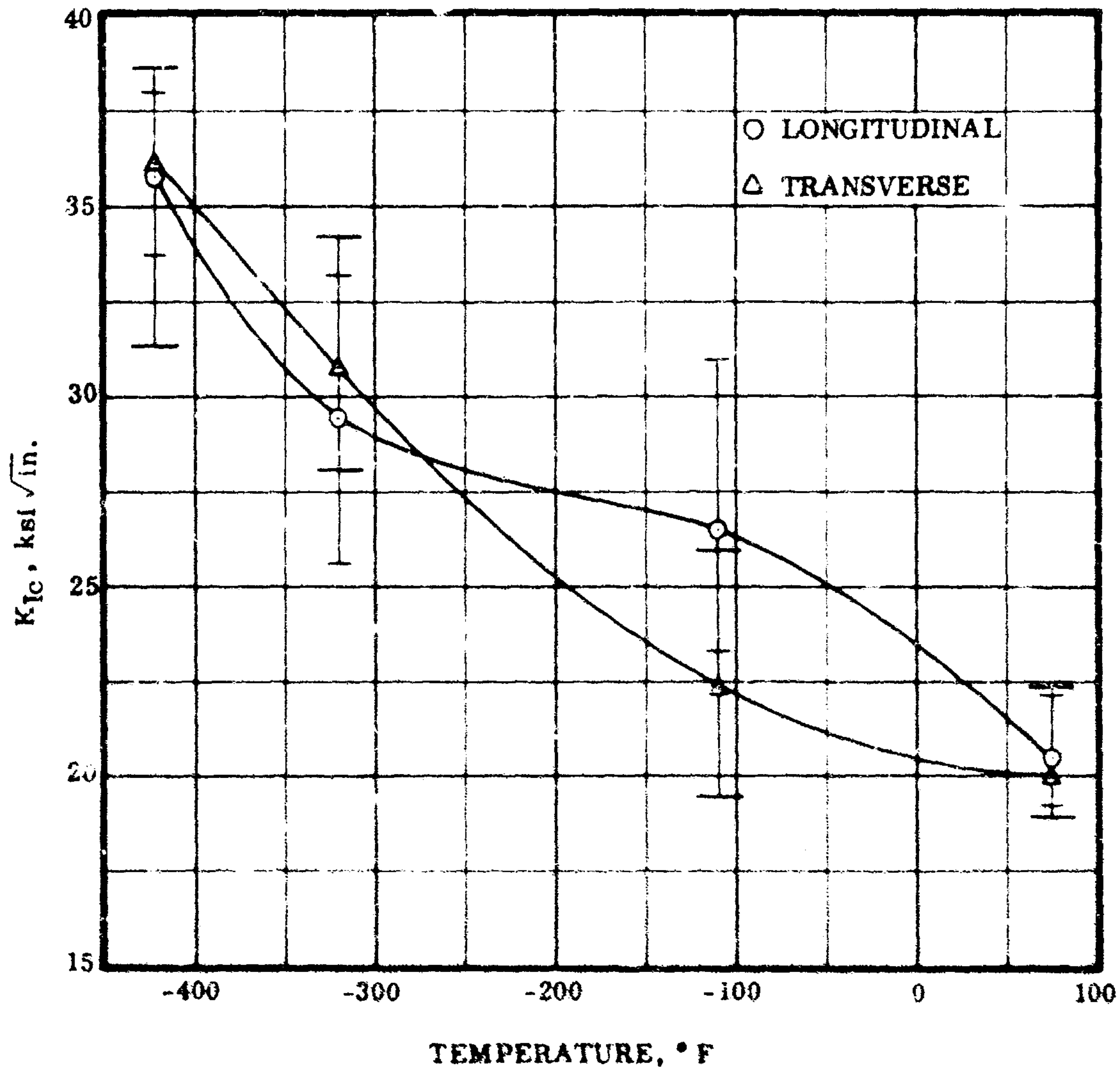

Figure 24. Variation of Plane Strain Fracture Toughness (K_{Ic}), With Temperature for X2021-T8 E31 Aluminum Alloy Using Single Edge Notch (SEN) Specimens

3. COMPARISON OF SPECIMEN CONFIGURATIONS FOR OBTAINING PLANE STRAIN FRACTURE TOUGHNESS. Some attempt has been made to relate plane strain to plane stress by Irwin and others. In addition, Hahn and Rosenfield (Reference 13) have successfully related K_{Ic} with tensile properties for various materials at room temperature, utilizing the strain hardening exponent. (Strain hardening exponents were not obtained in the present program.)

The values in this program should permit comparison of K_{Ic} values as obtained by SEN and CN specimens, although the specimen configurations probably violate several recommendations.

In all cases the average corrected K_{Ic} obtained through use of CN tests was significantly higher than those obtained in the SEN tests. Since the plane strain fracture toughness is a lower limiting value of crack intensity factor, K_1, it would appear that the SEN specimens are more likely to be true values. In some cases there was an overlap in the range of data at a particular temperature. (For example, the CN and SEN results at -423° F for X2021 show several similar results.)

On the other hand, the differences in K_{Ic} between the two test specimens for INCO 718 were consistently high, ranging from 29 to 46 percent. The closest agreement was for the 2021 alloy at -423°F, where the average values were 14 and 10 percent higher for CN than SEN tests (longitudinal and transverse respectively). It is conceivable that the results at other test temperatures could have had better agreement for the X2021 aluminum if more than three replicate tests were run.

Some suggest that the most valid data come from tests where the σ_N/σ_{ys} ratio is smallest. In this program, the lowest (by far) net fracture stress/yield stress ratios were for the two titanium alloys at -423°F. Differences in K_{Ic} for these materials ranged from 15 to 24 percent. However, at -423°F, the net fracture stress was approximately equal to the yield stress for the 2021 aluminum (CN tests), yet the differences in K_{Ic} were 14 and 10 percent for the longitudinal and transverse grain directions. Apparently σ_N/σ_{ys} ratios have no direct relationship to the accuracy of the K_{Ic} values.

SECTION VII

CONCLUSIONS

The overall objective of this program was to obtain comparative fracture data for six sheet alloys for usage at cryogenic temperatures. Tensile and notched tensile properties, as well as plane stress and plane strain properties were obtained for the following alloys at -423° F:

Titanium 5Al-2.5Sn (ELI)
Titanium 6Al-4V (ELI)
INCO 718 (Aged)
X2021-T8 E31 Aluminum
2219-T81 Aluminum
7039-T64 Aluminum

In addition, strength and fracture properties were obtained for INCO 718 and X2021 aluminum at room temperature, -110° F, and -320° F.

Sufficient tensile, notched tensile, center notched, and single edge notched specimens have been forwarded to the Air Force Materials Laboratory to permit testing of five of the alloys (all except INCO 718) at room temperature, -110° F, and -320°F. In addition, two calibrated strain gaged compliance gages were also sent to the AFML to aid in fracture testing.

1. As expected, the ultimate tensile strength, yield strength, and notched strength of INCO 718 (aged) increased with decreasing temperature. The same general trend continued for fracture properties, including net fracture stress, plane stress, and plane strain fracture toughness for both types of specimens used. The notch-unnotch ratio of the material dropped to slightly below unity at -423°F.

2. The new X2021-T8 E31 aluminum alloy also showed increased properties with a decrease in temperature. The notch-unnotch tensile ratio (K_t = 6.3) was just less than unity at all test temperatures. The elongation and all fracture properties also increased with a decrease in temperature. This material appears to be a promising alloy for use in cryogenic applications.

3. Except for the titanium alloys, the 3-inch-wide center notched specimens provide net fracture stresses that exceed 80 percent of yield strength for the two thicknesses tested (B = 0.063, 0.125).

4. The net stress at pop-in was well below yield strength for all alloys and temperatures tested in this program.

5. In all cases in this program, the average K_{Ic} (corrected for plastic zone) was significantly larger when obtained from the center notched specimens as opposed to those obtained by use of the single notched specimen.

6. Reasonable load-deflection curves can be obtained from 1/2-inch-wide single edge notched (SEN) specimens at -423° F. While determination of pop-in is not simple, it appears that reasonable results can be obtained by careful experimentation, providing that suitable compliance gages are available.

7. Determination of pop-in requires use of engineering judgment even if a graphic method is utilized. The so called tangent or secant methods are practical, although some judgment is still required.

SECTION VIII

RECOMMENDATIONS

1. It is suggested that the secant method of determination of the pop-in value for K_{Ic} as suggested by Brown and Srawley be tried for the remainder of the tests to be performed by the AFML. In addition, the methods used in this program should be used for a direct comparison.

2. If the calibration method of determining K_{Ic} is to be continued, it would be wise to work out a precise technique utilizing nondestructive test methods for determination and characterization of fatigue crack extension prior to applying the calibration loads.

3. In view of the number of publications appearing recently suggesting various techniques and relationships of fracture toughness, it seems prudent to search, record, analyze, and disseminate information on all recent literature. Although some agencies have published documents containing data, little work has been done in the area of analysis of existing data or substantiation of existing theories or techniques.

REFERENCES

1. Srawley, J. E. and Brown, W. F., Jr., Fracture Toughness Testing, NASA Technical Note TN D-2599, January 1965.

2. ASTM Standards, Part 31, p. 945, May 1967.

3. Fracture Toughness Testing and Its Applications, ASTM Special Technical Publication No. 381, American Society for Testing and Materials, 26 June 1964.

4. Brown, W. F. and Srawley, J. E., Plane Strain Crack Toughness Testing of High Strength Materials, ASTM Special Publication No. 410, March 1967.

5. Hanna, G. L. and Steigerwald, E. A., Development of Standardized Test Methods to Determine Plane Strain Fracture Toughness, AFML-TR-65-213, September 1965.

6. Hunsicker, H. Y. and Hess, J. H., "New Weldable High Strength Aluminum Alloys for Cryogenic Service, "Advances in Cryogenic Engineering, Vol. 11, p. 423, 1966.

7. Witzell, W. E., Hersh, M. S., and Anderson, R. T., A Survey of Welding and Inspection Techniques for 2219-T81 Aluminum Alloy, NASA CR-72097, January 1967.

8. Christian, J. L., Yang, C. T., and Witzell, W. E., Physical and Mechanical Properties of Pressure Vessel Materials for Application in a Cryogenic Environment, Part III, ASD-TDR-62-258, December 1964.

9. Campbell, J. E., Current Methods of Fracture-Toughness Testing of High-Strength Alloys with Emphasis on Plane Strain, DMIC Report 207, 31 August 1964.

10. Srawley, J. E., Jones, M. H., and Brown, W. F., Determination of Plane Strain Fracture Toughness. Materials Research and Standards, Vol. 7 No. 6, June 1967.

11. D'Annessa, A. T., Fracture Toughness of X7039-T6 Aluminum Alloy Plate Weldments, Technical Report 6-62-64-6, Lockheed MSD, Sunnyvale, Calif.

12. Tiffany, C. F., Lorenz, P. M., and Hall, L. R., Investigation of Plane Strain Flaw Growth in Thick Walled Tanks, NASA CR-54837, D2-20467-1, February 1966.

13. Hahn, G. T. and Rosenfield, A. R., Sources of Fracture Toughness: The Relation Between K_{Ic} and the Ordinary Tensile Properties of Metals, Metal Science Group, Battelle Memorial Institute, April 1967.

14. Boyle, R. W., "A Method for Determining Crack Growth in Notched Sheet Specimens," Materials Research and Standards, August 1962.

BIBLIOGRAPHY

Benjamin, W. D. and Steigerwald, E. A., Stress Corrosion Cracking Mechanisms in Martensitic High Strength Steels, AFML-TR-67-98, April 1967.

Brown, B. F., "A New Stress-Corrosion Cracking Test for High-Strength Alloys," Materials Research and Standards, Vol. 6, No. 3, March 1966.

Carman, C. M., Plane Strain Fracture Toughness of 5Al-2.5Sn ELI Titanium and 2219-T87 Aluminum Alloy Weldments, NASA P.O. C-35060A, Quarterly Progress Report, Frankfort Arsenal, October 1964.

Carman, C. M., Forney, J. W., and Katlin, J. M., Plane Strain Fracture Toughness of 2219-T87 Aluminum Alloy at Room and Cryogenic Temperature, NASA CR-54297, NASA LeRC, Cleveland, Ohio, August 1966.

Christian, J. L. and Hurlich A., Physical and Mechanical Properties of Pressure Vessel Materials for Application in a Cryogenic Environment, Part II, ASD-TDR-62-258, April 1963.

Christian, J. L. and Witzell, W. E., "Evaluation of the Effects of Specimen Configuration and Testing Variables on Crack Propagation Properties," Cryogenic Engineering Conference, 17 August 1964.

Hanna, G. L. and Steigerwald, E. A., Influence of Working Hardening Exponent on Crack Propagation in High-Strength Materials, AFML-TR-66-139, October 1966.

Kobayashi, A. S., On the Magnification Factors of Deep Surface Flaws, Boeing Co. Structural Development Research Memo No. 16.

Lanta, F. J. and Steigerwald, E. A., Influence of Work Hardening Coefficient on Crack Propagation in High-Strength Steels, AFML-TR-65-31, May 1965.

Paris, P. and Erodogan, P. E., "A Critical Analysis of Crack Propagation Law," Trans. ASME, T of Basic Engineering, December 1963.

Smith, F. W., Stresses Near a Semi-Circular Edge Crack, Ph.D. thesis, University of Washington, 1966. University of Michigan Microfilm Inc. No. 66-7901.

Srawley, J. E., Jones, M. H., and Gross, B., Experimental Determination of the Dependence of Crack Extension Force on Crack Length for A Single Edge Notch Tension Specimen, NASA Technical Note TN D-2396, August 1964.

Tiffany, C. F. and Masters, J. N., Investigation of the Flaw Growth Characteristics of 6Al-4V Titanium Used in Apollo Spacecraft Pressure Vessels, NASA CR-65586, NASA MSC, March 1967.

Witzell, W. E., Fracture Toughness of Stainless Steel Sheet at Cryogenic Temperatures, American Rocket Society Paper 2418-62, 4 April 1962.

Witzell, W. E., Fracture Mechanics - Development of Single Edge Notch and Slow Bend Evaluation Techniques, Convair Report GDA-ERR-AN-701, 31 December 1964.

Witzell, W. E., An Introduction to Crack Propagation in High Strength Sheet Materials, Convair Report MRG-286, 2 February 1962.

Yang, C. T., A Study of Law of Crack Propagation, Convair Report ERR-AN-64-489, ASME Paper No. 64, WA/Met-6.

Yang, C. T., Use of Critical Gross Stress as a Design Limit — A Design Concept for Brittle Fracture, Convair Report ERR-AN-1005, December 1966.

APPENDIX I

CALIBRATION OF CENTER NOTCHED SPECIMENS

An attempt was made to calibrate some of the center notched specimens at -423°F in the manner of Boyle (Reference 14). This technique was conducted as follows:

1. A machine notch 0.77 inch long was cut in the tensile specimen.
2. With the compliance gage installed, the specimen was loaded to a given load, less than the fracture load.
3. The specimen was unloaded and the notch was extended to 1.00 inch.
4. Step 2 was repeated.
5. Again, the specimen notch was extended, this time to 1.25 inches.
6. Step 2 was repeated.
7. Finally, the notch was extended to 1.45 inches.
8. With the compliance gage installed, the specimen was loaded to failure.

Using the four load-extension curves obtained from the previous technique, a plot was made as follows:

1. Determine $\frac{\pi a}{W}$ for each notch length.
2. Calculate $\frac{E v}{\sigma W}$

   where a = one-half the notch length

   W = specimen width

   σ = gross stress at the given load

   v = extension at the given load

3. Plot $\frac{\pi a}{W}$ against $\frac{E v}{\sigma W}$

This procedure differs from Boyle's in that the total extension of the compliance gage is used (at the preselected load). Boyle used one-half of the deflection of an extensometer over a 2-inch gage length. The compliance gage in the present program had a gage length of about 1/4-inch. There were two reasons for using the entire output of the compliance gage, namely 1) to obtain as much deflection as possible in order to more nearly duplicate Boyle's work, and 2) to minimize errors due to slight variations in location of this small gage. Since this is a calibration to be used for other tests, the actual length is not critical as long as the tests and the calibration are conducted under the same conditions.

The data for two materials (2021-T8 E31 aluminum and Ti 5Al-2.5Sn) along with a generalized curve are shown in Figure 25. This curve has a slightly greater slope than does the curve of Boyle.

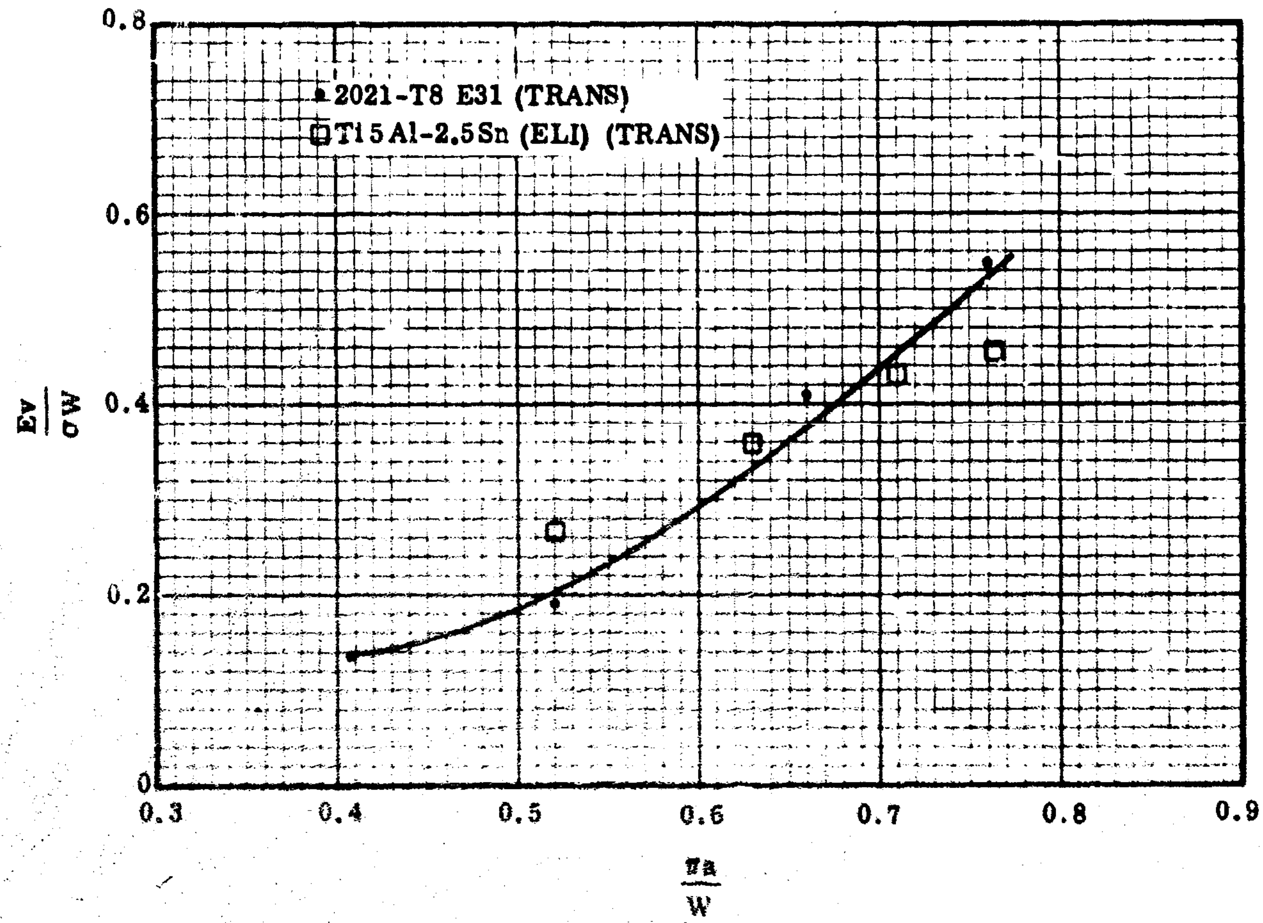

Figure 25. Calibration Curves for Center Notched Specimens of Selected Alloys at -423° F

APPENDIX II

FRACTOGRAPHY

INTRODUCTION. Each of the six alloys tested in this program was examined under light and electron microscopes. Fracture surfaces of the alloys were replicated and photographed under the electron microscope.

A failure in the loading pin hole area of an INCO 718 center cracked specimen prompted an examination of the leading edge of the crack. Under a light microscope it was determined that the leading edge of the crack was actually two cracks forking away from the original single crack. It was noted that the net stress at the failure of the grip of the specimen exceeded the net fracture stress of virtually all of the other similar specimens. It appears that when the crack splits into two cracks, the stresses at the tip of crack redistribute themselves, lowering the local stress concentration factor. As a consequence the ultimate gross stress is increased.

ELECTRON MICROSCOPY. Fractured surfaces were examined in several areas of interest, namely: 1) fatigue cracked area, 2) static cracked area, and 3) the transition between the fatigue and static crack. The INCO 718 nickel alloy and 2021 aluminum alloy fractures were examined for each test temperature. Fractures at -423° F were examined for all other alloys.

Electron fractographs for the 2021 alloy were similar for each of the test temperatures. Each of the three areas (fatigue, transition, static crack) is shown for room temperature tests in Figure 26. Fatigue crack growth is readily detected in the parallel striations in the photographs. As usual, fatigue planes bend toward discontinuities and are not necessarily parallel from area to area. The transition zone is quite clear, with striations stopping abruptly and dimples appearing shortly thereafter. The static crack area is normal, showing a somewhat ductile dimple pattern throughout.

Examination of the 2219-T81 aluminum alloy was made for tests performed at -423° F only. The results (Figure 27) show the same kind of patterns in the static cracked area but with much finer fatigue striations than were detected in the 2021 alloy. Since striations for the X2021 were consistent for different temperatures, there should be no temperature effect for this class of alloys. This characteristic should be examined more carefully after other tests are performed by the AFML.

Fractographs for the 7039-T64 aluminum alloy (not shown) are very similar to those for the 2021 material.

Titanium 6Al-4V (ELI) was also examined for tests performed at -423° F (Figure 28). Again, the static crack portion is normal and predictable. In this case, however, the fatigue striations are quite wide (coarse) and somewhat random in direction. Nevertheless, the transition zone is easily detectable.

The fractured surfaces obtained from Titanium 5Al-2.5Sn (ELI) specimens (Figure 29) tested at -423°F are very similar to those of the Ti 6Al-4V alloy except that the fatigue striations are more orderly and finer.

As in the 2021 series, the fractured surfaces of the INCO 718 were similar for each test temperature. Fractographs for the material test at -423°F, shown in Figure 30, again show normal fatigue striations and static fractured surfaces.

Fatigue Striations (8000X) | Transition Zone (8000X) | Static Crack (8000X)

Figure 26. Electron Fractographs for X2021 Aluminum Alloy at Room Temperature

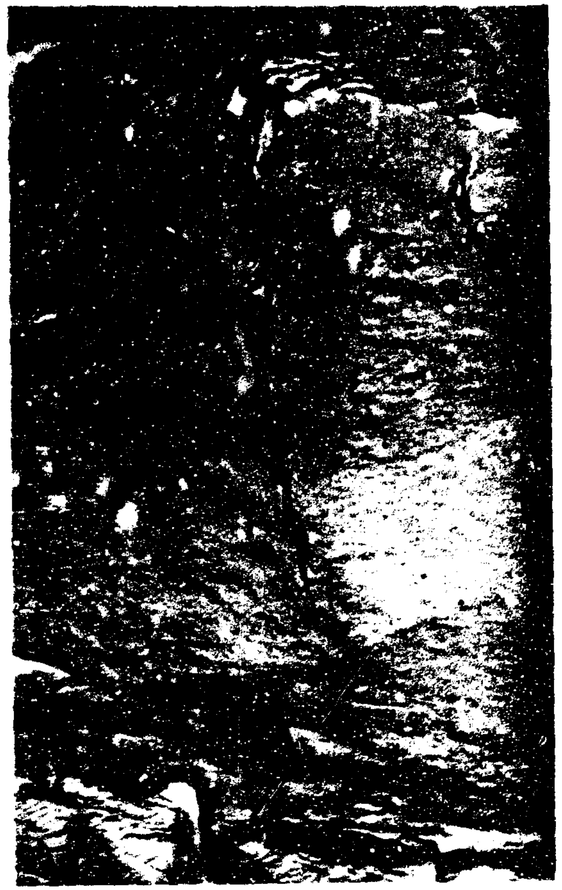

Fatigue Striations
(8000X)

Static Crack
(8000X)

Figure 27. Electron Fractographs of 2219-T81 Aluminum Alloy at -423°F

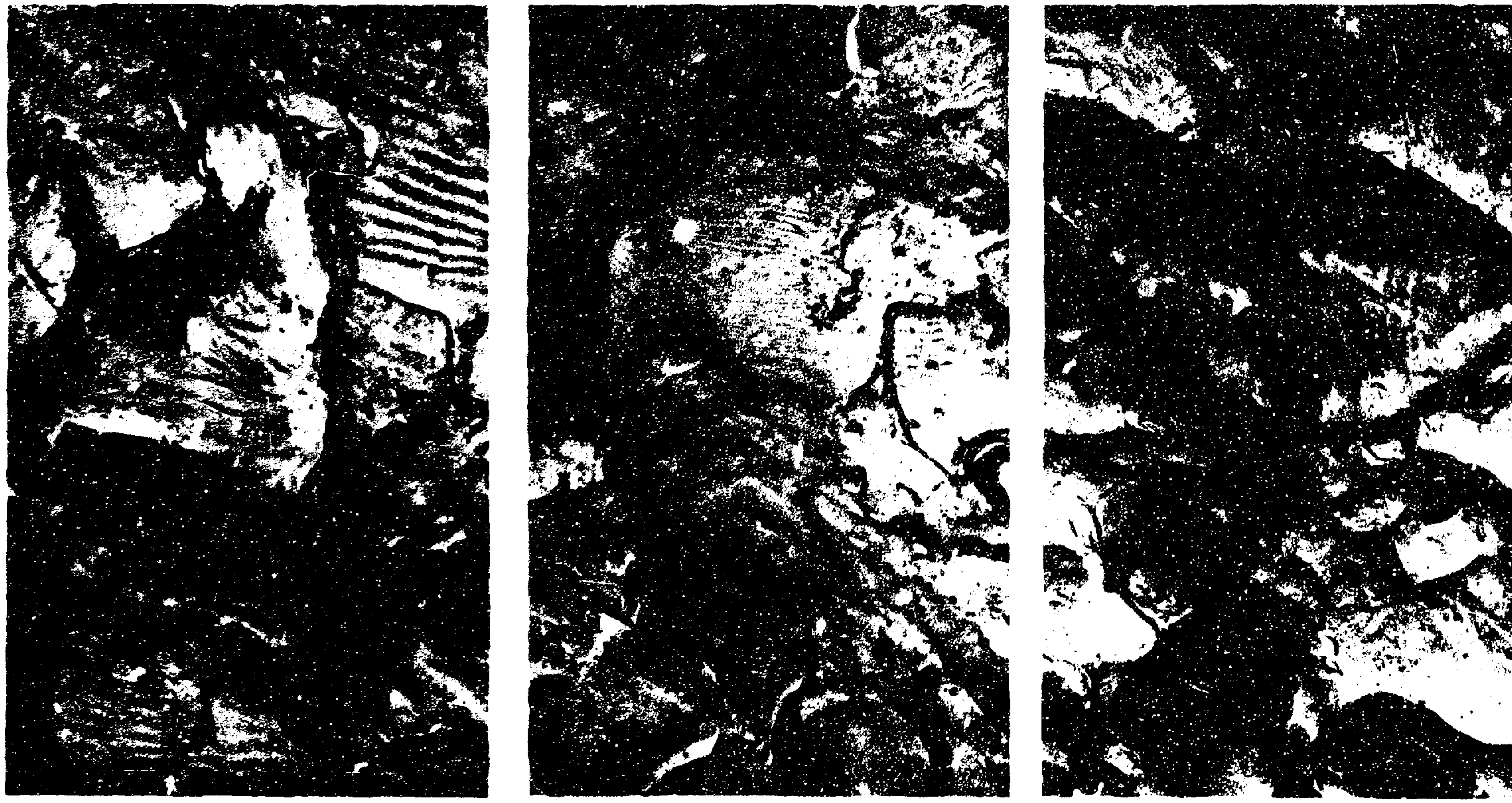

Fatigue Striations
(8000X)

Transition Area
(5000X)

Static Crack
(8000X)

Figure 28. Electron Fractographs of Titanium 6Al-4V (ELI) at -423° F

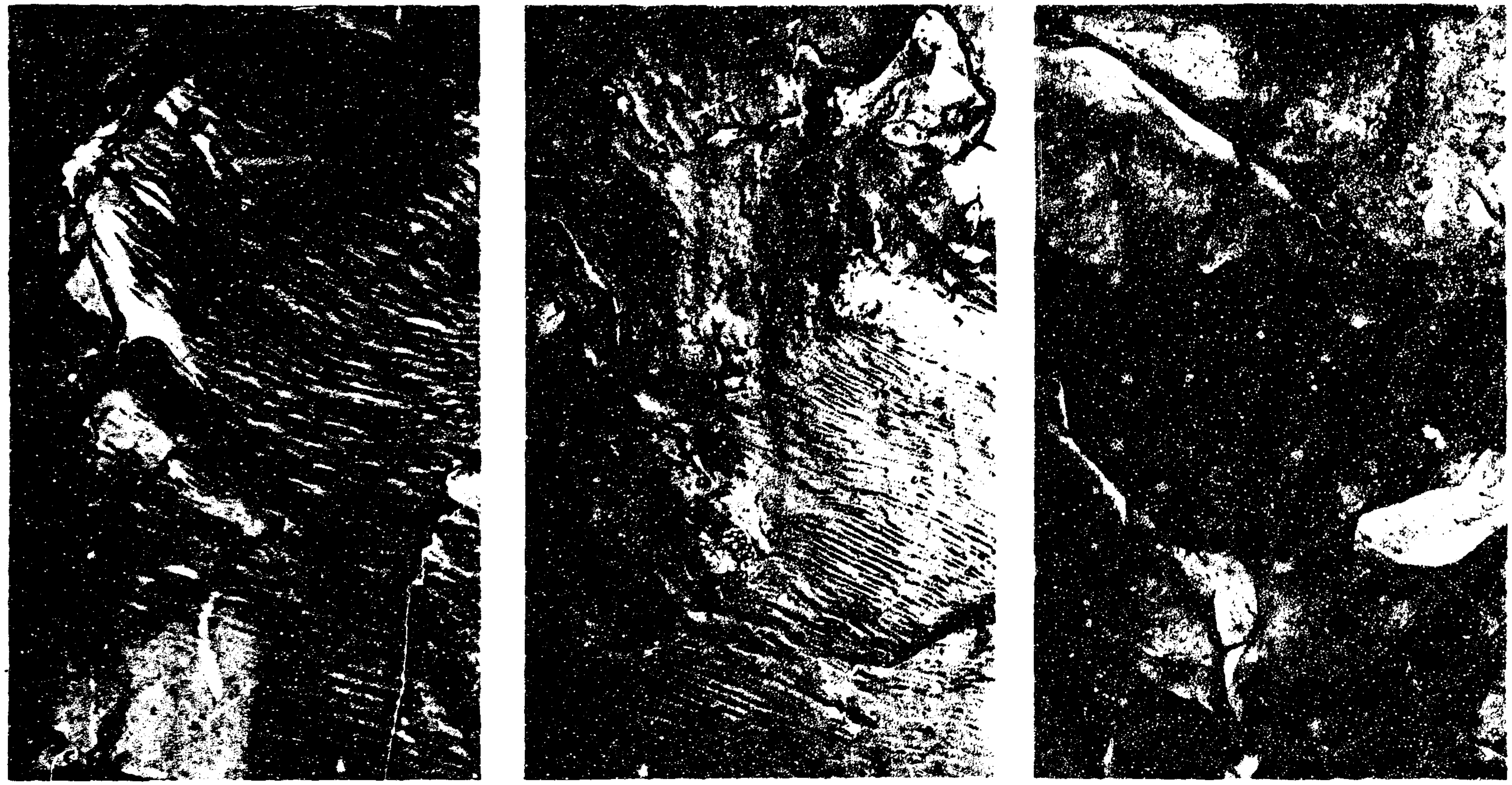

Fatigue Striations
(8000X)

Transition Area
(5000X)

Static Crack
(8000X)

Figure 29. Electron Fractographs of Titanium 5Al-2.5Sn (ELI) at -423° F

Fatigue Striations
(8000X)

Static Crack
(8000X)

Figure 30 Electron Fractographs of INCO 718 (Aged) at -423° F

UNCLASSIFIED

Security Classification

DOCUMENT CONTROL DATA - R&D

(Security classification of title, body of abstract and indexing annotation must be entered when the overall report is classified)

1. ORIGINATING ACTIVITY (Corporate author) Convair division of General Dynamics	2a. REPORT SECURITY CLASSIFICATION Unclassified 2b. GROUP Not Applicable

3. REPORT TITLE

FR^CTURE DATA FOR MATERIALS AT CRYOGENIC TEMPERATURES

4. DESCRIPTIVE NOTES (Type of report and inclusive dates)

Final Report. May 1966 to June 1967

5. AUTHOR(S) (Last name, first name, initial)

Witzell, William E.

6. REPORT DATE	7a. TOTAL NO. OF PAGES	7b. NO. OF REFS
November 1967	94	13

8a. CONTRACT OR GRANT NO. AF33(615)-3779	9a. ORIGINATOR'S REPORT NUMBER(S) GDC-ZZL67-017
b. PROJECT NO. 7381, Materials Application	
c. Task No. 738106, Design Information Development	9b. OTHER REPORT NO(S) (Any other numbers that may be assigned this report) AFML-TR-67-257
d.	

10. AVAILABILITY/LIMITATION NOTICES

Qualified requesters may obtain copies of this report from the Defense Documentation Center (DDC), Cameron Station, Bldg. 5, 5010 Duke Street, Alexandria, Virginia 22314

11. SUPPLEMENTARY NOTES	12. SPONSORING MILITARY ACTIVITY
	Air Force Materials Laboratory Research and Technology Division Wright Patterson Air Force Base, Ohio

13. ABSTRACT

Six potential aerospace alloys were evaluated for toughness at liquid hydrogen temperature (-423°F). They were: Titanium 5A1-2.5Sn (ELI), Titanium 6A1-4V (ELI), INCO 718 (aged) nickel alloy, Aluminum X2021-T8 E31, Aluminum 2219-T81, and Aluminum 7039-T64.

The first four materials were 0.063-inch thick; the last two were 0.125-inch thick. Sufficient specimens were manufactured to evaluate all of the alloys at four test temperatures, namely: room temperature, -110°F, -320°F, and -423°F.

~~Convair division~~ has ~~performed~~ tensile, notched tensile, center notched and single edge notch tests at -423°F for all alloys. In addition, the INCO 718 and X2021 aluminum alloys were investigated at the three other temperatures. The Air Force Materials Laboratory will perform the remainder of the tests at room temperature, -110°F; and -320°F.

An attempt was made to obtain both plane stress and plane strain fracture toughness data from the same center notched specimen. Except for the titanium alloys, the net fracture stress exceeded 80 percent of the yield strength for all alloys and test temperatures. In all cases, the net stress at pop-in was well below the yield strength of the material.

The pop-in net fracture stresses for the single edge notch specimens (obtained by a strain gaged compliance gage) were also well below the yield strength.

K_c and K_{Ic} values were calculated for all fracture specimens.

Both the INCO 718 and X2021 aluminum alloys showed good toughness properties as the temperature was decreased to -423°F.

DD FORM 1 JAN 64 1473

UNCLASSIFIED

Security Classification

14. KEY WORDS	LINK A		LINK B		LINK C	
	ROLE	WT	ROLE	WT	ROLE	WT
Fracture Toughness						
Aluminum Alloys						
Titanium						
INCO 718						
Cryogenic						
Plane Stress						
Plane Strain						

INSTRUCTIONS

1. ORIGINATING ACTIVITY: Enter the name and address of the contractor, subcontractor, grantee, Department of Defense activity or other organization *(corporate author)* issuing the report.

2a. REPORT SECURITY CLASSIFICATION: Enter the overall security classification of the report. Indicate whether "Restricted Data" is included. Marking is to be in accordance with appropriate security regulations.

2b. GROUP: Automatic downgrading is specified in DoD Directive 5200.10 and Armed Forces Industrial Manual. Enter the group number. Also, when applicable, show that optional markings have been used for Group 3 and Group 4 as authorized.

3. REPORT TITLE: Enter the complete report title in all capital letters. Titles in all cases should be unclassified. If a meaningful title cannot be selected without classification, show title classification in all capitals in parenthesis immediately following the title.

4. DESCRIPTIVE NOTES: If appropriate, enter the type of report, e.g., interim, progress, summary, annual, or final. Give the inclusive dates when a specific reporting period is covered.

5. AUTHOR(S): Enter the name(s) of author(s) as shown on or in the report. Enter last name, first name, middle initial. If military, show rank and branch of service. The name of the principal author is an absolute minimum requirement.

6. REPORT DATE: Enter the date of the report as day, month, year; or month, year. If more than one date appears on the report, use date of publication.

7a. TOTAL NUMBER OF PAGES: The total page count should follow normal pagination procedures, i.e., enter the number of pages containing information.

7b. NUMBER OF REFERENCES: Enter the total number of references cited in the report.

8a. CONTRACT OR GRANT NUMBER: If appropriate, enter the applicable number of the contract or grant under which the report was written.

8b, 8c, & 8d. PROJECT NUMBER: Enter the appropriate military department identification, such as project number, subproject number, system numbers, task number, etc.

9a. ORIGINATOR'S REPORT NUMBER(S): Enter the official report number by which the document will be identified and controlled by the originating activity. This number must be unique to this report.

9b. OTHER REPORT NUMBER(S): If the report has been assigned any other report numbers *(either by the originator or by the sponsor)*, also enter this number(s).

10. AVAILABILITY/LIMITATION NOTICES: Enter any limitations on further dissemination of the report, other than those imposed by security classification, using standard statements such as:

(1) "Qualified requesters may obtain copies of this report from DDC."

(2) "Foreign announcement and dissemination of this report by DDC is not authorized."

(3) "U. S. Government agencies may obtain copies of this report directly from DDC. Other qualified DDC users shall request through ______."

(4) "U. S. military agencies may obtain copies of this report directly from DDC. Other qualified users shall request through ______."

(5) "All distribution of this report is controlled. Qualified DDC users shall request through ______."

If the report has been furnished to the Office of Technical Services, Department of Commerce, for sale to the public, indicate this fact and enter the price, if known.

11. SUPPLEMENTARY NOTES: Use for additional explanatory notes.

12. SPONSORING MILITARY ACTIVITY: Enter the name of the departmental project office or laboratory sponsoring *(paying for)* the research and development. Include address.

13. ABSTRACT: Enter an abstract giving a brief and factual summary of the document indicative of the report, even though it may also appear elsewhere in the body of the technical report. If additional space is required, a continuation sheet shall be attached.

It is highly desirable that the abstract of classified reports be unclassified. Each paragraph of the abstract shall end with an indication of the military security classification of the information in the paragraph, represented as *(TS)*, *(S)*, *(C)*, or *(U)*.

There is no limitation on the length of the abstract. However, the suggested length is from 150 to 225 words.

14. KEY WORDS: Key words are technically meaningful terms or short phrases that characterize a report and may be used as index entries for cataloging the report. Key words must be selected so that no security classification is required. Identifiers, such as equipment model designation, trade name, military project code name, geographic location, may be used as key words but will be followed by an indication of technical context. The assignment of links, roles, and weights is optional.